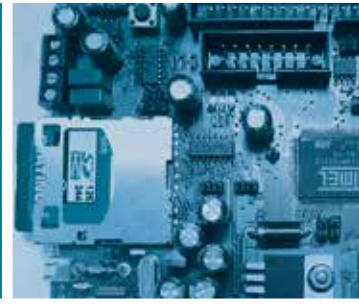
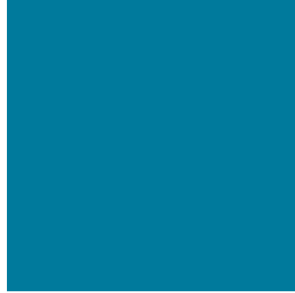
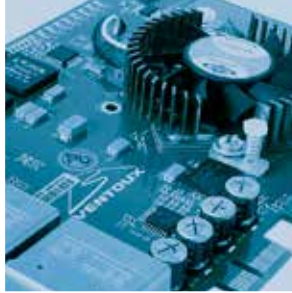
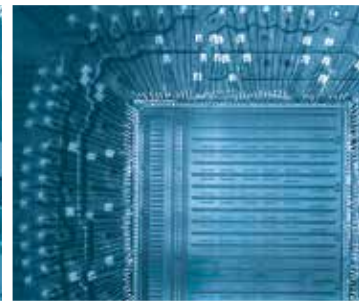
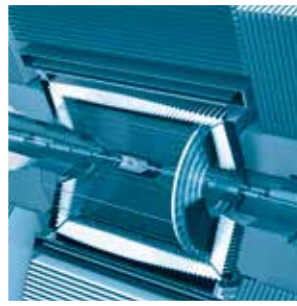
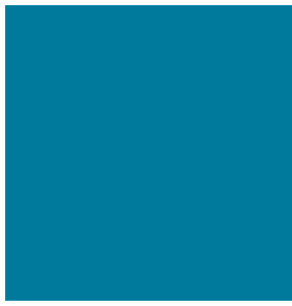


ziti



UNIVERSITÄT  
HEIDELBERG  
ZUKUNFT  
SEIT 1386



---

---

# 2011 ANNUAL REPORT

## JAHRESBERICHT

---

---

# CONTENTS

<b>PREFACE</b> .....	<b>4</b>
Letter to the Reader .....	4
<b>INSTITUTE</b> .....	<b>6</b>
Introduction .....	6
Some Key Numbers 2011 .....	6
Research Groups .....	7
Teaching .....	7
B.Sc. Applied Computer Science.....	7
Diploma Computer Engineering .....	7
M.Sc. Computer Engineering .....	8
<b>RESEARCH</b> .....	<b>10</b>
Chair of Automation Project Overview .....	10
Chair of Circuit Design Project Overview .....	16
Chair of Computer Architecture Project Overview .....	30
Chair of Computer Science V Project Overview .....	44
Chair of Computer Vision, Graphics and Pattern Recognition Project Overview .....	60
Chair of Optoelectronics Project Overview .....	86
Research Group Advanced Computer Architecture .....	108
Research Group Advanced Detectors for Scientific and Medical Applications .....	110
Research Group Application Specific Computer .....	112
Research Group Accelerated Scientific Computing .....	114
Research Group Dependable Robotics (DeBot) .....	116
Research Group High-Speed Short Range Interconnects .....	118
Research Group Next Generation Network Interfaces .....	120
Research Group Process Control (ProCon) .....	122
Research Group Unmanned Aerial Vehicles .....	124
Research Group Virtual Patient Analysis (ViPA) .....	126
<b>DATA</b> .....	<b>130</b>
Members and Staff .....	130
Third-party-funded Projects .....	135
Selected Project Partners .....	138
Publications .....	141
Patents .....	150
Colloquia and Conferences .....	150

## published by

Institut für Technische Informatik als  
zentrale Einrichtung der Universität Heidelberg  
B6, 26  
68159 Mannheim

## designed by

formamentum, Büro für visuelle Kommunikation

## used fonts

Linotype Univers  
Jenna Sue



*Dear Reader,*

This is the second annual report of the Institute of Computer Engineering (ZITI) since it was transferred from the University of Mannheim to the University of Heidelberg in 2008. The aim of this report is mainly to give you an overview of the research activities carried out at the ZITI in 2011.

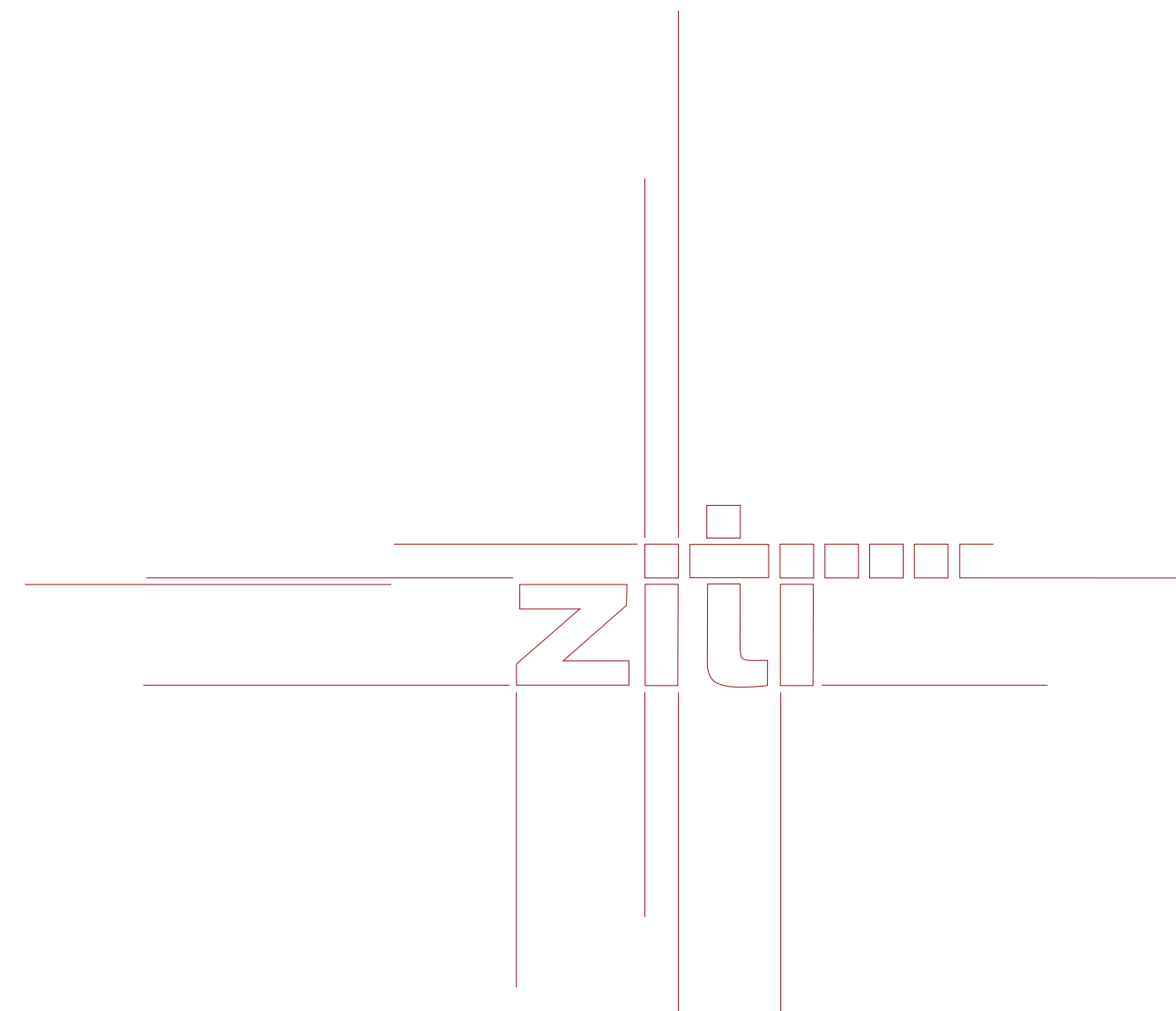
The chairs of the institute are divided between the Department of Physics and Astronomy and the Department of Mathematics and Computer Science. ZITI collaborates successfully with research initiatives in Heidelberg. Our new assistant professor, Holger Fröning has established his chair and focuses his research on high-performance computing architectures. The newly established Master of Computer Engineering was successfully started in winter term 2011/2012. The institute founded its 10<sup>th</sup> research group "Unmanned Aerial Vehicles". The research areas of the institute can be summarized as:

1. Advanced Computer Architectures
2. High-Performance Computing
3. Process Control and Dependable Systems
4. Next-Generation Networks
5. Advanced Detector Technology

The research topics indicate a focus on high performance in every aspect of computing. The architecture group deals with the utilization of an increasing degree of parallelism and all the challenges involved there. In the network group, optical networks with terabit communication bandwidth and microsecond latency are addressed. The unique mixture of computer engineers and physicists enables ambitious research programs.

We hope that this report will capture your interest and provide some insight into the structure and the aims of ZITI.

Karl-Heinz Brenner  
*Executive Director*





## INSTITUTE

### Institute of Computer Engineering/Institut für Technische Informatik als zentrale Einrichtung der Universität Heidelberg

#### Introduction

The Institute of Computer Engineering (ZITI) is dedicated to the understanding, implementation and optimization of high-performance systems. ZITI's application-oriented research and development complements the University of Heidelberg's focus on fundamental science research.

ZITI applies the latest research from computer engineering to instrumentation, data acquisition and processing in physics, astronomy, biology, medicine and other natural and life sciences. Furthermore ZITI develops integrated hardware and software solutions for high-performance and application-specific computing.

ZITI is recognized for its excellence in specialized research areas like high-performance interconnects, active optical cables, pixel detectors and scalable memory architectures.

From the beginning, ZITI has integrated cutting-edge technologies to enable our graduate students to meet future challenges in industry and research, as evidenced by our spin-off activities.

In October 2011 a new juniorprofessorship for Computer Engineering has been added to the portfolio of ZITI.

#### Some Key Numbers 2011

Chairs	6
Professors	7
Secretaries	6
Technicians	2
PhD Candidates and Research Assistants	89
Research Groups	10
Projects	27
Funding (spent)	2.208.294 €
Partners	50
Publications	54
Patents	1
Colloquia and Conferences	4

#### Research Groups

With the new founding of the institute, ZITI has established a number of research groups, which enable an exchange between different disciplines and provide young scientist with an opportunity to enhance their scientific skills and pursue their own research goals.

In June 2010, the following research groups were founded by advanced research assistants:

- Advanced Computer Architecture
- Application Specific Computing
- Accelerated Scientific Computing
- High Speed Short Range Interconnects
- New Detectors for Scientific and Medical Applications
- Next Generation Network Interfaces
- Process Control
- Dependable Robotics
- Virtual Patient Analysis

Research groups act independently under the umbrella of ZITI. They can work interdisciplinarily and foster cooperation between chairs. The research groups are led by group speakers. They have a sharing in ZITI resources.

#### Teaching

Apart from various lectures held in the Department of Physics and Astronomy as well as the Department of Mathematics and Computer Science, ZITI mainly provides lectures in three programs: Applied Computer Science (B.Sc.), Computer Engineering (Diploma), and Computer Engineering (M.Sc.).

#### B.Sc. Applied Computer Science

The B.Sc. Applied Computer Science is hosted by the Department of Mathematics and Computer Science and is mainly organized by the Institute of Computer Science. It combines knowledge from Mathematics, Computer Science, Computer Engineering, Physics, and Electrical Engineering. Students must complete 180 CP, usually within 6 semesters. In the program, students can choose a major in Computer Engineering, which includes

- Practical Course Measurement Techniques
- Physical Basics of Computer Engineering
- Signals and Systems
- Digital Circuitry
- Elective module

It is also possible to visit single courses without majoring in Computer Engineering.

#### Diploma Computer Engineering

Due to its history at the University of Mannheim, ZITI is also still involved in teaching activities for the diploma program Computer Engineering in Mannheim. Students already enrolled in the program before the transfer of the Institute to the University of Heidelberg can complete their studies on regular terms until 2012. In 2011, 67 students graduated from the program. In the winter term 2011/12, 28 students were still enrolled in the program.



### M.Sc. Computer Engineering

In 2011, ZITI established the new master's program for Computer Engineering (M.Sc. TI) in winter 2011/12. It is hosted by the Department of Physics and Astronomy. The lectures and application-oriented courses have been designed to educate students in areas of high industrial demand. This program provides a pool of qualified students for ZITI's Ph.D. programs. The nominal duration of the Master in Computer Engineering is 4 semesters.

The M.Sc.TI at Heidelberg University addresses graduates from B.Sc. programs in Computer Science or Natural Sciences with a sufficient minor in Computer Science (>24 CP). According to their personal interest, students can focus on one of the following areas

- Hardware Design,
- Application-Specific Computing,
- Photonic and Optical Signal Processing, or
- Intelligent Autonomous Systems.

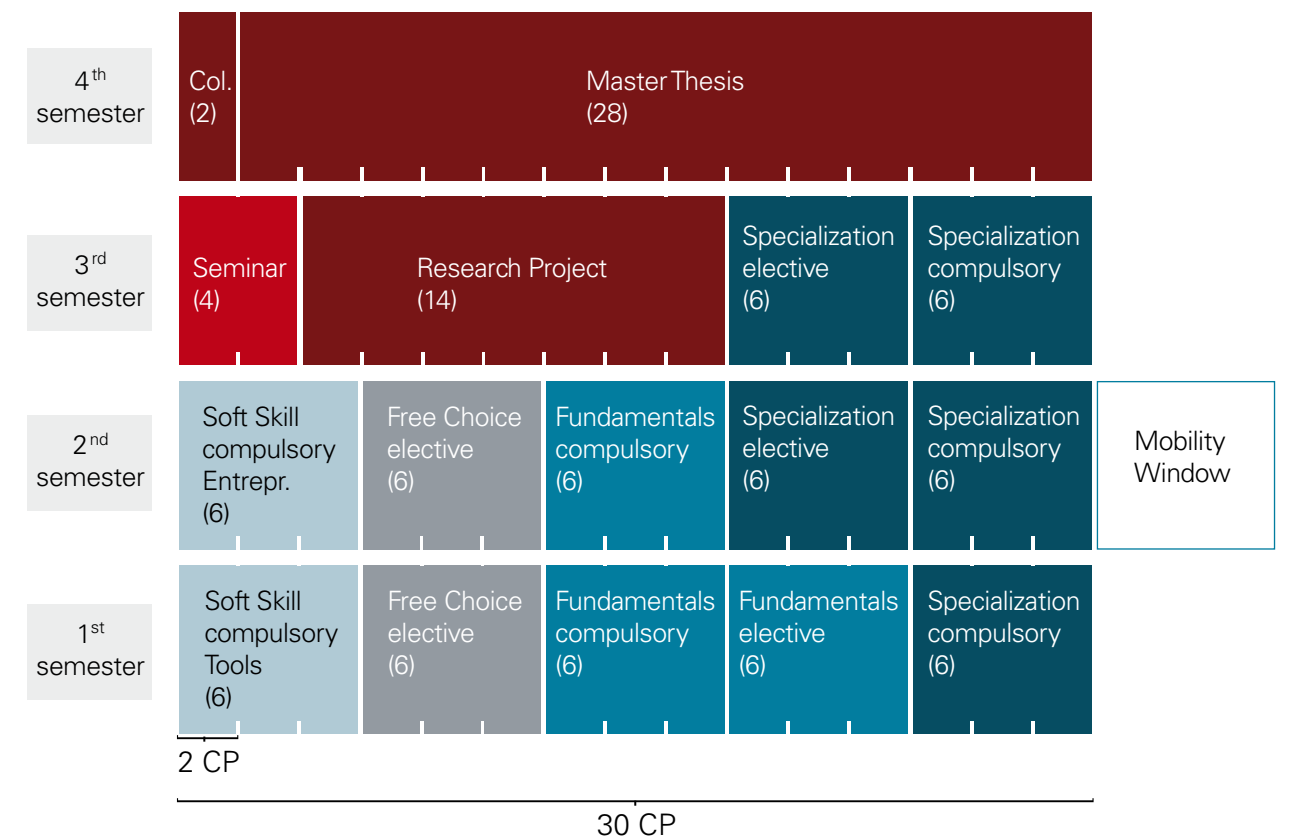
The courses can be classified into four different types, marked in different colors:

- Fundamentals (■, 3 modules),
- Soft skills (■, 2 modules),
- Free courses (■, 2 modules) and
- Specialization (■, 'Major', 5 modules)

In each type, a certain number of modules (or CP) has to be passed. Some modules are compulsory and must be passed, while others are elective modules which can be chosen from various options. Finally, some modules can be chosen freely. Modules in the specialization usually belong to one of four fields of computer engineering (majors). The third semester, also includes

- a seminar ■ (horal presentation of a specialized subject, 4 CP ), and
- a student research project ■ in a research group, which can also be used as a preparation for the master thesis ■ (14 CP).

The master thesis with a final colloquium covers the complete fourth semester.





## CHAIR OF AUTOMATION PROJECT OVERVIEW

Prof. Dr. sc. techn. Essameddin Badreddin

CYCLOBOT ..... 12  
A. Wagner, E. Nordheimer, E. Badreddin

ERGONOMIC HUMAN-FRIENDLY WHEELCHAIR MOTION ..... 14  
K. A. Tahboub, E. Badreddin

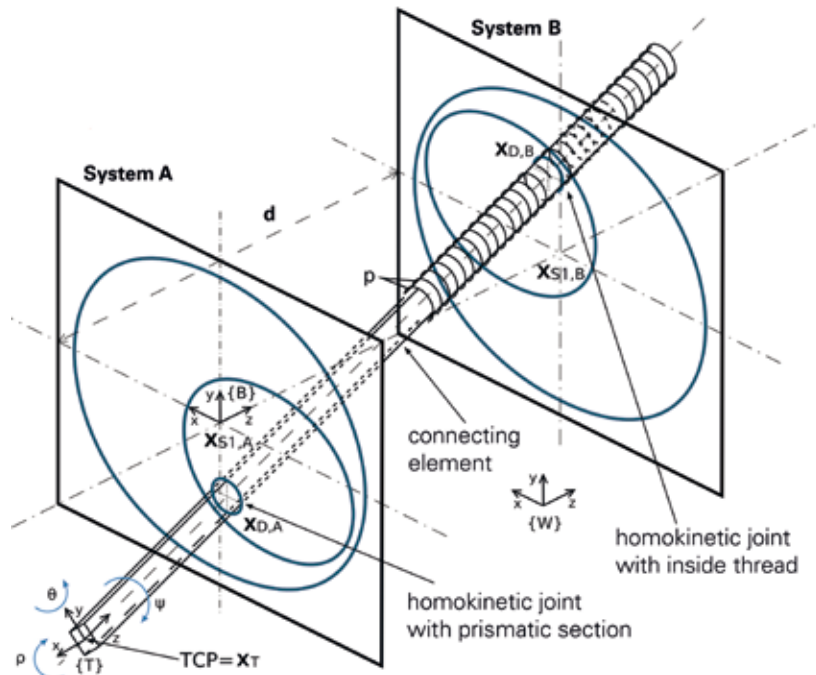


Fig.1: System A and B and the connecting element that is mounted in two homokinetic joints

## CYCLOBOT

A. Wagner, E. Nordheimer, E. Badreddin

The aim of the CYCLOBOT project is to construct and to put a bone-mounted surgical robot into operation for milling of cavities during joint replacement. For this purpose a manipulator with small dimensions yet with a sufficiently large workspace is desirable.

One of the most important criterions for a surgical robotic instrument is the ratio of volume and active workspace, which depends strongly on the chosen kinematic typ. Within the CYCLOBOT project, a novel combination of serial and parallel kinematics, the so-called hybrid kinematics or EPIZAKTOR-kinematics has been proposed [1], which promises an advantageous large workspace while providing small dimensions of the robot itself and good mechanical properties such as number of kinematic elements, weight, and dynamic behaviour.

This novel hybrid kinematics provides six degrees of freedom (6 DOF). It uses two disc systems with 3 DOF each. Each disc system can be described as a virtual nonredundant serial 2-link planar manipula-

tor with a homokinetic joint as a wrist. A connecting element or end-effector is attached to the two disc systems by homokinetic joints (Fig.1).

One of these joints has a prismatic inner geometry so that it provides the rotation of the end-effector around its axis while the other joint is provided with a lead screw to move the connecting element in its axis.

For the first functional prototype (Fig.2) a cascaded kinematics-based control approach for velocity and pose control with singularity avoidance in real-time has been developed. The hybrid kinematics uses rotating movements of the drives (Fig.2, a) only, which are actuated by brushless DC motors (Fig.2, b). The implemented models of the inverse and forward kinematics together with coupling matrices of the disc's dependences allow control of position and orientation of the end-effector in 6 DOF simultaneously.

Each disc system contains kinematics constraints, the so-called singularities in the centre and on the edge of each disc system. An algorithm for singularity avoidance has been developed. It is based on the real-time evaluation of the feasible joint velocities and vicinity to these unreachable singular positions.

### Singularity Avoidance in real-time

The real-time modification of the angular velocities of the robot's discs avoids the singular positions in the centre of the workspace. As soon as the path-errors appear as a result of the singularities, they are compensated through suitable path-corrections by using redundant DOFs near singularities. The algorithm has been validated both in the developed simulation process and in the real-time control system.

Experimental results for different test trajectories have shown that the robot can reach sufficient sta-

tic and dynamic position accuracy according to the requirement of complex task in orthopedic surgery [2]. This makes the device attractive for the milling cavities with round shape into bone. The control system with singularity avoidance in real-time allows also to handle of arbitrary trajectories considering kinematics constraints.

Supported by: DFG-PROINNO II  
Total Support Amount: 500.000 Euro

### References

- [1] Pott PP, Schwarz MLR, Heute S, Weiser P, Wagner A, Badreddin E, "Novel hybrid kinematics with small dimensions and large workspaces make medical robots convenient for orthopaedic surgery". Proc. of the CARS, Berlin, Germany, 2009.
- [2] Wagner A, Nordheimer E, Merscher M, Heute S, Weiser HP, Pott PP, Badreddin E, Schwarz MLR, "Kinematics-Based Position-Control of the 6-DOF Surgical robot EPIZAKTOR". In: CAOS 2011, 2011.

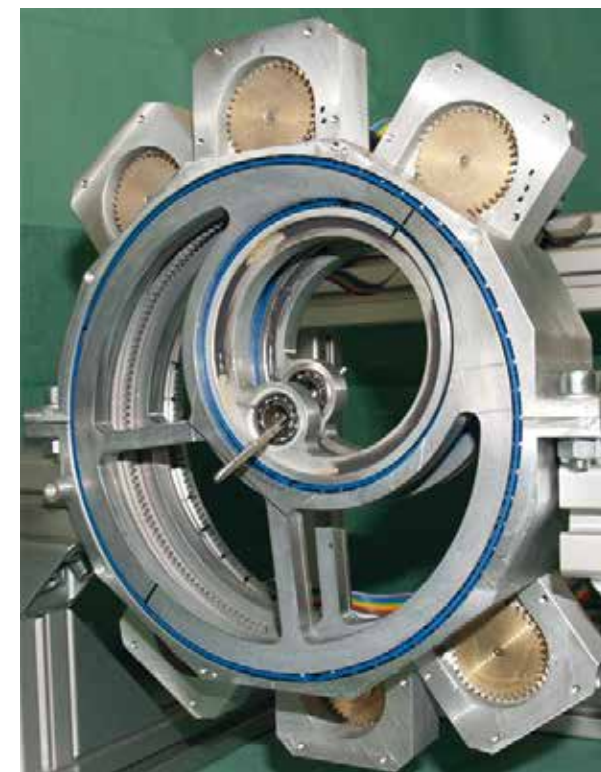


Fig. 2 (a): Epizactor – first functional prototype of the CYCLOBOT (Drives)

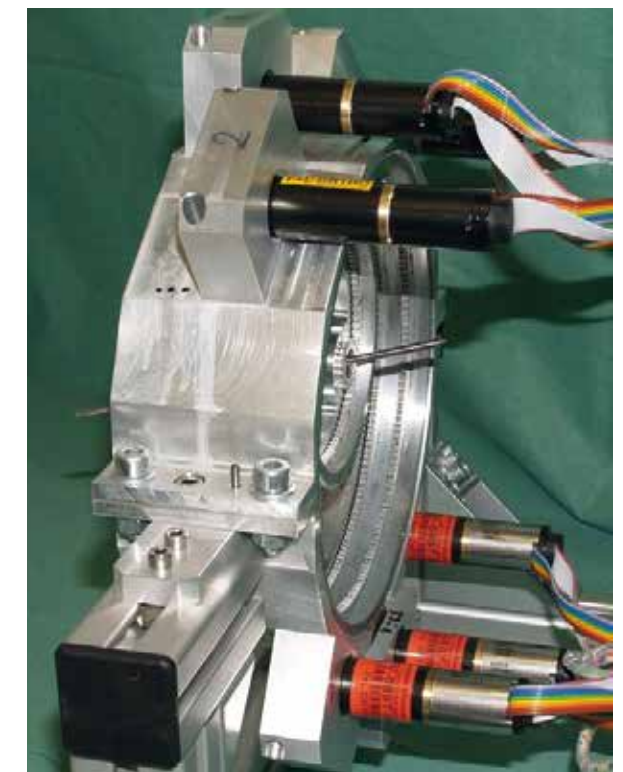


Fig. 2 (b): Epizactor – first functional prototype of the CYCLOBOT (Motors)

## ERGONOMIC HUMAN-FRIENDLY WHEELCHAIR MOTION

K. A. Tahboub, E. Badreddin

The main idea of this project is to minimize the unwanted reaction forces acting on the human as a result of the wheelchair's motion. A biomechanics multi-segment model of a human sitting on a wheelchair has been developed. Literature review on sitting posture exposed to vertical and horizontal vibration indicated that vibration transmissibility becomes critical to human comfort at certain frequencies in the low-frequency range. Thus a notch filter is proposed to be implemented to act on the commanded acceleration (or velocity) signal.

The wheelchair control is based on a model of the human sitting posture when exposed to horizontal seat perturbations. Vibrations to robotic wheelchairs are investigated in order to make suggestions for enhancing user's comfort and safety.

Fig.1 shows the trunk, which is represented as an inverted pendulum. The trunk is inherently unstable causing a major problem for people with spinal cord injuries. Consequently, trunk muscles must maintain upright sitting posture while disturbing forces are generated by seat motion.

In contrast to reflexes the observed muscle activation pattern with its complexity and independence of muscle stretch lead to the suggestion that the responses are centrally generated [1]. Co-activation of antagonist muscles to produce stability by increasing the stiffness of the trunk is recognized. Furthermore, the vestibular system seems to play a minor role compared to proprioception (rotation of pelvis and hip movement) and cutaneous receptors measuring the pressure distribution under buttock and thigh.

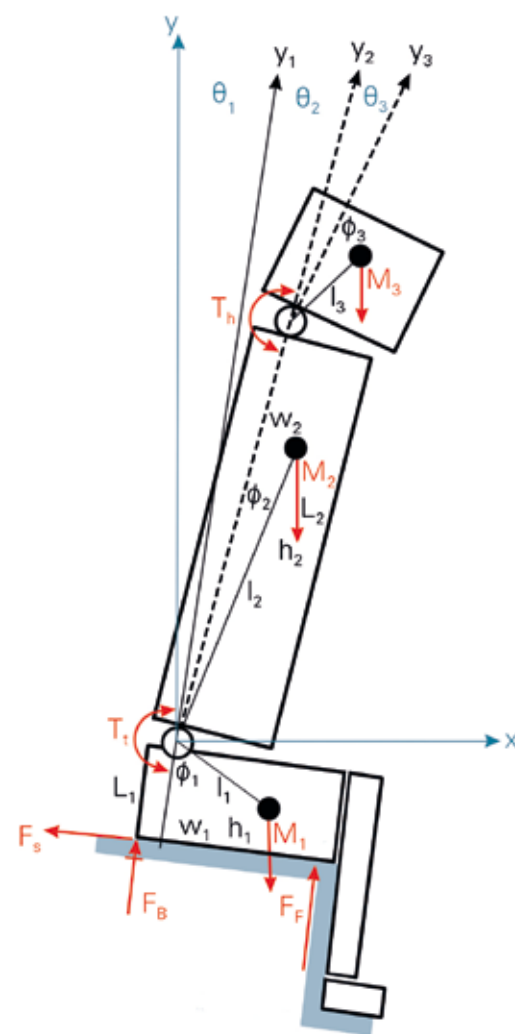


Fig.1: Schematic diagram of a seated human

In contrast to several published inert biomechanics models for human seated posture which consider neither active nor reactive control through the muscles, the biomechanics model proposed in this project (Fig.1) incorporates a simplified active control law composed of an inner stabilizing loop and an

external tracking loop [2]. Simulation results based on this biomechanics model correspond with published experimental results. Transmissibility function of seat vibration to the head, demonstrates a considerable amplification of transmitted vibration at frequencies around the peak frequency of 3Hz. This amplification is felt as discomfort to the wheelchair motion. For improving wheelchair user's acceptance, comfort, and feeling of safety, it is proposed in this work to limit the wheelchair acceleration in the frequency range where transmissibility is high. This implies applying a band-stop filter around the 3-Hz frequency.

The realization of the concept was started by implementing two inertial measurement units (one attached to the wheelchair while the other to the body of the human user) and to connect them to the wheelchair system (Fig. 2).

These units will be used to identify vibration transmissibility and apparent mass functions for different sitting postures. This will enable for the verification of the derived biomechanics model and for choosing the appropriate notch filter frequencies.

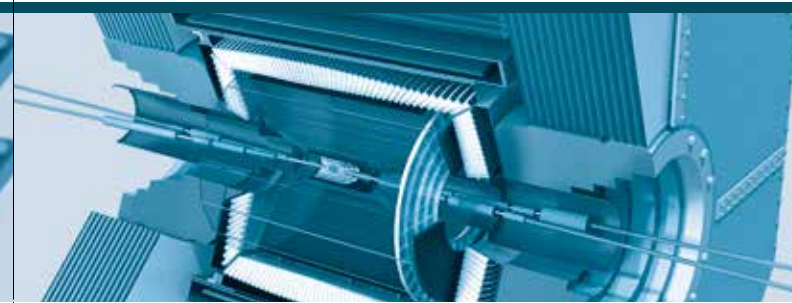
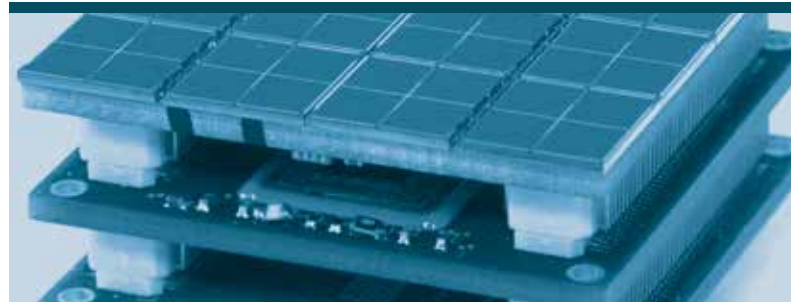
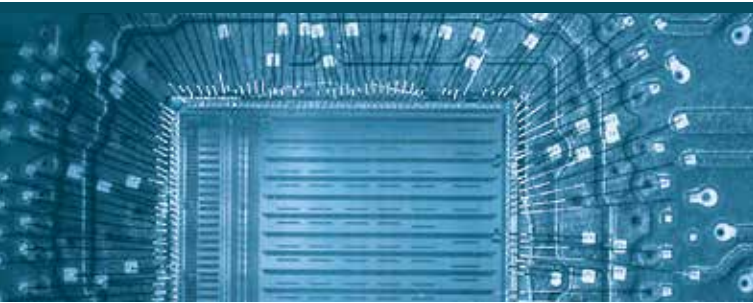


Fig.2: Assistance Wheelchair System based on a conventional electrical-powered wheelchair B600 (OttoBock Healthcare GmbH). The wheel-chair is equipped with a number of additional sensors and a real-time control computer.

### References

[1] Forssberg, F., Hirschfeld, H., "Postural adjustments in sitting humans following external perturbations: muscle activity and kinematics," Experimental Brain Research, Vol. 97, pp. 515–527, 1994.

[2] Tahboub, K. A., Badreddin E., "Human Sitting Posture Exposed to Horizontal Perturbation and Implications to Robotic Wheelchairs," International Conference on Intelligent Robotics and Applications, Aachen–Germany, 2011.



## CHAIR OF CIRCUIT DESIGN PROJECT OVERVIEW

Prof. Dr. Peter Fischer

HIGH PERFORMANCE SIMULTANEOUS PET / MRI IMAGING .....	18
M. Ritzert, I. Sacco, P. Fischer	
PIXEL READOUT ASIC FOR THE DSSC DETECTOR AT XFEL .....	20
F. Erdinger, M. Kirchgessner, J. Soldat, P. Fischer	
THE NOVEL INTERPOLATING SILICON PHOTOMULTIPLIER .....	22
P. Fischer	
THE PIXEL VERTEX DETECTOR OF THE BELLE-II EXPERIMENT .....	24
J. Knopf, C. Kreidl, I. Peric, L. Raffelt, P. Fischer	
THE SPADIC AMPLIFIER / DIGITIZER ASIC FOR THE TRD OF CBM .....	26
T. Armbruster, M. Krieger, I. Peric, P. Fischer	
THE XNAP FAST 2D X-RAY PHOTON DETECTOR .....	28
C. Thil, P. Fischer	

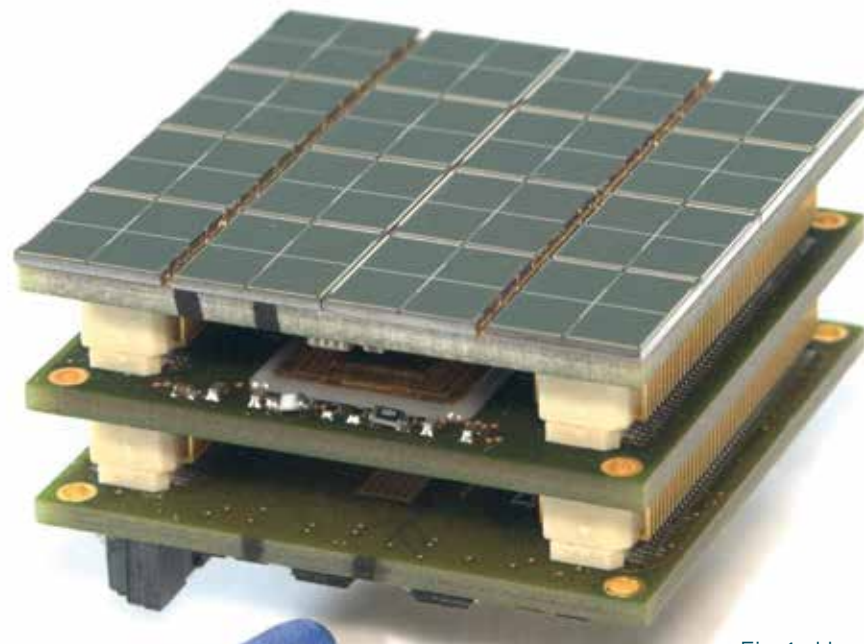


Fig.1: Hyperimage Detector stack with Silicon Photomultipliers, ASICs and Control board. Crystals which convert the Gammas from positron annihilation into optical photons are placed on the top surface of the SiPMs on the uppermost boards.

## HIGH PERFORMANCE SIMULTANEOUS PET/MRI IMAGING

M. Ritzert, I. Sacco, P. Fischer

Medical imaging techniques like CT (Computed Tomography), MRI (Magnetic Resonance Imaging) or PET (Positron Emission Tomography) provide very different types of information, like the tissue density, highly resolved morphological information, or functional information, i.e. the distribution of radioactive tracers in cancer studies. A hot topic in medical imaging research is to combine several such modalities, if possible in a single instrument (as compared to available consecutive image acquisitions).

The EU funded 'Hyperimage' project and its successor, the EU project 'Sublima' are developing simultaneous PET/MRI systems with ultimate performance. In such a simultaneous system, the location of radioactive tracers is determined by the PET system and the association to organs is made by the MRI image. The continuous stream of MRI information will further allow compensating for unavoidable patient motion (breathing, heart beat) during the lengthy PET exposure times of several 10 minutes, with significant improvement in image quality.

The Hyperimage PET system is based on magnetic field insensitive Silicon Photomultipliers (SiPMs) to detect scintillation light from small LYSO crystals, read out by dedicated PETA ASICs which are developed entirely in our group.

Each ASIC channel contains a fast hit detection, an energy ADC and a time measurement with an intrinsic resolution of below 20 ps.

Very compact modules with an active area of  $\sim 3 \times 3$  cm<sup>2</sup> and 64 individual sensor elements have been designed in our group (fig.1).

In order to further improve performance and to possibly increase the number of SiPM channels, a new concept has been prototyped with the ISIS1 chip: The amplifier inputs have very low impedance (few Ohms) for ultimate SiPM speed and a variable input dc potential to correct for variations in the SiPM breakdown voltage. The hit signals generated by fast discriminators in several channels are ORed to one single output line which is processed in an off-chip TDC, for instance implemented in an FPGA. This allows reading out several channels with a single line, thus simplifying module design. The channels ID and the energy information (generated by a charge-to-time converter) are attached to the hit signal and are decoded in the FPGA as well.

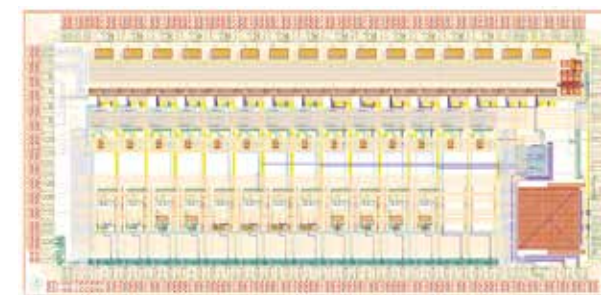


Fig.2: Layout of the ISIS1 test chip

The prototype chip (fig.2) has been successfully tested and used for energy and coincidence time readout of crystals. As an example, fig.3 shows an energy spectrum of a <sup>22</sup>Na source obtained by analyzing the encoded ISIS information in an FPGA. Several circuit parts of the ISIS chip are presently being used for the design a next generation PETA ASIC.

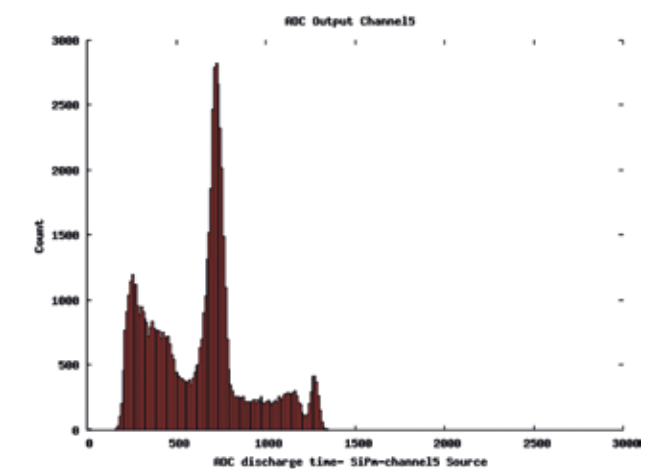


Fig.3: <sup>22</sup>Na energy spectrum taken with SIPM and the ISIS1 chip. The large peak are Gammas with 511 keV.

The Hyperimage Project is supported by EU FP7 under Grant Agreement No. 201651, Sublima under No. 241711. Collaboration is with Philips research, FBK, MSE, Technolution, PDPC, King's College, EPFL and the Universities of Delft, Ghent and Klinikum Aachen.

## PIXEL READOUT ASIC FOR THE DSSC DETECTOR AT XFEL

F. Erdinger, M. Kirchgessner, J. Soldat, P. Fischer

Synchrotron X-ray sources are popular and valuable facilities for material studies and fundamental research. A next big step in intensity and brilliance will be made by the XFEL free electron laser which is being constructed at DESY in Hamburg. In order to exploit the unprecedented possibilities of the machine, the XFEL GmbH is funding the development of advanced 2D detector arrays which can image photons of only a few keV energies with  $\sim 100 \mu\text{m}$  spatial resolution at an image frame rate of up to 4.5 MHz.

One such innovative system will be the  $1024 \times 1024$  pixel DSSC (DEPFET Sensor with Signal Compression) detector which consists of silicon sensors with intrinsic nonlinear amplification bump bonded to large ( $\sim 1.3 \times 1.5 \text{ cm}^2$ ) specialized pixel ASICs with 4096 channels each. Every channel of this chip contains an analogue interface to the sensor, a low noise filtering amplifier, an 8 Bit (single slope) ADC and a local static memory to store the amplitude values during the photon burst of  $\sim 1 \text{ ms}$  duration. The data is then read out in the XFEL cool-down period of 99 ms, before the next burst arrives.

Our group is coordinating the ASIC development, is responsible for the digital local storage & control and, most importantly, for the interconnection and integration of all building blocks to a compact pixel layout of  $204 \times 229 \mu\text{m}^2$  size, as shown in fig. 1.

We are further assembling larger pixel arrays and design local and global circuitry for configuration, control and fast data readout.

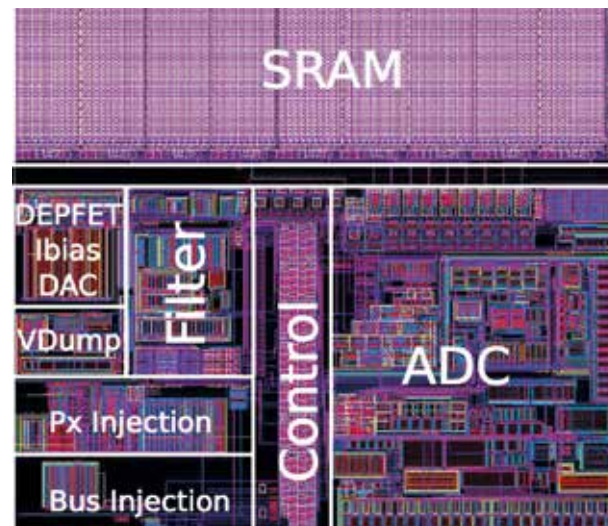


Fig. 1: Layout of one pixel of the DSSC ASIC

After several small prototype chips, matrix chips with  $8 \times 8$  pixels are available. In order to characterize the chips and to operate them with connected and biased DEPFET sensors, a common readout infrastructure has been developed by our group (see fig. 2 and caption).



Fig. 2: Setup for measurements with the DSSC pixel ASIC with DEPFETs: A small piggy back board with the ASIC (center, light green) is connected to a base board which has two ZIF connectors to hold a

DEPFET ceramic board. Bias voltages are provided by a programmable board on the left. Control and readout is performed through an FPGA and a USB interface by a board on the right side.

As an example, fig. 3 shows a measurement of the energy spectrum of an X-ray source, taken with the above setup: The X-rays are absorbed in the DEPFET sensor and the generated electron hole pairs lead to a drain current increase. This current is amplified, filtered and digitized by one pixel of the matrix chip. The data is buffered in the RAM and read out after a while. The spectrum demonstrates that our goals for system noise can be reached.

The setup has also been used to demonstrate the feasibility of power cycling, i.e. of switching off the ASIC in the burst gaps and turning it on again just before the next burst: Measurements show that the chip is ready to take data after only  $\sim 50 \mu\text{s}$ .

The final chip will contain a complex logic to steer the data taking, to produce timing signals, to provide memory addresses/control and to read out the data. This logic has been defined in HDL and has successfully been prototyped on a test chip.

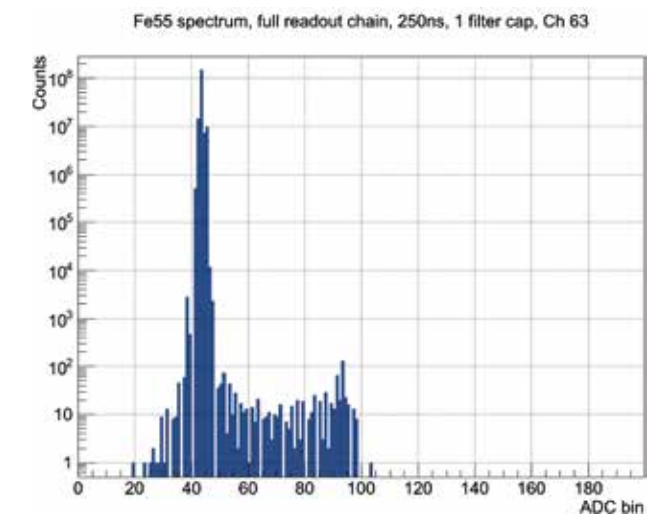


Fig. 3: Amplitude spectrum of a  $^{55}\text{Fe}$  source delivering X-rays of 5.9 keV measured with a linear DEPFET and one pixel of the MM2 matrix chip. The iron signals are located at  $\sim 90$  ADC counts. The large baseline peak allows a determination of system noise. Gaps on the x axis are from missing codes of the pixel ADC used.

Supported by XFEL GmbH. Cooperation with MPI HLL Munich, DESY, Universities Milano, Bergamo & Siegen.

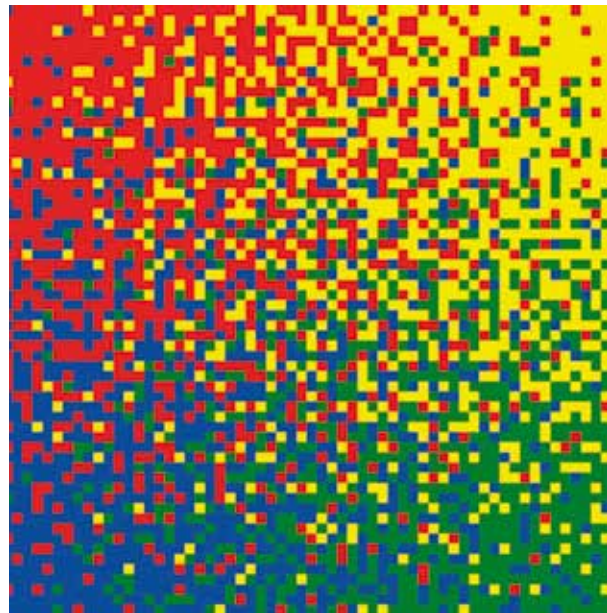


Fig.1: Cell assignment of the ISiPM to the four 'corner' signals.

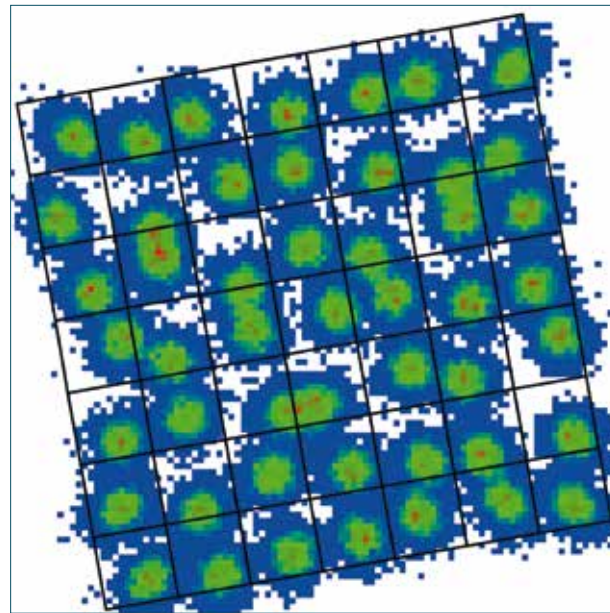


Fig.2: Simulated flood map with 7 × 7 crystals standing on a ISiPM with 100 × 100 cells.

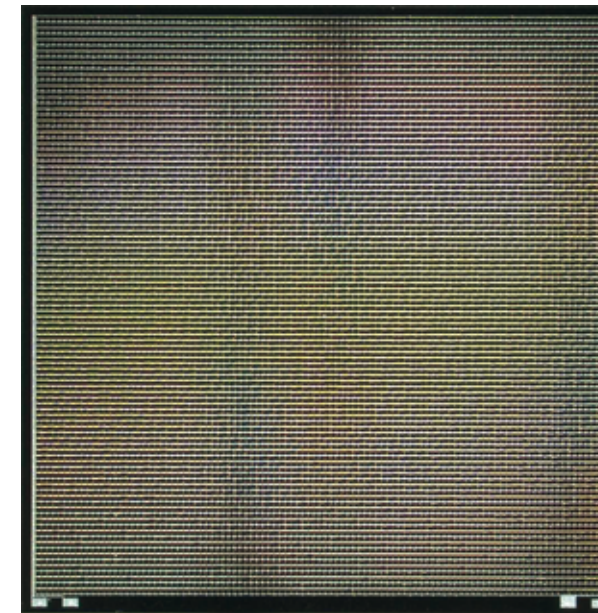


Fig.3: Photograph of the first ISiPM device with 100 × 100 cells.

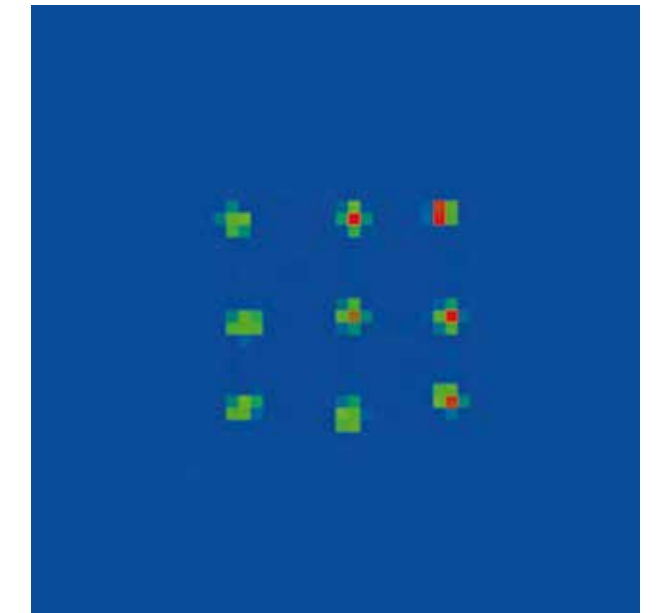


Fig.4: Flood map of 3 × 3 LYSO crystals (see text).

## THE NOVEL INTERPOLATING SILICON PHOTOMULTIPLIER

P. Fischer

Silicon Photomultipliers (SiPMs) are solid state photo detectors which consist of many (1000s) avalanche diodes with separate bias resistors connected in parallel. Their advantages of high gain, amplitude information, compactness and insensitivity to magnetic fields make them more and more popular for photon detection in calorimetry or PET, where light from scintillation crystals is detected. In order to measure the impact point of high energetic gamma particles with high precision, the crystals are often segmented into many small elements (millimetre pitch). The identification of the hit crystal is achieved by delicate light spreading onto larger SiPMs or by many small SiPMs. Both methods have drawbacks like edge effects or the need for many electronics channels.

A novel device, the Interpolating Silicon Photomultiplier (ISiPM) can provide a solution. It provides the spatial position of photon clusters with high resolution on a single device without light sharing. The APD cells of the ISiPM area are not connected to a *common* readout electrode, but each cell is connected to *one of several* (mostly 4) output channels. The most straight forward embodiment is a rectangular device with four outputs located (conceptually) in the corners.

The assignment of each cell to one of the channels (fig.1) is chosen such that the centre of gravity of an arbitrarily shaped group of cells can be reconstructed as (for instance) the weighted sum of the corner signals. Due to the finite size of the

cells, this exact goal can only be approximated and residual systematic errors remain. An algorithm has been developed to produce fractal assignment maps with homogeneous reconstruction properties.

Fig.2 shows the simulation of an array of crystals standing on such a device and being illuminated with X-rays. Most crystals can be clearly identified. The systematic deviations of the reconstructed positions are from binning effects of the cell assignment.

First prototype devices have been fabricated at FBK/Trento/Italy according to our design (fig.3). They have been successfully operated in a simple test setup. When placing an array of 3 × 3 LYSO crystals with 2 mm pitch on the device and illuminating with 511 keV gammas from a <sup>22</sup>Na source, all crystals can be very clearly resolved (fig.4). First tests with smaller pitches are promising.

The device will allow high resolution gamma detection with a small number of channels with possible applications in calorimetry or PET.

*A patent for the device has been filed.*

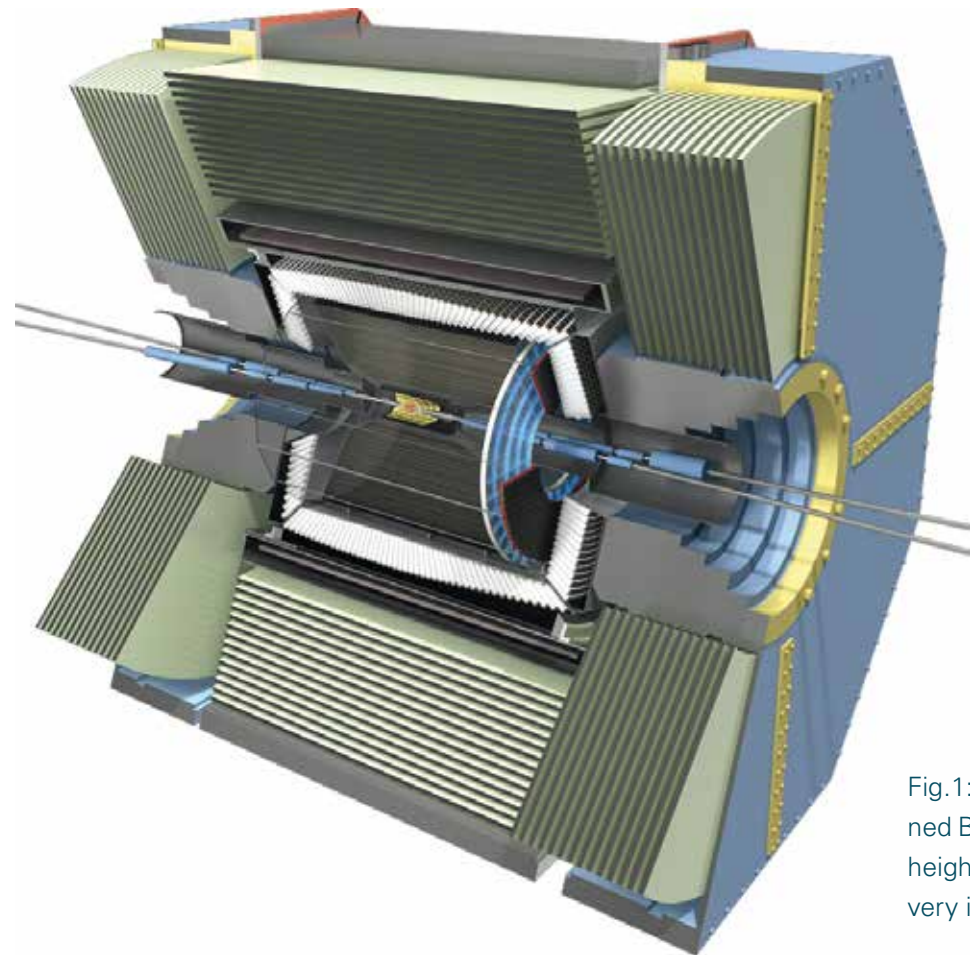


Fig.1: Artists view of the planned Belle-II detector with a total height of ~5 m. The PXD is the very innermost (red) part.

## THE PIXEL VERTEX DETECTOR OF THE BELLE-II EXPERIMENT

J. Knopf, C. Kreidl, I. Peric, L. Raffelt, P. Fischer

The Belle Experiment at the KeK Accelerator Centre in Japan has made significant contributions to B-Meson physics, in particular to parity violation. The topic being still very relevant for understanding the fundamental forces of nature, Japan has decided to upgrade the KeK machine to a much higher luminosity (~x10), in order to produce significantly more collisions for more detailed studies with better statistics. In order to cope with the resulting enormous event and data rates, and to provide state of the art measurements of the collision products, the existing Belle detector will be upgraded within the next ~3 years.

This Belle-II detector (Fig.1) will also contain a novel pixel detector (PXD) in the very central part of the experiment to improve the measurement precision of the particle decay position.

The challenging requirements for the PXD in terms of radiation length (minimal amount of material in the particle flight path), speed, noise and radiation tolerance cannot be satisfied with any available detector technology. The PXD collaboration is therefore developing a novel type of detectors based on amplifying silicon sensors (DEPFETs).

Silicon sensor modules of a size of  $\sim 1.2 \times 10 \text{ cm}^2$  will be arranged in two layers closely around the (vacuum) beam pipe (Fig.2). Each sensor has a thinned active area of only  $75 \mu\text{m}$  thickness and is subdivided into low noise amplifying unit pixel elements of  $\sim 50 \times 50 \mu\text{m}^2$  size. The pixels are connected in a xy-pattern and are read out row-wise at high speed.



Fig. 2: PXD Design. The (gray) active module layers will be placed around the beam pipe (not shown) at radii of 13/22mm.

The ASICs to control the sensor rows and to read out the column current signals are being developed by our group. They use bump bonding for a compact module design (Fig.3). Therefore, interposers to allow for wire bonding had to be designed. After manufacturing at the HLL Munich, chip were bumped and flipped by our group.

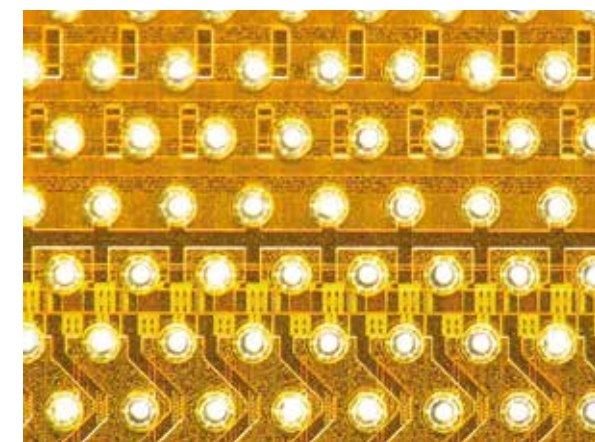


Fig. 3: Bumps on DCD readout ASIC

The successful operation of several modules has been confirmed by test beam measurements by the collaboration.

The interconnection of the sensor matrix and of all ASICs must be achieved on 3 metal layers on the silicon itself. The design of this complicated 'all-silicon' structure is done in our group. In order to prototype this delicate object, an electrical dummy module (no active sensor) has been designed (Fig. 3) with many test features included. It is presently being manufactured at the HLL.



Fig.4: Layout of the electrical dummy module ( $\sim 1.5 \times 15 \text{ cm}$ ). The sensor matrix will be at the bottom right, 6 Switcher chips are located at the top, and 4 DCD readout chips and 4 data handling processor ASICs on the right. A flexible capton cable will be glued and bonded at the right end.

*Supported by bmbf under contact number 05H09VH8. Main partners are MPI Munich, Universities of Bonn, Aachen, Siegen, Valencia, Barcelona, Krakau,...*

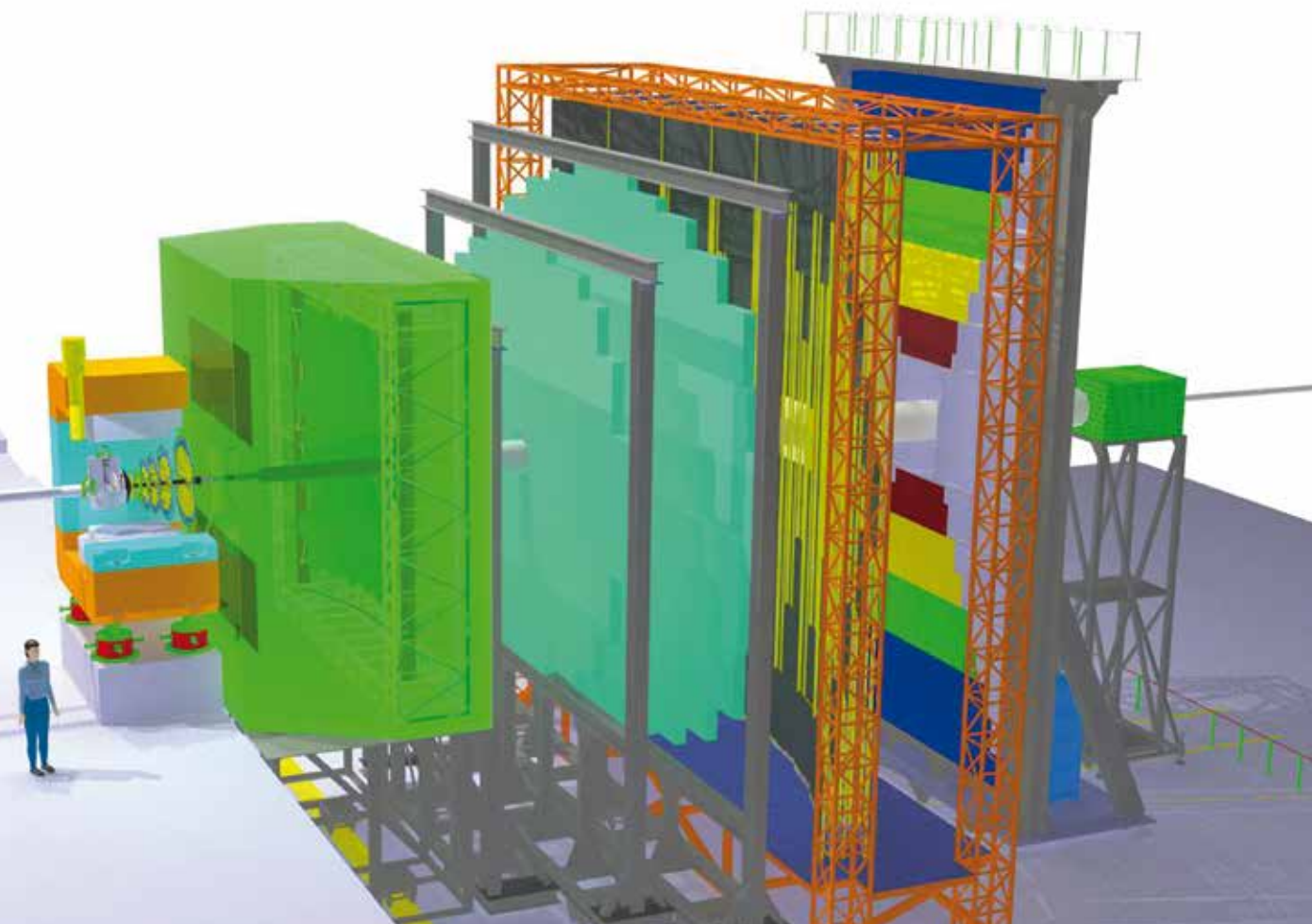


Fig. 1: Planned CBM Experiment at FAIR/GSI. The TRD detectors are the green circular structures in the centre.

## THE SPADIC AMPLIFIER/DIGITIZER ASIC FOR THE TRD OF CBM

T. Armbruster, M. Krieger, I. Peric, P. Fischer

The FAIR facility (Facility for Antiproton and Ion Research) which is being constructed at the GSI in Darmstadt will deliver very intense proton and ion beams to study, among many other physics goals, nuclear matter at very high temperature and density.

The CBM experiment (Compressed Baryonic Matter) will be searching for evidence of the Quark-Gluon-Plasma and will study the phase transitions and the density of state.

The CBM collaboration, composed of about 50 institutes, is developing the fixed target detector sketched in fig.1 to reach the various physics goals. Several different sub-detectors will be used to measure particle tracks and to identify their type, energy and momentum with high precision. One component is a large Transition Radiation Detectors (TRD) which can localize particle tracks and distinguish between different particle types (electrons,

protons). The TRD is composed of a 'radiator' structure where a traversing high energetic particle generates a burst of X-ray photons and a gas filled gap where the X-ray photons are absorbed again. The absorption process generates free electrons which drift to the backside where they are amplified in high electric fields. The generated charge cloud finally induces electrical signals on pad electrodes with a size of some cm<sup>2</sup>.

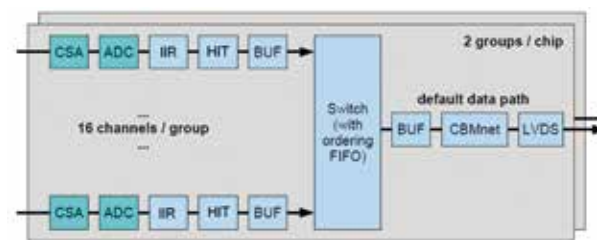


Fig. 2: Block diagram of SPADIC 1.0.

The signals of 100.000-500.000 pad electrodes must then be amplified, digitized and processed with a specialized integrated circuit, the SPADIC (Self Triggered Pulse Amplification and Digitization ASIC[1], fig. 2) which is developed by our group.

A part from a versatile low noise frontend and an 8-9 Bit ADC, each SPADIC channel contains a sophisticated digital logic to process the digitized data: An Infinite Impulse Response (IIR) filter can be used to remove baseline fluctuations and ion tails from the detector. This filter has been studied & optimized in great detail to minimize the hardware effort (number of bits in internal processing and for coefficients). Hits are then automatically detected and a programmable subset of the hit data is cut out of the data stream. Multiple hits and triggers from/to neighbors are possible. The hits are buffered and injected into a serial readout interface while maintaining time ordering. The serial interface is the first ASIC implementation of the CBM-Net protocol developed by the chair of computer architecture for CBM.

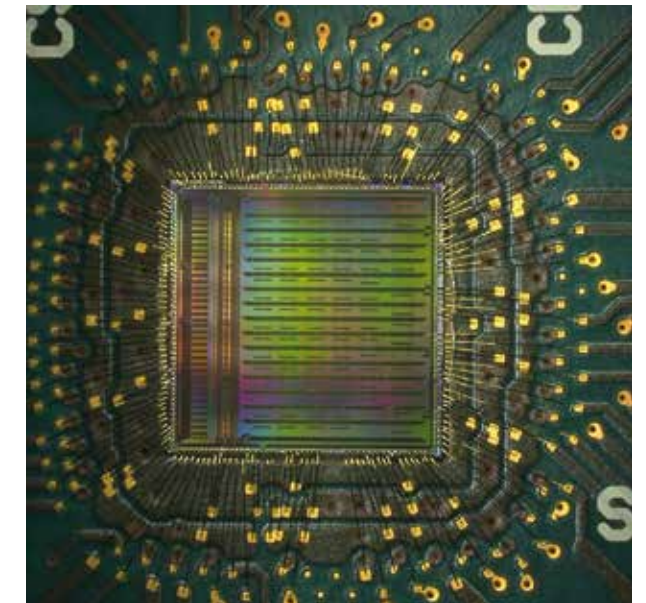


Fig. 3: Photograph of the bonded SPADIC 1.0 ASIC. The analogue parts + ADCs of the 32 channels are on the left side, the major part of the chip is covered by digital logic.

After several prototypes for the analogue blocks and ADC, the first full size chip, SPADIC 1.0, with 32 full channels has been designed and submitted. It contains an improved version of the frontend (two polarities for possible application with other detectors in CBM like the RICH) and a significant amount of digital logic which required a large tooling effort (RAM generators, FIFOs, ...). Initial tests have shown that the chip can be configured and that ADC data can be correctly read out.

*Supported by BMBF (06HD9120I). Cooperation with the CBM Collaboration, mainly GSI and the universities Frankfurt, Münster, Heidelberg.*

### References

[1] <http://spadic.uni-hd.de>

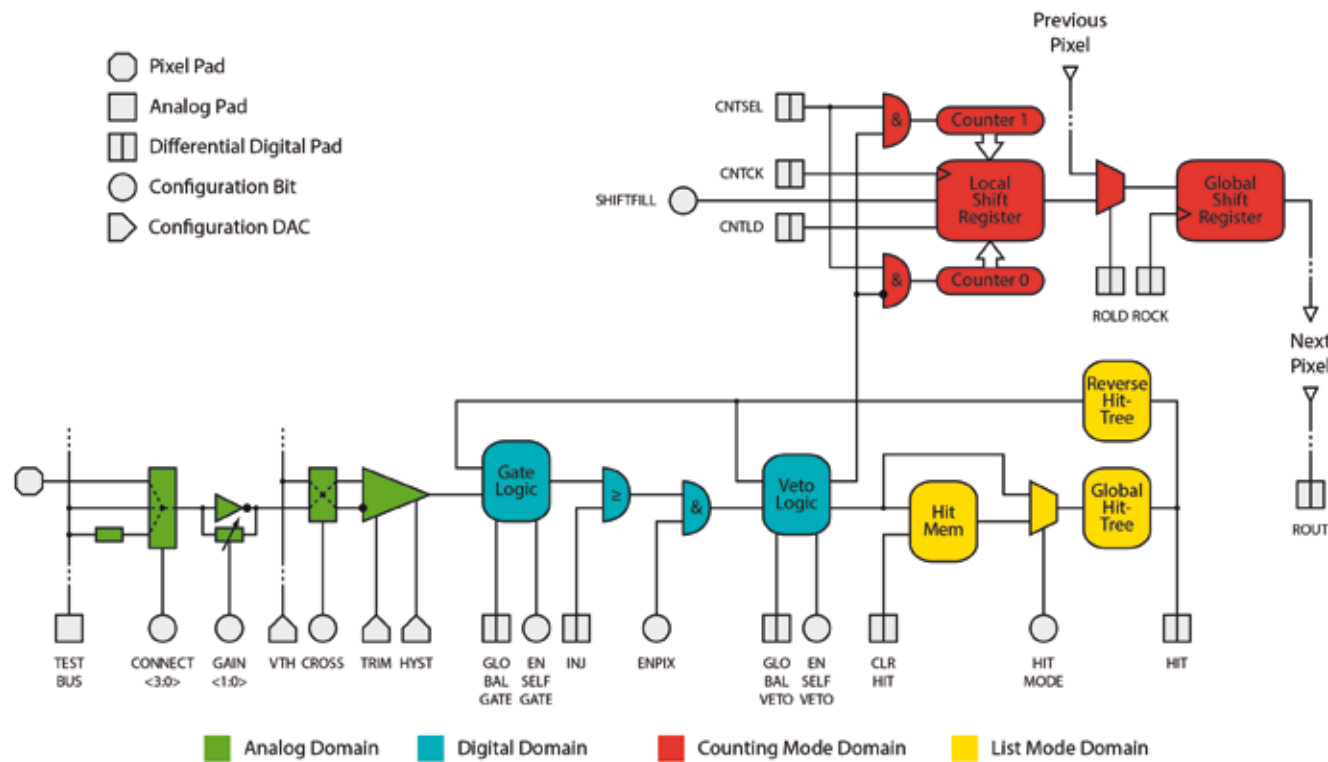


Fig.1: Architecture of the APA chips

## THE XNAP FAST 2D X-RAY PHOTON DETECTOR

C. Thil, P. Fischer

Synchrotron light sources like the European Synchrotron Radiation Facility ESRF in Grenoble use their intense, focussed X-ray photon beams to generate diffraction patterns on crystallized samples or to study the atomic composition by fluorescence techniques. Fluorescence photons can be distinguished from prompt (scattered) photons by the arrival time differences at the detector, which can vary from few nanoseconds to microsecond. At present, such X-ray sensitive photon detectors with nanosecond resolution consist of very few (max. 10) individual pixels only, so that scans over a larger acceptance are very time consuming.

The XNAP project (Xray Nanosecond Array of Pixels) has been initiated by the detector R&D group at the ESRF with the goal to develop an array of  $32 \times 32$  X-ray sensitive pixels with a time resolution in the ns range. The detector is based on thick, fully depleted APDs (provided by an industry partner) and a readout ASIC developed in our group. Each pixel of the chip contains a fast transimpedance input stage with variable polarity to amplify the weak APD signals, a discriminator with programmable threshold to digitize the information and a fast OR tree to flag the hit to an external Time-to-Digital converter on a shared output (lower part in fig.1).

In addition, the number of hits within a certain time window can be counted by fast counters with programmable depth. Two counters allow dead time free operation. A test chip with  $4 \times 4$  pixels has been bump bonded to sensors, the final  $16 \times 16$  pixel ASIC of  $5 \times 5 \text{ mm}^2$  size is ready as well.

The assemblies use two different types of APDs (divided anode and divided cathode). They have been characterized with light pulses, X-rays from radioactive sources, with X-rays from a micro-focus X-ray generator at ESRF and recently with direct synchrotron light from the ESRF ring.

Fig.2 shows the count rate as a function of the detection threshold when illuminating with X-rays from  $^{55}\text{Fe}$  of 5.9 keV. A plateau with close to full detection efficiency is reached before the noise becomes dominant.

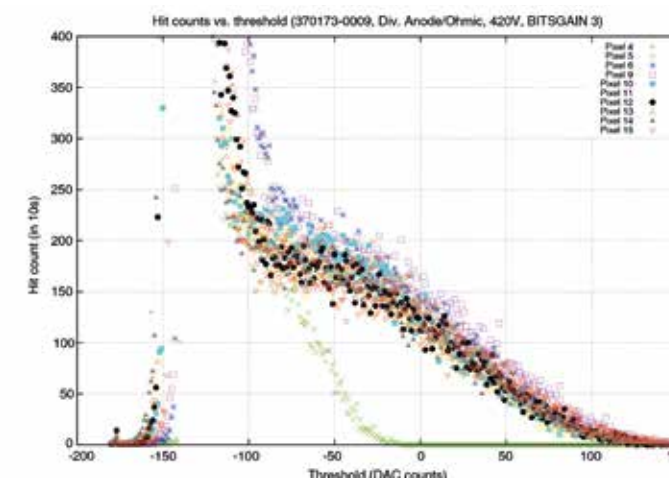


Fig.2: Count rates vs. Threshold for several pixels ( $^{55}\text{Fe}$ ).

Fig. 3 shows the count rate in one pixel for increasing illumination. The chip saturates at  $\sim 100 \text{ Mcps}$ , which is consistent with a paralyzable dead time of  $\sim 4 \text{ ns}$  for Poisson distributed hits and which is an order of magnitude better than traditional electronics.

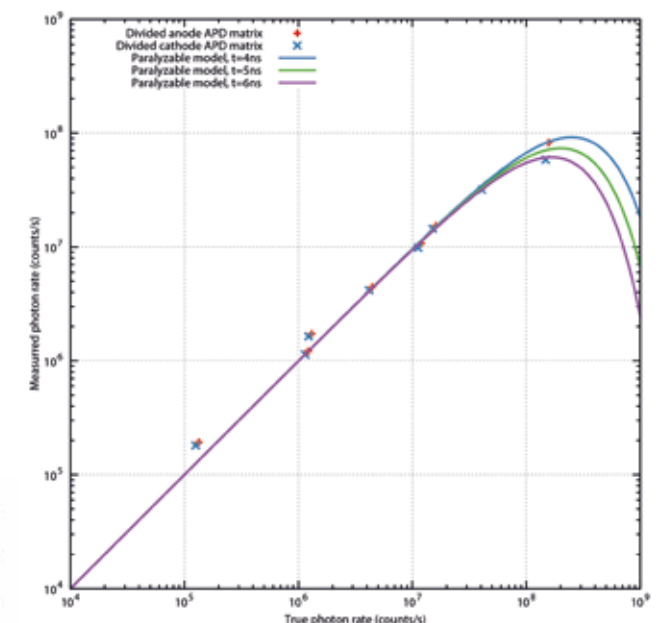
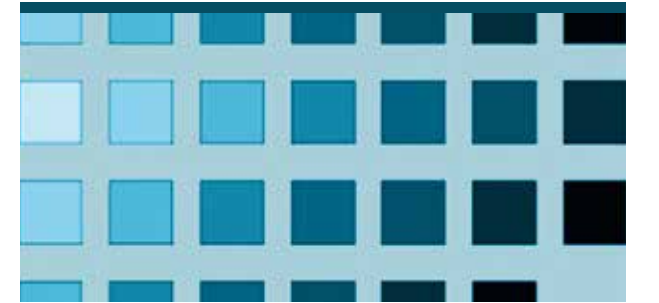
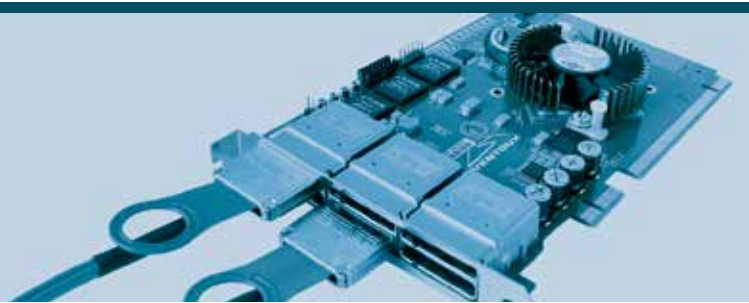


Fig.3: Count rate in APA1.1 vs. incident particle rate

These and further results have led to a choice of preferred sensor. The fully system should be ready by the end of 2012.

Supported by ESRF and DESY. Cooperation with ESRF (P. Fajardo), DESY (H. Graafsma), Excellitas, Sping-8 (A. Baron).



## CHAIR OF COMPUTER ARCHITECTURE PROJECT OVERVIEW

Prof. Dr. Ulrich Brüning

CHAIR OF COMPUTER ARCHITECTURE .....	32
Prof. U. Brüning and team	
CADENCE .....	36
Kapferer, U. Brüning	
HIGH FREQUENCY TRADING ACCELERATION USING FPGAS .....	38
C. Leber, B. Geib	
SIMULATING FUTURE MEMORY INTERFACES .....	40
H. Litz, N. Burkhardt, M. Watson, U. Brüning	
THE CBMNET V2.0 IMPLEMENTATION AND NETWORK STRUCTURE DESIGN WITHIN THE CBM PROJECT AT FAIR .....	42
F. Lemke, S. Schenk, U. Brüning	

## CHAIR OF COMPUTER ARCHITECTURE

### Prof. U. Brüning and team

The ZITI Chair of Computer Architecture at the University of Heidelberg has the expertise to design complex hardware/software systems. As system architects we cover not only the operation principles but include the technology and the software to build real working prototypes. The Computer Architecture Group (CAG) holds a profound expert knowledge in the area of design space analysis, hardware design of processors and devices, interconnection networks, and software driver development, especially for the construction of large computing clusters based on PC technology.

All levels of system design are covered, starting at the application programming interface, e.g. the message passing interface library (MPI), through the efficient design of device drivers finishing at custom build hardware devices based on standard cell ASIC and FPGAs.

Goals of the applied research activities are to cover a broad range of methodologies for the design of complete high performance systems with the possibility to optimize every level and educate students on the various real world topics.

The group mainly focuses on the design of parallel architectures, which achieve their high performance by improving communication between computational devices/units. Scaling such systems is a great challenge to the architecture of the interconnection networks (IN) and the network interface controllers (NIC). Special attention is paid on the interface between software and hardware to setup communication instructions.

Beside a number of interesting industrial projects, the chair focuses its internal research on the question of latency reduction in various application areas. Interconnects and interconnect switches on the network side and host interfaces and device control at the host side suffer significantly on designs which are not optimized for latency reduction or latency hiding. The EXTOLL project is an examples where a holistic optimization approach leads to a very low latency and high performance network interface controller (NIC), which was operational in 2009 and has been demonstrated at the ISC10 in Hamburg and at the largest supercomputer conference and exhibition SC10 in New Orleans (US).

In 2011 a spin-off company EXTOLL GmbH was founded in order to leverage the research results of the EXTOLL research project and try to raise venture capital to manufacture a high performance ASIC. A licensing agreement between EXTOLL GmbH and the University of Heidelberg was signed. Since then cooperative effort has been made to promote the EXTOLL interconnect solution. There have been two exhibitions which are of high importance for the HPC community and EXTOLL/CAG has been jointly presented the results at the ISC 11 in Hamburg and at the SC11 in Seattle, USA. Due to the continuing support of the Federal Ministry of Economics and Technology (BMWi) in the EXIST program through 2011 we have been able to improve the business plan and approached venture capital companies to finance the ASIC production. We have entered the BW business plan contest and have won the first price in the category of start-ups.



Fig.1: EXTOLL/CAG booth at the SC2011 in Seattle

The EXTOLL NIC in FPGA technology is comparable to fast industrial ASIC designs from the perspective of latency. To improve the IN also on bandwidth we developed in cooperation with Samtec and the HyperTransport Consortium a high density board edge connector (HDI6) for up to 10Gbit/s per lane providing 12 bidirectional lanes with a total bandwidth of 240Gbit/s. The development of a prototype was supported by the BMBF [2].

The EXTOLL interconnect technology has been selected as interconnect for a large research prototype with the Juelich Supercomputing Center (JSC) as the main contractor. A project proposal has been

written in a European consortium and was granted in 2011 by the EU. Due to some delay in the IP negotiations the DEEP project [3] started with a delay of 5 month in December 2011. It is one out of three large FP7 framework programs. The CAG will work on the adaptation and optimization of the EXTOLL interconnect to the new Intel processor KNC (many integrated cores MIC).

Due to our presentations at the SC10 we could acquire another industrial partner for the application of EXTOLL. KLA-Tencor is supplying the wafer scanner technology to most of the wafer fabs today. They have to solve the problem of massive increase in bandwidth and server processing capacity in the near future and EXTOLL would be a well fitting technology. A project with a grant of 100k USD for a first prototype test using Xilinx V7 FPGAs has been executed.

In 2007, the HyperTransport Center of Excellence was founded together with AMD and since then it is operated by the Computer Architecture Group. HyperTransport (HT) is the processor interface of AMD CPUs and can be used to interconnect CPUs in a coherent and non-coherent way. The CAG developed their own HT cores and could utilize this technology in some projects with AMD and other industrial partners to build HT-based devices. In February 2011 we hold the Second Symposium for HyperTransport™ Technology in combination with the International Workshop on HyperTransport Research and Applications (WHTRA) with international participation.

Because of the difficult economic situation of AMD in 2011 sponsoring was significantly reduced and the CAG continued the HT work for internal use.

The server manufacturer AIC approached the CAG in order to set up a common cluster project with their HTX capable servers. The HTX FPGA board "Ventoux" was adapted and tested and a first 9 node system with EXTOLL interconnect was presented at the SC11. This connection to AIC provided a perfect way to produce our FPGA board Ventoux at the Taiwanese manufacturing plant of AIC for a reasonable price, which could not be achieved in Germany.

A new industrial partner has been found for low latency interconnect applications, where a new project with about 145 k Euro was started in 2011 and a "High frequency trading" (HFT) application was developed for this company.

A 10GEthernet interface was added to our basic HT based host interface. Specific functional units for the support of trading have been successfully implemented.

In the area of memory interconnects, the CAG has been in contact for some time with Micron and this led to a Research Grant of 30k USD to evaluate new interconnect structures for non-volatile storage based on PCM.

For the CBM project a new 3 year project proposal has been prepared and submitted to the BMBF. The grant is expected in 2012.

In order to design and develop such complex hardware components the CAG runs some internal developments in the area of EDA tools for closing specific design gaps. This is mainly done for productivity reasons and for raising the level of abstraction in the design phase.

The FSMDesigner4 for design of finite state machines has been improved to the next release 5. The development of the tool has been continued as an open source project on Source Forge.

Furthermore, tools and scripts have been developed simplifying automatic generation of parametrized HW-structures, like a Register File generator, on-chip Crossbars, FIFOs, etc. In addition to the RF-HDL code, SW drivers are generated automatically to test the RF in PCIe and HT devices. For most of the projects, a common methodology for mapping hardware to FPGAs and ASICs with the same source code is used.

The CAG of the University of Heidelberg is member of the Cadence Academic Network and plays a major role in this network, as we are the "Lead University for Functional Verification". The Cadence Academic Network is a university/industry collaboration to support and improve Universities activities in the design of analog and digital semiconductors and to educate students with the latest tool generation. For the verification of complex hardware the CAG has invested in the verification methodology based on UVM. In close cooperation with the University of Bristol (Prof. Kerstin Eder) the course material from the Bristol verification course has been extended and used for a new master degree course for hardware verification.

We have continued our close collaborations with the research group of Prof. Jose Duato from the Universidad Politécnic de Valencia, where a new Prof. Frederico Silla joined the cooperation. The Memscale implementation has its roots in his group. With Prof. Rehm from the Technical University of Chemnitz we have done work in the area of non-blocking collective operations. In the area of chip design the CAG is working with Prof. Stefan Heinen from the RWTH Aachen.

A new collaboration with ST Microelectronics could be established for the test of optical components for high speed serial communication. First information exchange has been proceeded and results are expected in a longer time frame.

#### References

- [1] Zuwendungsbescheid vom 18.08.2010 der PTJ: EXIST-Forschungstransfer: EXTOLL – Innovative skalierbare Hochleistungs-Rechnersysteme, Förderkennzeichen: 03EFT5BW24.
- [2] BMBF Development of AOC prototype, 03VWP0002
- [3] FP7 DEEP Research Grant, RI-287530

## CADENCE ACADEMIC NETWORK

S. Kapferer, U. Brüning



The Cadence Academic Network [1] was founded in 2007 by Cadence Design Systems, a global vendor of EDA software. The goal of the initiative is to establish a network among European universities together with Cadence in order to share knowledge and expertise in the field of analog and digital design. As one of three founding member universities the University of Heidelberg, in particular the Chair of Computer Architecture, took on its role as lead university in the field of advanced SoC (System-on-Chip) verification.

Since then the network has grown considerably and currently consists of 11 lead institutions covering eight methodologies ranging from Advanced Verification, Analog-Mixed Signal, and Digital Design to PCB Co-Design, thus incorporating the whole range of design and implementation of microelectronic circuits. Although lots of universities are based in Germany there are several other lead institutions in the EMEA region, e.g. in Sweden, England or Italy. Furthermore the network includes more than 20 contributor universities and research institutes from all over Europe. The ability to access leading-edge methodologies from industry allows the integration of teaching material into lectures that benefit students with a state-of-the-art education as well as industry because their future employees are already equipped with practical skills acquired in their studies.

Since 2008 the Cadence Academic Network is also visible at the annual CDNLive! EMEA conference. A special academic track at the conference allows uni-

versities to present their academic work or curricula to academic peers and attendees from industry. The program committee and program chairs are selected from the lead institutions and review all submissions entered for the academic track. The track itself is fully integrated into the conference and the accepted submissions are visible to all visitors in the conference guide. Interest in the academic track has also grown considerably in the last years, reaching its peak at this year's conference with 147 individuals attending a session in the track (a 50% increase since 2010), out of these 76 were coming from industry.

Over the last years researchers from the Computer Architecture Group held several invited talks detailing research projects at the group and education at the University of Heidelberg. Other talks at the conference promoted open source EDA tools (FSM Designer) and verification environments (e.g. for the HyperTransport ecosystem) that were developed internally and are free to use for other universities. With the beginning of 2011, the Cadence Academic Network started to provide its technical information and a discussion forum via the LinkedIn network. It offers advanced possibilities to receive tailored information and also a platform for discussions with fellow researchers as well as Cadence employees. The "Cadence Academic Network" group [2] acts as the main portal, whereas several subgroups such as "Advanced Verification Methodology" provide a platform for special interests in a particular technical field. The groups are moderated by the lead institutions of the academic network, ensuring a constant flow of information and discussions. The lead institutions usually review the available material to provide a short summary together with a recommendation for other users.

The main LinkedIn group is already followed by more than 360 members, not only from European academia but from institutions and companies all over the world.

The Cadence Academic Network also was the source for a successful collaboration of the Computer Architecture Group with another network member, RWTH Aachen University, for a joint project to combine our expertise in digital design and verification with Aachen's knowledge in analog design at small technology nodes. This collaboration is still going on and led to the development of a fractional PLL for a TSMC 65nm GP process.

*Cadence and the Cadence logo are registered trademarks of Cadence Design Systems, Inc.*

### References

- [1] [http://www.cadence.com/support/Pages/academic\\_network.aspx](http://www.cadence.com/support/Pages/academic_network.aspx)  
 [2] <http://www.linkedin.com/groups?gid=2839375>

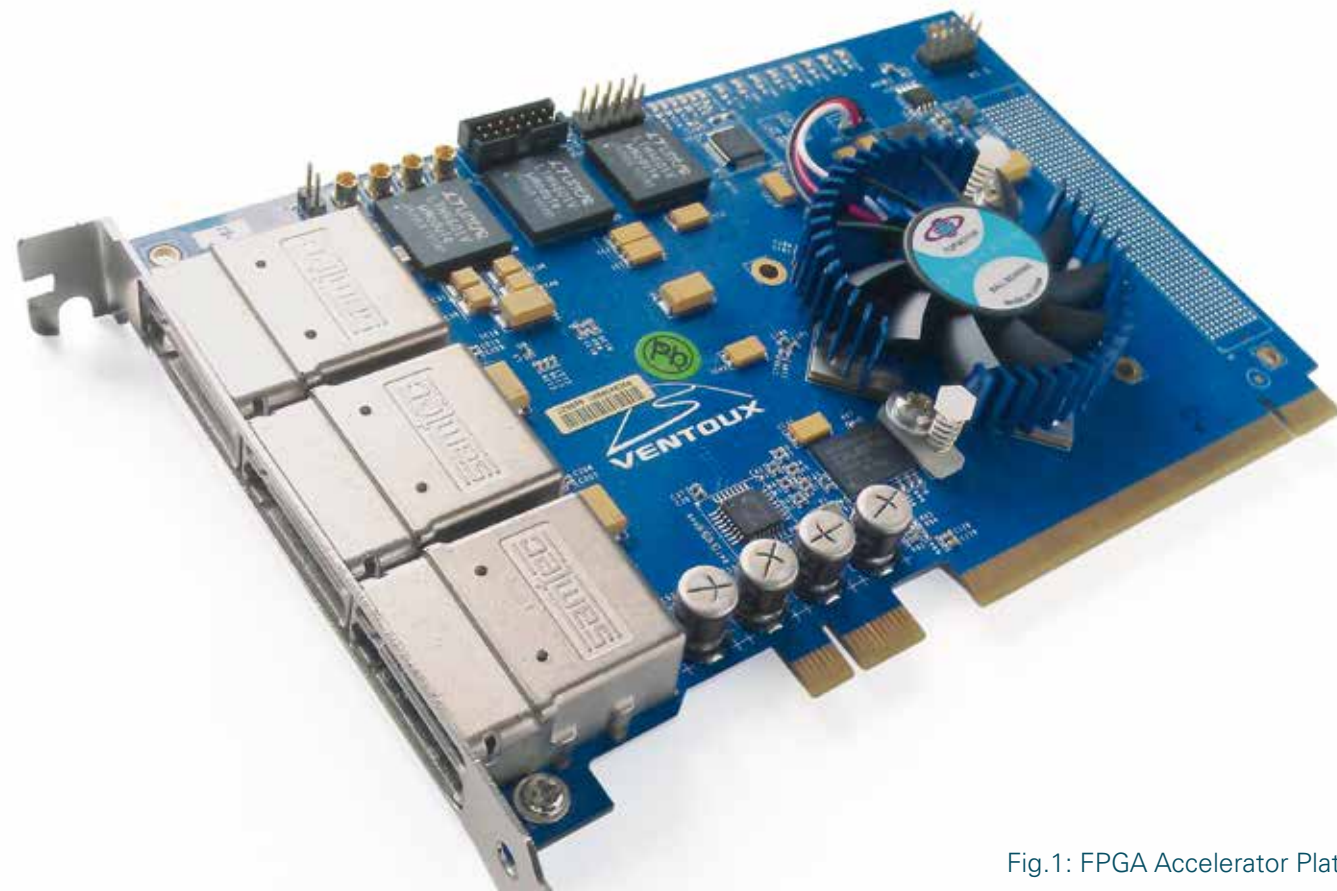


Fig.1: FPGA Accelerator Platform

## HIGH FREQUENCY TRADING ACCELERATION USING FPGAS

C. Leber, B. Geib

High Frequency Trading (HFT) has received a lot of attention over the past years and has become an increasingly important element of financial markets. The term HFT describes a set of techniques within electronic trading of stocks and derivatives, where a large number of orders are injected into the market at sub-millisecond round-trip execution times. High frequency traders utilize a number of different strategies, including liquidity-providing strategies, statistical arbitrage strategies and liquidity detection strategies. All strategies have in common that they

require absolute lowest round-trip latencies as only the fastest HFT firm will be able to benefit from an existing opportunity.

Electronic trading of stocks is conducted by sending orders in electronic form to a stock exchange. In common systems the so-called market feeds which provide real time information about stock prices are received via usual network interface. Feed handlers transmit the data using UDP and TCP/IP encapsulated in Ethernet packets. The feed itself is transmit-

ted using the FAST protocol. In 2010 the Computer Architecture Group of the University of Heidelberg has developed a Field Programmable Gate Array (FPGA) based Accelerator for receiving, decoding and interpreting such market feeds [1]. As a platform for the trading engine, our in-house developed HTX board is used, which is shown in 1.

This project was continued in 2011 with the goal to optimize the pipeline structure and the Ethernet MAC to reduce the latency much further.

An open source 10GEthernet MAC was selected as base for the optimization. The latency of this MAC has been reduced by more than 30% by using sophisticated techniques for CRC checking and pipeline stage reduction.

This optimized trading accelerator has been tested in a new developed SW/HW Co-Testing environment. By using this verification environment many bugs could be removed from the trading software. After successful verification first tests at the stock exchange has been executed.

The result of this research project is a significant acceleration of the complete trading process. This allows the sponsoring company to perform more trades successfully, which benefits the complete financial environment as the company can thereby provide liquidity to the market.

*Supported by: HFT Trading Company (Industrial Research Grant 145.000 EUR)*

### References

[1] Christian Leber, Benjamin Geib, Heiner Litz: "High Frequency Trading Acceleration using FPGAs"; FPL 2011, September 5-7, 2011, Chania, Greece.

## SIMULATING FUTURE MEMORY INTERFACES

H. Litz, N. Burkhardt, M. Watson, U. Brüning

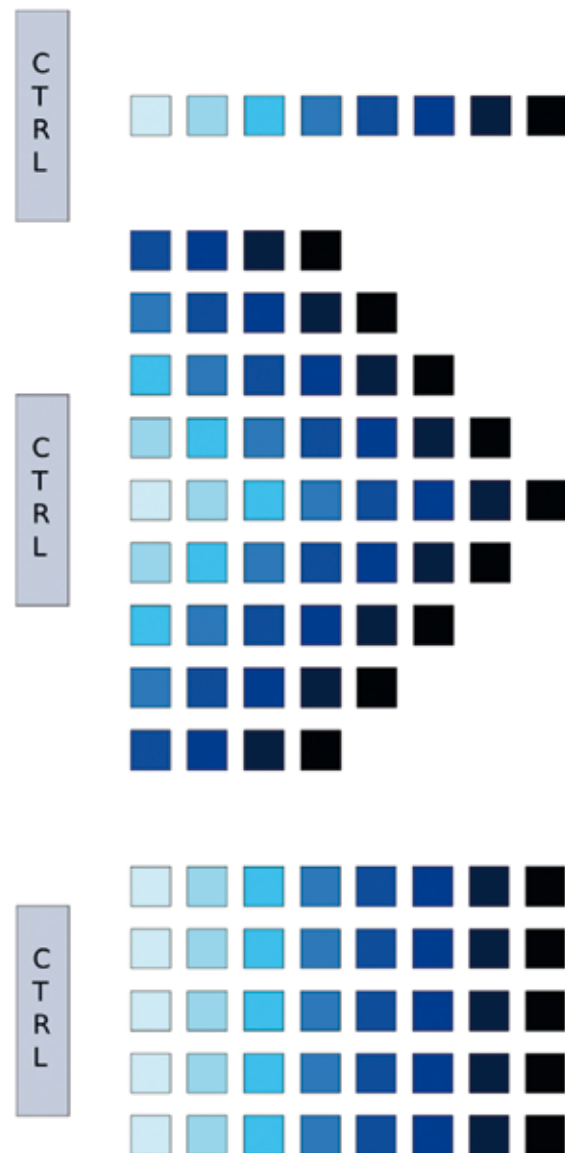


Fig.1: Visualizing the number of network hops needed to reach memory nodes with chain, grid, and multi-chain topologies. Darker nodes require more hops to reach than lighter nodes

Single-threaded processor performance has not continued to scale. Multi-core and Many-core architectures are the norm. As more processing cores are added, the degree of parallelism increases. This increase in processing parallelism requires a corresponding increase in memory access parallelism in order to avoid starving the computing resources. One way to increase parallelism is by adding multiple memory interfaces to the processor package. This is prohibitively expensive for all but the highest-margin products, because modern DDR DRAM interfaces are wide and relatively high power.

The objective of this work is to explore the design space for a high-speed, narrow memory interface. The interface must be as power-efficient as possible, and provide improved performance that can be scaled into the future. In order to provide sufficient memory capacity, the devices must be able to form a network.

Figure 1 shows how the latency is affected by connecting multiple memory devices into a chain, a grid with one connection to the memory controller, or a mesh, with multiple chains of memory devices connected to a single controller.

The chain topologies requires two connections per memory node, while the grid topology requires four connections.

A packet-based network allows the interface to scale smoothly with the interface width, with error detection and correction provided by cyclic redundancy codes (CRC).

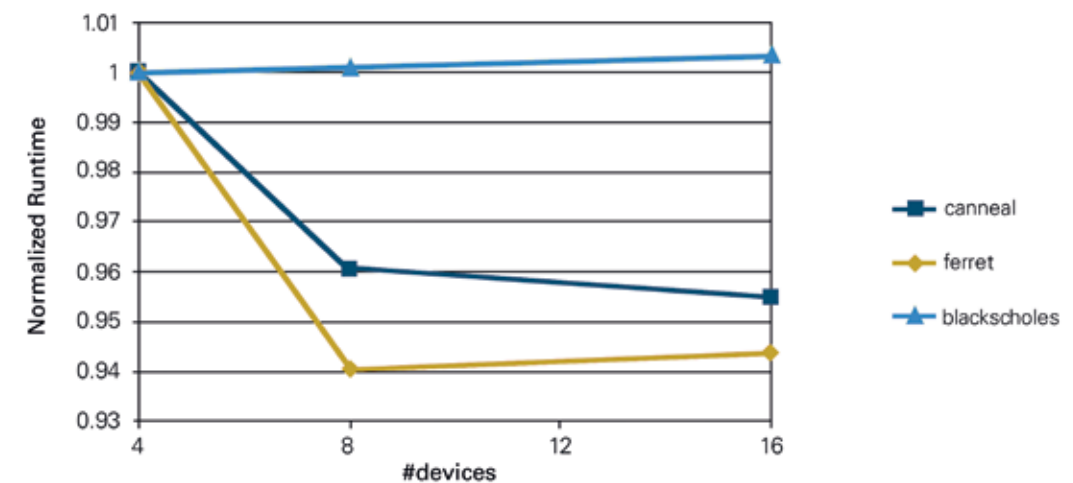


Fig. 2: Normalized runtimes for three benchmarks from the PARSEC benchmark suite

Gem5, a full-system simulator which is widely used in academic research, is employed to estimate the performance impact of the architecture on the system. A new memory model, built on the existing DRAM model connects to the default DEC alpha system. Benchmarks from the PARSEC benchmark suite are used to measure the effects of design decisions.

Figure 2 illustrates the effects of increasing the number of memory devices for three of the PARSEC benchmarks. The effect depends on the amount of parallelism in the benchmark. Two of the applications show some performance increase as more devices are added, while the third shows a performance decrease, corresponding to the increased average latency experienced by the program. As the parallelism of workloads continues to

increase with the number of processing cores, the number of workloads which benefit from additional memory resources will also increase.

Cooperation: Micron Technology Mostafa Abdulla

## THE CBMNET V2.0 IMPLEMENTATION AND NETWORK STRUCTURE DESIGN WITHIN THE CBM PROJECT AT FAIR

F. Lemke, S. Schenk, U. Brüning

The Compressed Baryonic Matter (CBM) experiment at the Facility for Antiproton and Ion Research (FAIR) at GSI Darmstadt needs an optimized Data Acquisition (DAQ) system. The Computer Architecture Group's (CAG) activities within the CBM Collaboration focus on designs and implementations concerning the DAQ network system.

The CBMnet V1, the first protocol implementation, was intensively tested within the CBM DAQ system showing excellent results [1]. Due to new requirements, the CBMnet V2.0 has been designed and implemented. The most important new features are link-based retransmission, perfectly fitting into the new flow control scheme, and a support for unbalanced communication delivering more lanes supporting higher bandwidth in FLES direction than for FEE control towards the detector region.

In addition, developments have been done to support new SPARTAN 6 FPGAs. This guarantees the usability for new planned ROC versions. Hardware has been assembled and tested to build-up larger test beam read-outs at the beginning of 2012 using up to five DCBs. One of them is used as control system and four DCBs, which are

connected to ABBs, support up to  $4 \times 4 = 16$  ROCs running in parallel supporting different kinds and amounts of FEBs. The implementation of the CBMnet V2.0 that is used as final version for the CBM DAQ network led to the development of a generic module block, which can be used for different FEE ASICs. The generic module structure with CBMnet V2.0 as built-in block for FEE ASICs is shown in Figure 1.

This generic module has already been integrated into a first FEE ASIC chip. Additionally to CBMnet V2.0 it delivers a register file with control modules for user defined and global control and configuration of the ASIC, I2C modules for test and bring up, and automatic link bring-up and configuration support.

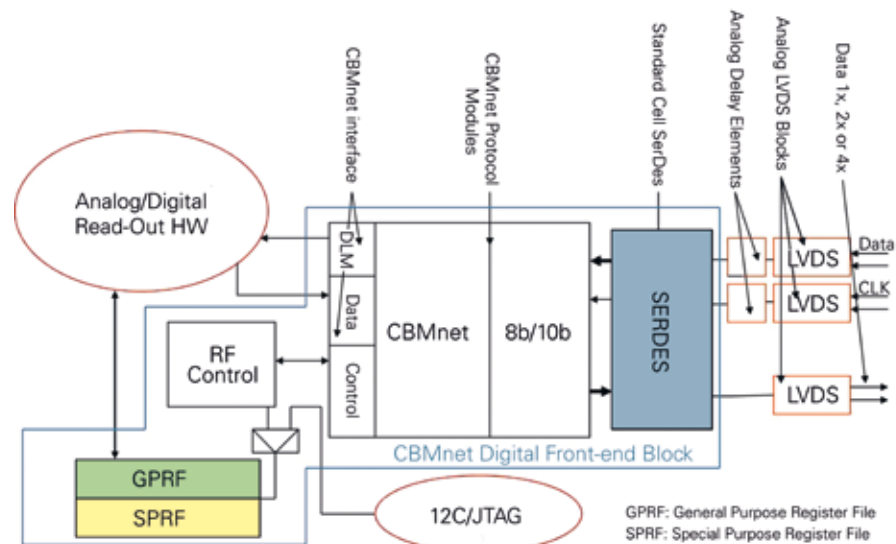


Fig. 1: Generic CBMnet Module Structure

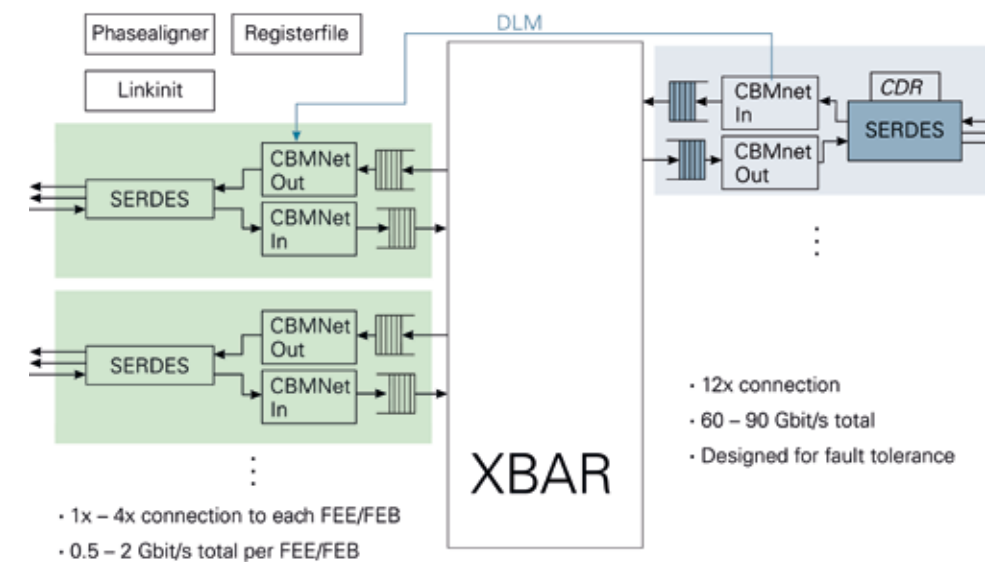


Fig. 2: HUB ASIC Structure

The Silicon Tracking System (STS) poses the most demanding requirements for bandwidth and density of all CBM detectors.

A total of 17000 ASICs, producing 300 - 500GB/sec data, must be read-out in the very confined space available for electronics, calling for a much denser and more radiation tolerant solution than the FPGA based ROCs currently used in early prototyping setups. The proposed DAQ chain is based on a HUB ASIC, responsible for data aggregation, synchronization and rate conversion. An overview of the planned HUB ASIC structure is presented in Figure 2. It mediates between the front-end ASICs, which can be connected with 1, 2 or 4 LVDS lanes operated at 500 Mbps, and the optical links operated with at least 5 Gbps. The number of links per HUB is yet to be optimized to meet the density and total cost targets. A plausible value is four 5 Gbps links per HUB, which would allow to support 10 to 40 FEE ASICs per HUB. To achieve the required density for the electrical to optical conversion the usage of active optical cables (AOC) technology with 12 lanes seems to be the most promising solution. This allows using COTS components at this stage.

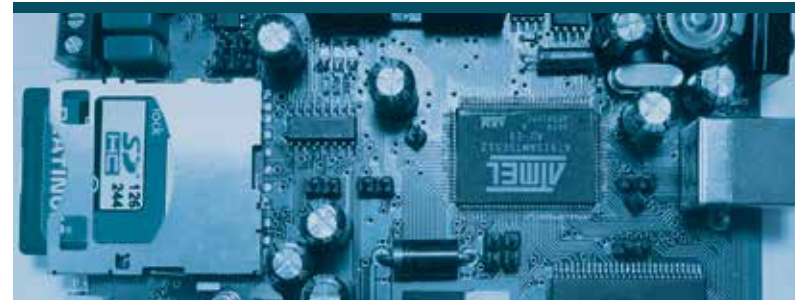
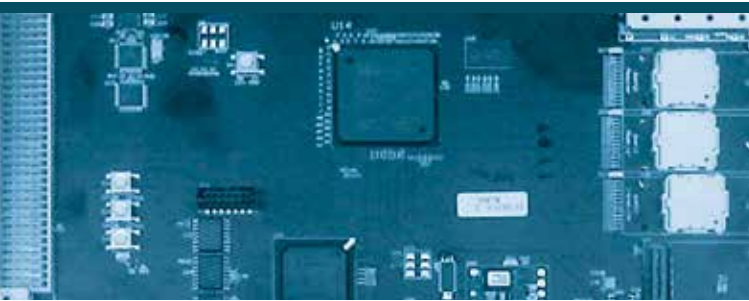
Analysis and research concerning the AOCs [2] has been done, but further analysis for the opto-converter board is required.

For the next year first prototyping steps and radiation tests for AOCs are planned.

Supported by: BMBF (06HD91171), Cooperation with GSI

### References

- [1] Lemke F., Schenk S., Brüning U., "Experiences and results using the CBMnet protocol including precise time synchronization and clock distribution," Deutsche Physikalische Gesellschaft EV (DPG11), Frühjahrstagung, Muenster, Germany, March 21-25, 2011.
- [2] Wohlfeld D., Lemke F., Froening H., Schenk S., Brüning U., "High Density Active Optical Cable: from a Concept to a Prototype," SPIE Photonics West, Optoelectronic Interconnects and Component Integration XI, San Francisco, California, January 22-27, 2011.



## CHAIR OF COMPUTER SCIENCE V PROJECT OVERVIEW

Prof. Dr. Reinhard Männer

DAQ AND READOUT SUBSYSTEMS FOR ATLAS .....	46
M. Kretz, A. Kugel, R. Männer, N. Schroer	
DEVICE MECHANISM: STRUCTURED DEVICE DRIVER DEVELOPMENT .....	48
R. S. F. Silva, G. Marcus, R. Männer	
HARDWARE-/SOFTWAREPROJECT: EMBEDDED SYSTEMS .....	50
A. Wurz	
MICROSIM – A MEDICAL TRAINING SIMULATOR FOR MICROSURGICAL TASKS .....	52
N. Hüsken, O. Schuppe, E. Sismanidis, R. Männer	
NEUROSIM – THE PROTOTYPE OF A NEUROSURGICAL TRAINING SIMULATOR .....	54
F. Beier, E. Sismanidis, R. Männer	
ONLINE PROCESSING OF CELL IMAGES USING AN OPENCL TO FPGA COMPILER .....	56
M. Gipp, G. Marcus, R. Männer	
XFEL DSSC DAQ – A READOUT SYSTEM FOR THE DSSC DETECTOR OF THE EUROPEAN XFEL .....	58
T. Gerlach, A. Kugel, R. Männer	

## DAQ AND READOUT SUBSYSTEMS FOR ATLAS

M. Kretz, A. Kugel, R. Männer, N. Schroer

Detector readout and data-acquisition for the ATLAS experiment at the LHC at CERN is a continuous activity of the group since many years. In 2011 the prototype of the new back-of-crate (BOC [1], see) card has been produced, which connects to a new part – the inner B-layer (IBL) – of the ATLAS pixel detector, to be installed in 2014 [2].

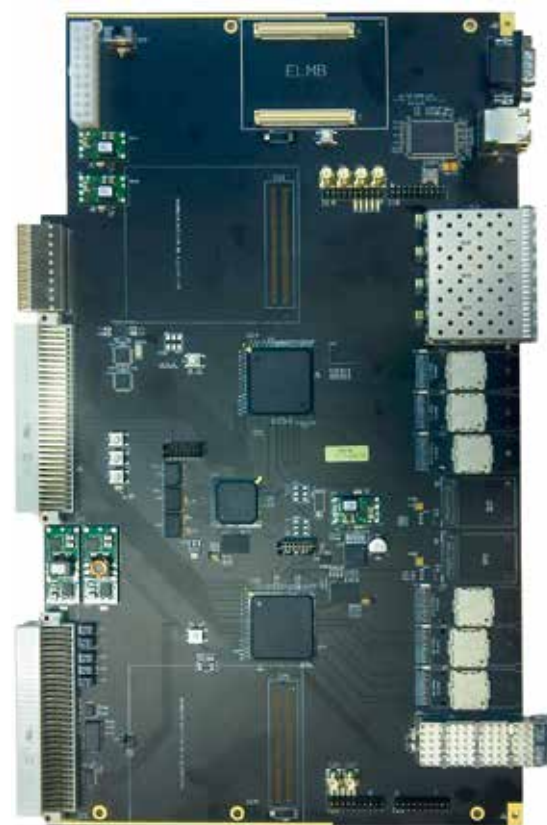


Fig.1: Prototype BOC

Testing was performed in close cooperation with the groups at Bologna, Göttingen and Wuppertal. All important functional blocks could be tested suc-

cessfully. The guidelines for the re-design were finalized.

A demonstrator [3] of the firmware elements was developed and tested prior to the BOC production on evaluation hardware and subsequently ported to the BOC hardware.

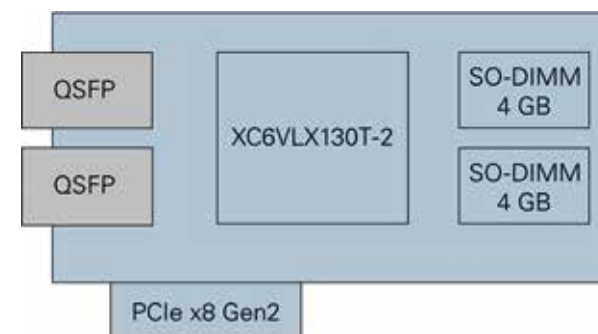


Fig.2: ROBIN-NP

For the TDAQ area a new development project was launched aiming at a successor of the current ROBIN data-acquisition card. A high-level design of the new ROBIN-NP (Fig.2) was prepared and presented to the community.

The new design differs in two main properties from the current design:

- No local processor
- Matching input-output bandwidths

The current ROBIN software and firmware was modified to create an initial functional prototype for the new design.

In view of the beginning LHC upgrade programme new DAQ and detector readout architectures are being evaluated, based upon three flavours of hardware infrastructure:

- VME or direct successor (the status quo)
- ATCA (a younger industry standard)
- PC-farms (used at higher levels already)

Based upon the experience with the current DAQ system, a PC-based detector readout architecture was proposed in late 2011 which minimizes the amount of custom hardware used in detector readout. Similar to the ROS system a set of custom PC-peripheral cards provide custom I/O and processing functionality to a PC-farm which deals with the high data-rate from the detectors. Farm interconnects can be added via a high-performance commodity network, if required. The peripheral cards also provide data to a fast trigger system and the ROS. An initial sketch of this architecture is shown in Fig.3.

*Supported by: BMBF (05H09VHA), Cooperations: CERN, Wuppertal University, NIKHEF (NL), RHUL (UK), INFN Bologna (I)*

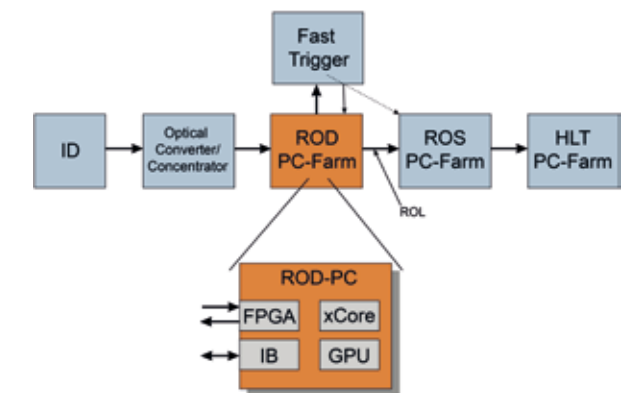


Fig.3: PC-based Readout

### References

- [1] N. Schroer et al., The ATLAS IBL BOC prototype, Proceedings of Topical Workshop on Electronics for Particle Physics Conference 2011, Vienna, Austria, 26–30 Sep 2011, <http://cdsweb.cern.ch/record/1394273/files/ATL-INDET-PROC-2011-029.pdf>
- [2] A. Polini et al., Design of the ATLAS IBL Readout System, Proceeding of 2nd International Conference on Technology and Instrumentation in Particle Physics, Chicago, IL, USA, 9–14 Jun 2011, <http://cdsweb.cern.ch/record/1393406/files/ATL-INDET-PROC-2011-028.pdf>
- [3] J. Ancu et al., The ATLAS IBL BOC Demonstrator, Proceedings of 2011 IEEE Nuclear Science Symposium and Medical Imaging Conference, Valencia, Spain, 23–29 Oct 2011, <https://cdsweb.cern.ch/record/1401224/files/ATL-INDET-PROC-2011-038.pdf>

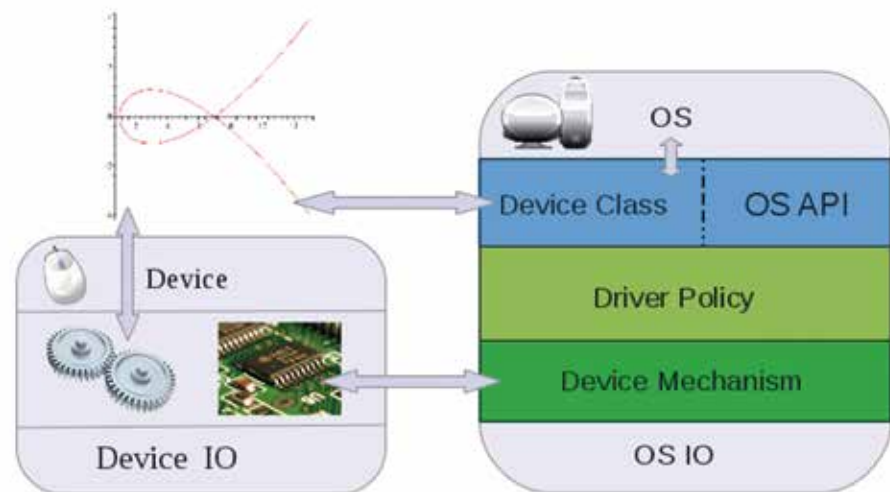


Fig.1: System functionality integration through device and driver

## DEVICE MECHANISM: STRUCTURED DEVICE DRIVER DEVELOPMENT

R. S. F. Silva, G. Marcus, R. Männer

Device drivers are error-prone especially because the development methods of hardware and software are independent. Interaction between software and hardware is informally specified, and interface testing is rarely designed.

This situation is stressed when a device is intended to be hosted by a computer where drivers account for up to 70% of operating system failures. In an operating system, the device driver has not only to comply with the device interface but also with a possible device class interface, and the kernel specific API. The major problem lies in the flexibility of these interfaces. The operating system interfaces are non-standard or not fully specified, and the device has its custom interface.

Furthermore, the steady rise of new devices requires fast development of device drivers. Thus, drivers are re-used creating so called monolithic drivers. These approaches imply that the upcoming devices have to maintain the old device interface to some extent. Less certain, however, is the compli-

ance of the new devices with the non-explicit device interface constraints that the driver expects. Finally, registers used for device control cannot be natively represented by programming languages. Hence, up to 30% of driver code deals with error-prone bit operations.

We have therefore proposed a new separation of concerns in the device driver development process by modeling policy and mechanism separately. A device mechanism is a unique interface that exposes the generic functionality implemented by the device exposing a consistent software interface. The policy uses the mechanism to implement the features required by the operating system, effectively matching both interfaces. The device mechanism together with its proposed systematic composition enhances code reuse by coherently defining a device interface which can be used throughout platforms.

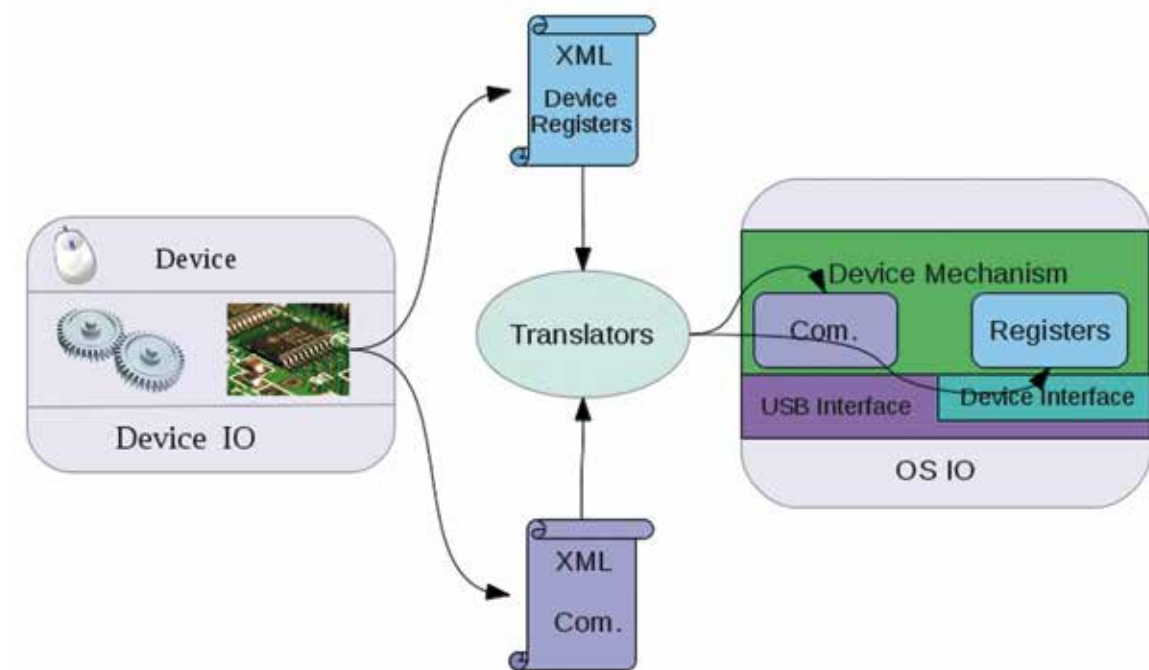


Fig. 2: Systematic composition workflow

The systematic composition provides the hardware semantic missing in program languages, i.e. named registers are provided for access instead of register addresses and bit operations. The actual mapping between the semantics and the physical layer is done using an XML file conformant with the IP-XACT standard. This also provides the capability of linking the hardware and software design teams to share the register map definitions. Besides, we define an XML Schema for the description of USB communication which completes a device's access by providing a description of the communication layer. Furthermore, we extended the IP-XACT description and our underlying framework to support programmed IO through which register accesses can be bound to USB packets.

The explicit described access information allows the access to be engineered in a standard way instead of arbitrarily defining disconnected parameters and access functions. This enhances the cohesion of these elements. Hence, a malfunction

of an element implies necessarily that it has been wrongly described narrowing the search for the fault. Furthermore, elements, its subelements and properties can be checked for correctness in their context.

As a case study, we define the device mechanism for an existent webcam driver also reusing it for a user space driver. The result is a clearer and more complete code which enabled us to find two implementation bugs. Moreover, register accesses are augmented with permission controls and access rules without adversely affecting the performance of the driver.

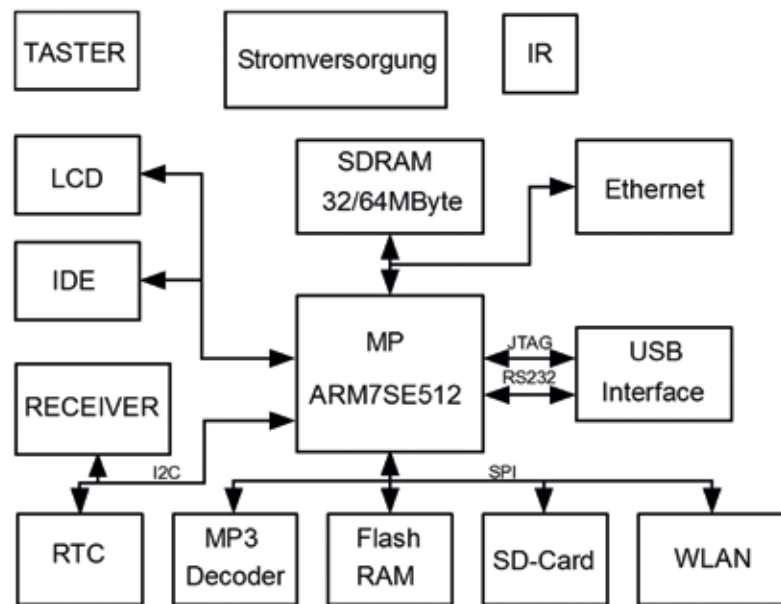


Fig.1: Circuit diagram

## HARDWARE-/SOFTWAREPROJECT: EMBEDDED SYSTEMS

### A. Wurz

The project encloses the realisation of a microcontroller circuit for implementing of an Internet-/UKW radio and a MP3 player.

The realization is based on an ARM7 processor with external SDRAM (32 MB) and FLASH RAM (4 MB). The board includes the following hardware components: Ethernet interface (10/100Mbps), interface for SD/SD-HC cards, MP3 decoder, real-time clock (RTC), ADC + DAC, interface for LCD graphics display, infrared port, a radio chip and USB-Interface.

As development environment the Eclipse C/C++ Development Toolkit is used. The programming of the processor occurs with OPENOCD using USB and FTDI JTAG- Interface.

The following software functions were implemented:

- File system FAT32 for SD-Card, FLASH-RAM and RAM-Disk
- USB Mass Storage Device of SD-Card, FLASH-RAM and RAM-Disk
- RDS radio for UKW + LW/MW/KW
- Internet radio [1]
- Synchronisation of the RTC with time Server
- Keyboard query to the service with graphics support

All functions were tested in 2011 successfully. It is planned to implement in 2012 a WLAN interface.

### References

- [1] M. Bloch: Implementing of an Internet radio. Hardware and software project: Embedded systems



Fig.2: Board with microcontroller

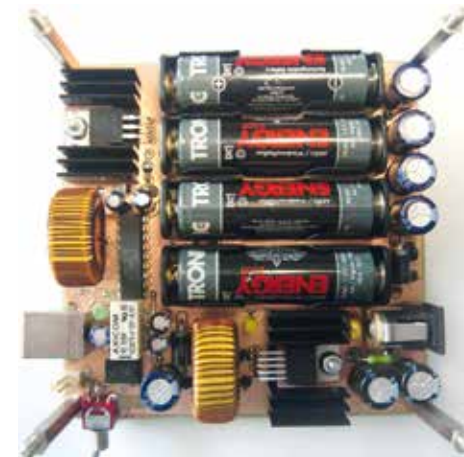


Fig.3: Power supply, battery charger, accumulators



Fig.4: LCD display



Fig.1: Tracking box

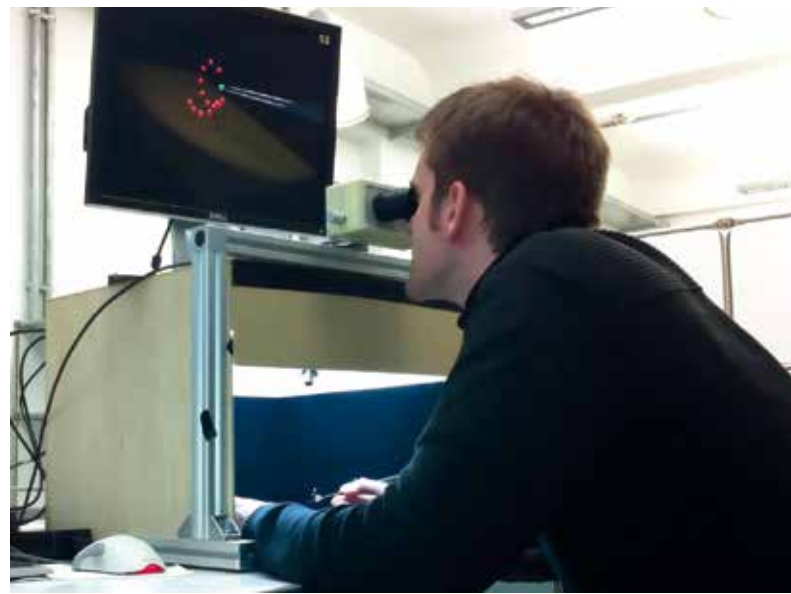


Fig.2: Stereo display

## MICROSIM – A MEDICAL TRAINING SIMULATOR FOR MICROSURGICAL TASKS

N. Hüsken, O. Schuppe, E. Sismanidis, R. Männer

Microsurgical techniques are used in a wide field of surgery, such as reconstructive and plastic surgery, ophthalmology and for re-/transplantation tasks. Typical tasks include the anastomosis of blood vessels and nerves in an order of magnitude of 1mm in diameter. Both the hand-eye coordination through a microscope and the handling of affected objects (vessels, tissue, instruments and sewing thread) itself need extensive training. Nowadays, simulators based on virtual reality (VR) are widely used as they present a perfect training system superior to conventional methods. With the help of medical simulators, virtual scenes can be modelled. The users can interact with the scene and train realistic operations without any risks for the patient. In addition, the users' performance can be measured and compared; even rare cases can be trained at any time.

MicroSim is a prototype VR-based simulator for microsurgical tasks. In order to provide an interface as native as possible to the user, we use original instruments tracked by an optical tracking system. Real-time simulation algorithms allow the interaction between the tracked forceps and virtual objects like tissue, vessels and sewing thread. The simulated scene is rendered in 3D and can be seen through a stereo display.

A multi-sensor camera made by VRmagic GmbH with four image sensors is used for image acquisition. The camera includes a Field Programmable Gate Array (FPGA) for image preprocessing. Image data is transferred via USB to the PC. Using a multi-sensor camera simplifies the operation: exposures

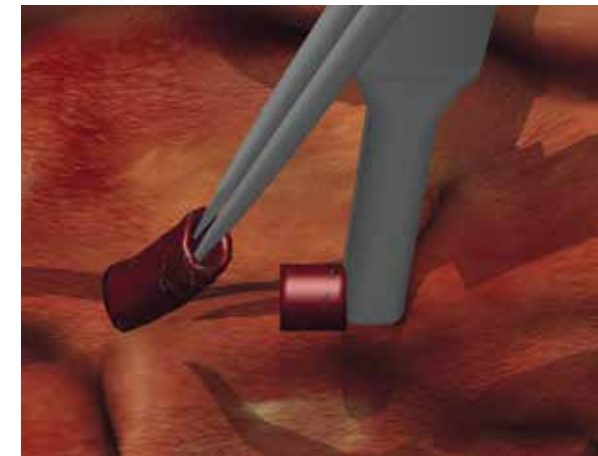


Fig.3: Simulation of blood vessels

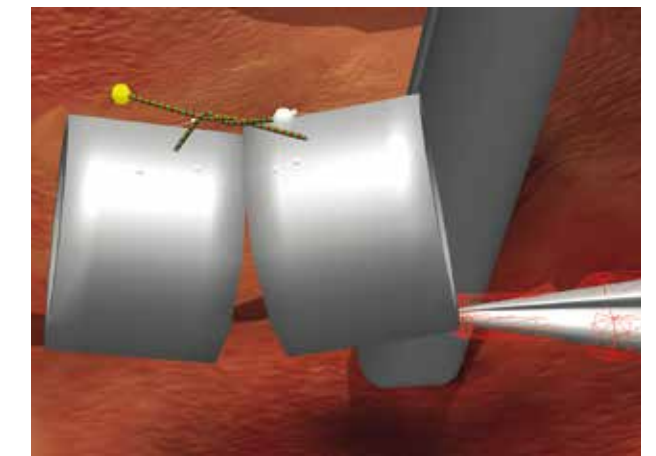


Fig.4: Simulation of sewing thread

are synchronised, all image data is streamed to one FPGA and only one USB port is needed. The camera sensors are mounted in a box which can be accessed by the user through one open side. The dimensions of the box are approx. 45x40x30cm<sup>3</sup>, which provides sufficient space for microsurgical tasks.

A working prototype uses a marker-based tracking: each forceps is equipped with 3 passive markers which allows the reconstruction of translation, orientation and opening of the forceps. Furthermore, an edge-based markerless approach is currently being developed.

The simulation algorithms use tetrahedron meshes in order to simulate blood vessels and surrounding tissue. The interaction between forceps and tissue has to be calculated in real-time. Tissue can be moved or grabbed. It is also possible to injure the tissue which leads to topological changes of the mesh. A non-elastic thread can be simulated. The thread interacts with the tissue so that it is possible to sew two interrupted blood vessels.

Several training modules have been developed: In abstract tasks, basic skills like hand-eye coordination can be trained. Medical modules simulate a real-world scenario.

*MicroSim is being developed in cooperation with the VRmagic GmbH, Mannheim. The project is kindly supported by German Bundesministerium für Wirtschaft und Technologie (BMWi) under grant ZIM (KF2351202SS9) and Aesculab AG, Tuttlingen, sponsor of the forceps.*



Fig.1: NeuroSim



Fig.2: Real operation

## NEUROSIM – THE PROTOTYPE OF A NEUROSURGICAL TRAINING SIMULATOR

F. Beier, E. Sismanidis, R. Männer

Neurosurgical interventions on the human brain are complicated and highly risky. Although minimal invasive techniques are used more often, there is still need for open surgical interventions, which can be accomplished only by very well trained and experienced surgeons. “See one, do one, teach one” is the most common axiom for acquiring medical skills although this method might endanger patients. Another possibility is the training on plastic models, living animals or dead bodies. So there is a great need for an efficient training environment that is realistic without involving real patients or animals. Virtual reality (VR) can be used in order to implement such a training system. Apart from the pro-

erties mentioned, VR-simulators have several advantages: Surgical tasks are reproducible and can be trained at any time, even if the case is rare. The surgeon’s skills are measured objectively and the result can be compared to other users

NeuroSim is the prototype of a VR-based simulator, that uses original instruments and a real surgical microscope in order to generate a native interface, compare figure 1 and 2. It uses optical and inertial tracking methods to estimate position and pose of the instruments as well as of the microscope that can be freely positioned in order to get a suitable view at the surgical area. Real-time simulation algo-

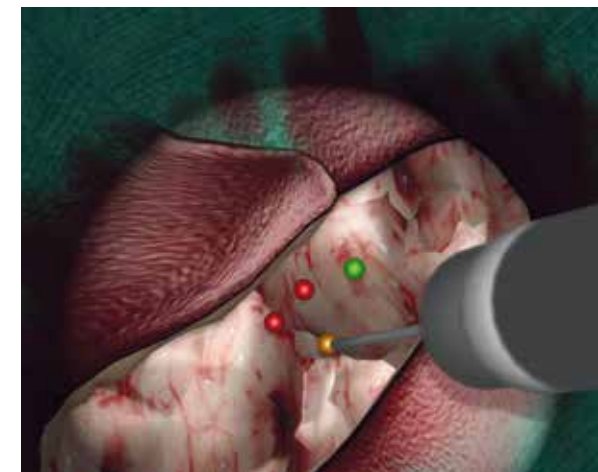


Fig.3: Abstract training module

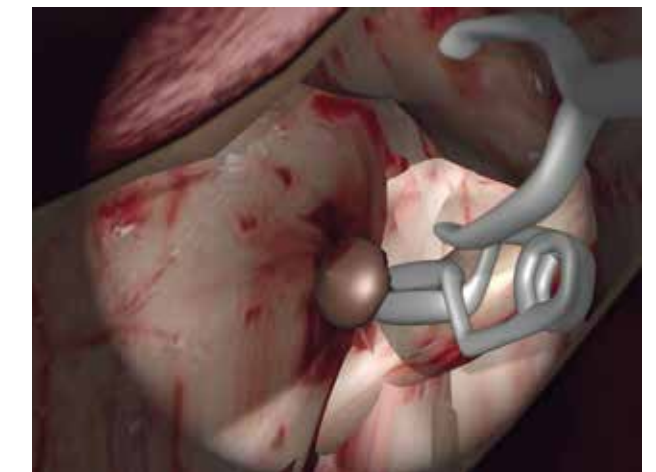


Fig.4: Aneurysm training module

gorithms calculate the interaction between the instruments and the tissue. The virtual scenario is shown stereoscopically in microdisplays that are mounted on the microscope.

NeuroSim features abstract training modules to train basic skills, e.g. the hand-eye coordination while working through a microscope (figure 3), as well as modules with real medical content. The first medical training procedure is the clipping of a cerebral aneurysm, see figure 4. The software design is modular and based on training modules, so more medical procedures or different abstract tasks can be added in the future.

*The simulator has been developed in cooperation with the Department of Neurosurgery of the Medical Faculty Mannheim, University of Heidelberg and VRmagic GmbH in Mannheim.*

*The project is kindly supported by Leica Microsystems GmbH, sponsor of the surgical microscope.*

### References

- [1] F. Beier, S. Diederich, K. Schmieder, R. Männer. NeuroSim – The Prototype of a Neurosurgical Training Simulator. *Studies in Health Technology and Informatics*, 163:51–56, 2011.
- [2] F. Beier, E. Sismanidis, A. Stadie, K. Schmieder, R. Männer. An Aneurysm Clipping Training Module for the Neurosurgical Training Simulator NeuroSim. *Studies in Health Technology and Informatics*, 173:42–47, 2012.
- [3] F. Beier. The Integration of a Neurosurgical Microscope as an Interface to a Medical Training Simulator. *Virtual Reality Conference (VR)*, 2012 IEEE, 2012.

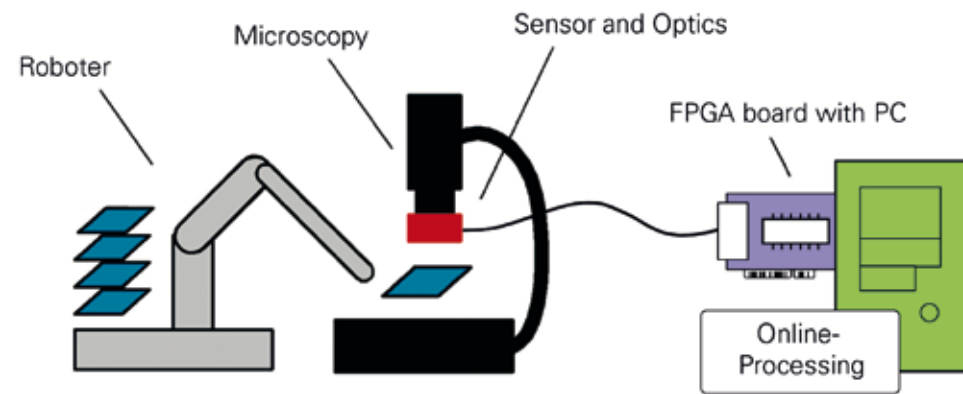


Fig.1: Set up of a Microscope connected to a FPGA to process images online

## ONLINE PROCESSING OF CELL IMAGES USING AN OpenCL TO FPGA COMPILER

M. Gipp, G. Marcus, R. Männer

The biologist in the VIROQUANT-Project have the demand to easily program FPGAs to process cell images online (in real-time). FPGAs can be connected to the sensors of a microscopy directly (fig 1.) and receive a pixel stream of images. Simple image processing algorithms are applied on the pixel stream to process it online. With hardware description languages one can program FPGAs, but they expect a fundamental knowledge of hardware and logic design, which biologist usually not have.

OpenCL is a parallel portable language for GPUs and multi core CPUs. It is widely used and easy to learn without any hardware design knowledge.

This project presents a developed OpenCL compiler prototype to open up the use of FPGAs as part of a Phd thesis [1].

Fig.1 shows the novel system architecture of the OpenCL to FPGA compiler. It is structured in three parts A, B and C described below.

(A) OpenCL Runtime Environment. Each OpenCL implementation bundles a set of standard function to communicate with the OpenCL device in our case to the FPGA. Only a basic subset of the standard is implemented to access the board memory, start the execution of kernel function on the FPGA and run the OpenCL compiler, see (B).

(B) VHDL Compiler. The compiler translates OpenCL kernel functions into a VHDL pipeline at the runtime. We use a C front end from LLVM which translates the kernel code into an intermediate representation language (IR) and an optimizer which

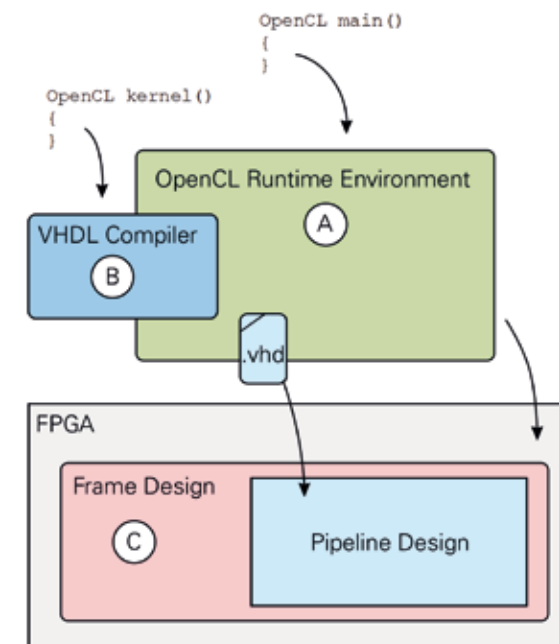


Fig.2: Overview and interaction of the developed components.

reduces the size of the IR code. A parser reads the optimized IR code and generate an abstract syntax tree (AST) in memory. Similar to the generated AST a second AST is build which consists of building blocks respectively to the logic of the IR instructions. From the building blocks within the second AST the VHDL code can be derived. Finally the VHDL code represents a pipeline with the logic of the OpenCL kernel function.

(C) Frame Design. It offers an environment to the VHDL pipeline to interact with the PCIe interface to the memory. The Frame Design has a memory controller, a PCIe core and a DMA logic to interact with the Runtime Environment functions from (A). The task are to transfer data from the host to the board memory, exchange the pipeline with dynamically partial reconfiguration, start the computation of the pipeline and provide a data flow from memory to the pipeline.

This project comprise several advantages other developments do not have in total. First, a simple parallel, well known language (OpenCL) can be used to efficiently program FPGAs without any hardware knowledge. Second, The kernel code is translated into a pipeline with streaming capabilities. And third the programmer do not need to take care of any data flow tasks.

Supported by: VIROQUANT

### References

[1] Gipp, M. „Online- und Offline-Prozessierung von biologischen Zellbildern auf FPGAs und GPUs“, Universität Heidelberg, 2012 (submitted)

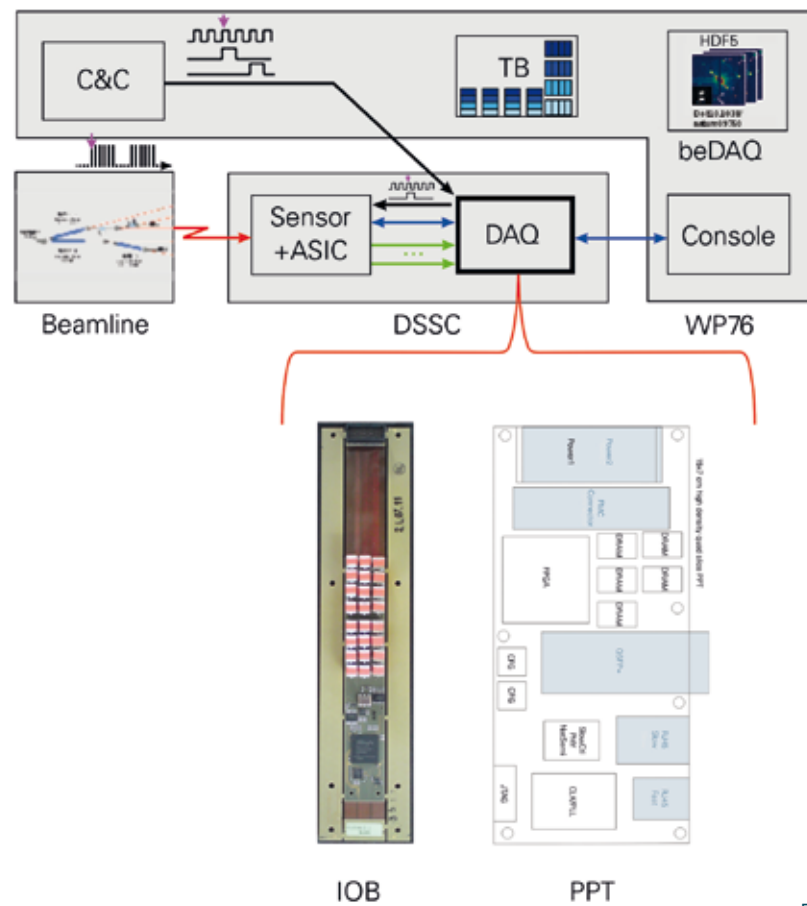


Fig. 1: XFEL/DSSC DAQ Architecture

## XFEL DSSC DAQ – A READOUT SYSTEM FOR THE DSSC DETECTOR OF THE EUROPEAN XFEL

T. Gerlach, A. Kugel, R. Männer

DSSC [1][2] is one 2-D megapixel detector being built for the European XFEL at DESY, Hamburg. The detector specific DAQ subsystem [3] of DSSC is under development by the ZITI group since 2009 and comprises two custom FPGA cards. In total 16 I/O-boards (IOB) are located close to the detector head, each servicing 64k pixel. Mechanically 4 IOBs are grouped into one detector quadrant which in turn is connected to one control and transceiver boards (PPT) located at the patch panel on the boundary of the detector. Each PPT connects via four 10GE links to the external train-builder (TB) box.

An initial version of the IOB is available. The functionality of the PPT is emulated by the MPRACE-2 rapid-prototyping platform<sup>1</sup>.

In 2011 the main focus of the DAQ development has been on further implementation of the I/O Board firmware, and its test environment. Several measurements on the prototyping hardware have also been carried out successfully.

<sup>1</sup> See also ZITI annual report 2008-2010

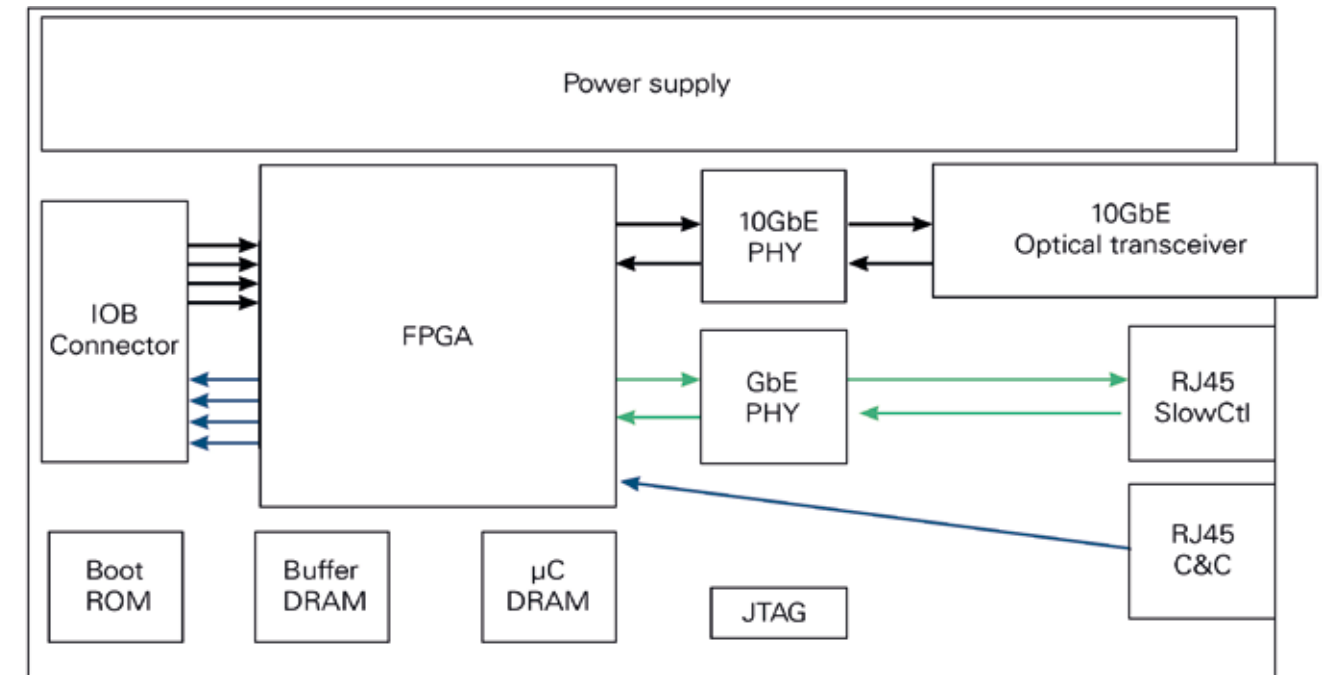


Fig. 2: Single PPT Slice

The I/O Board firmware component's capabilities have been further extended. A slow control interface module has been developed, which provides a simple custom serial communication protocol between the PPT emulation hardware and the I/O Board. The MOSFET driver controllers have been implemented as well.

The MPRACE-2 firmware has been extended by a software based user interface running on the MicroBlaze soft core CPU, enabling full access to the test environment hardware components. In cooperation with the ASIC development group, a VETO strategy was defined, and presented to the WP76 in a "DSSC VETO Specification Document". The design of the PPT modules has been sketched down to the component level, assuming the availability of low-cost 10GE capable FPGAs in 2012. The basic unit is one "slice" interfacing to one IOB at the detector end and to one 10GE link at the TB end. The design of such a slice is shown in Fig. 2.

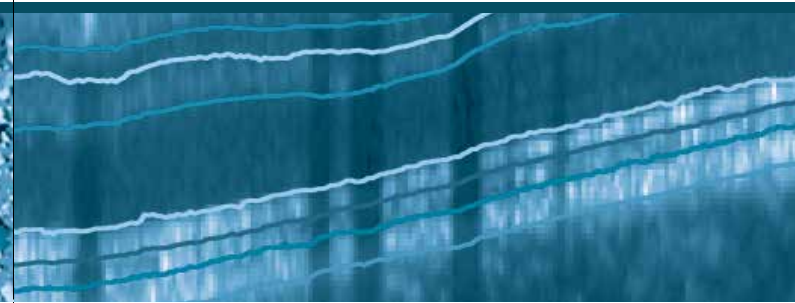
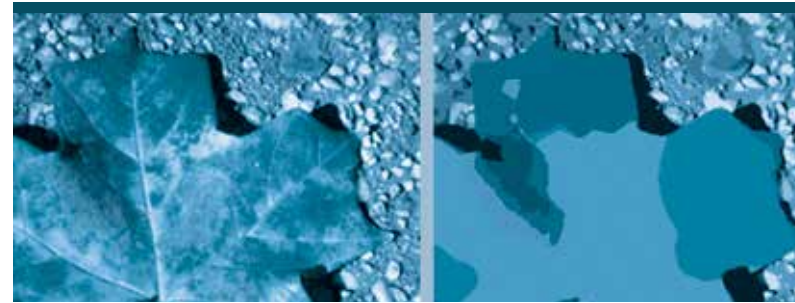
The goal for the final design is the integration of four slices into one PPT card, with four IOB interfaces and four 10GE links.

A major milestone for the DSSC DAQ project was the successful pass of the Go/NoGo review in October 2011.

Supported by: XFEL GmbH

### References

- [1] M. Porro et al; Development of the DEPFET sensor with signal compression: A large format X-ray imager with mega-frame readout capability for the European XFEL, Proceedings of 2011 IEEE Nuclear Science Symposium and Medical Imaging Conference, Valencia 23–29 Oct. 2011, pp.1424–1434
- [2] P. Lechner et al., DEPFET active pixel sensor with non-linear amplification, Proceedings of 2011 IEEE Nuclear Science Symposium and Medical Imaging Conference, Valencia 23–29 Oct. 2011, pp.563–568
- [3] T. Gerlach et al., The DAQ readout chain of the DSSC detector at the European XFEL, Proceedings of 2011 IEEE Nuclear Science Symposium and Medical Imaging Conference, Valencia 23–29 Oct. 2011, pp.156–162



## CHAIR OF COMPUTER VISION, GRAPHICS AND PATTERN RECOGNITION PROJECT OVERVIEW

Prof. Dr. Christoph Schnörr

CONVEX MODELS AND GLOBAL OPTIMIZATION  
FOR IMAGE SEGMENTATION AND LABELING ..... 62  
J. Lellmann, D. Breitenreicher, J. H. Kappes, F. Becker, C. Schnörr

DISCRETE TOMOGRAPHY FOR PARTICLE IMAGE VELOCIMETRY ..... 65  
S. Petra, F. Becker, C. Schnörr

GENERATIVE MODELING OF APPEARANCE AND SHAPE  
FOR MEDICAL IMAGE ANALYSIS ..... 68  
F. Rathke, S. Schmidt, C. Schnörr

GLOBALLY OPTIMAL IMAGE SEGMENTATION BY MULTICUTS ..... 70  
J. H. Kappes, M. Speth, B. Andres, F. Hamprecht, C. Schnörr

IMAGE DENOISING WITH ADAPTIVE TOTAL VARIATION ..... 74  
F. Lenzen, F. Becker

INFERENCE IN MARKOV RANDOM FIELDS  
BASED ON PRIMAL-DUAL CONVEX OPTIMIZATION ..... 77  
B. Savchynskyy, S. Schmidt, J. H. Kappes

PEDESTRIAN PATH PREDICTION USING LEARNED MOTION MODELS ..... 80  
C. Keller, C. Schnörr

VARIATIONAL METHODS FOR IMAGE SEGMENTATION WITH SHAPE PRIORS ..... 82  
B. Schmitzer, C. Schnörr

VARIATIONAL RECURSIVE JOINT ESTIMATION OF SCENE STRUCTURE  
AND EGOMOTION FROM MONOCULAR IMAGE SEQUENCES ..... 84  
F. Becker, F. Lenzen, C. Schnörr

## CONVEX MODELS AND GLOBAL OPTIMIZATION FOR IMAGE SEGMENTATION AND LABELING

J. Lellmann, D. Breitenreicher, J. H. Kappes, F. Becker, C. Schnörr



Fig.1: Application of the proposed approach for finding optimal partitions. Left: Original image. Center: Selection of seed regions by the user. Right: Histogram-based multiclass segmentation. The originally combinatorial problem is relaxed to a convex problem and solved globally optimal using specialized algorithms. The spatially continuous framework avoids discretization-based artifacts and allows to obtain solutions with sub-pixel accuracy.

In this project, we study approaches to construct convex formulations of variational problems in image processing. We focus on problems that can be approximated by convex partitioning problems on continuous image domains. Using specially developed algorithms, these problems can be globally optimized even for very general data terms, which allows to clearly separate modeling and optimization effects.

### Background and Goals

One of the key problems in image analysis is the partitioning problem. Here one seeks to decompose a given image domain  $\Omega \subseteq \mathbb{R}^d$  into several regions according to some data consistency and spatial coherency constraints.

Classical applications include image- or 3D volume segmentation and 3D reconstruction. In many cases the resulting problems can be formulated as convex optimization problems, which allows to solve them to global optimality. Any undesired or unexpected results can thus be attributed to the model, which is a clear advantage for model development. Moreover, using a *lifting* technique [1], many originally non-convex variational problems such as image registration and optical flow can be reduced to higher-dimensional convex partitioning problems. In this project, we focus on deriving convex relaxations for partitioning problems and developing efficient numerical solvers.

In contrast to grid- or graph cut-based methods, we consider the problem in the functional-analytic framework and from a spatially continuous perspective, i.e. we regard the image domain as a

connected set rather than a finite set of individual points. In contrast to “discretize first” approaches, this “analyze first” approach allows to get a deeper insight into the underlying problem, obtain sub-pixel accurate solutions, and abstract from inaccuracies caused by the discretization.

### Methods and Results

The task of segmenting the image domain  $\Omega \subseteq \mathbb{R}^d$  into several regions  $P_1, \dots, P_l$  can be posed as finding a labeling function  $u: \Omega \rightarrow \{1, \dots, l\}$  minimizing

$$\inf_{u: \Omega \rightarrow \{1, \dots, l\}} \int_{\Omega} \langle u(x), s(x) \rangle dx + J(u), \quad (3)$$

where  $s: \Omega \rightarrow \mathbb{R}^l$  constitutes the local data fidelity term, and the regularizer  $J(u)$  ensures a certain smoothness of the boundaries.

A way to solve this originally combinatorial problem is to allow intermediate solutions, i.e. to relax the constraint set to  $u: \Omega \rightarrow \Delta_l$ , where  $\Delta_l$  is the  $l$ -dimensional unit simplex. By a suitable extension of the regularizer  $J$  to this enlarged feasible set, one obtains a *relaxed* problem. From the solution of the relaxed problem, an approximate – and, in the case of two labels, exact – solution of the original problem can then be recovered.

This is particularly appealing in cases where  $J$  can be extended in a convex way, since then the overall problem can be solved to global optimality without potentially getting stuck in local minima. It is there-

fore of central importance to characterize regularizers for which such extensions exist, and to provide ways to construct such extensions. We focus on a class of regularizers where jumps between labels are penalized differently according to an interaction potential  $d$ , i.e. boundary length weighted by some scalar  $d(i, j)$  depending on the labels  $i$  and  $j$  of the adjoining regions (Fig. 2). In [4] we considered the special class of *Euclidean distances*, which are naturally handled by the above model. Non-Euclidean distances can still be approximated by offline solving an auxiliary convex problem.

Under several reasonable assumptions on the regularizer, we showed that any interaction potential must be a metric [4].

In addition, we extended an existing result [1] to show how a regularizer can be constructed for any such interaction potential. This completely characterizes the class of interaction potentials.

Regarding optimization, the model (3) can be posed as a (convex-concave) saddle-point problem. We studied several methods to solve such problems, with a special focus on primal-dual methods that allow to solve the problems to a prescribed accuracy and provide optimality certificates [4]. Compared to existing methods, the proposed Douglas-Rachford method is robust and works on many synthetic and real-world problems without further parameter tuning. When combined with an improved rounding technique, the approach allows to recover very good solutions of the original combinatorial problem with sub-pixel accuracy, and without the staircasing artifact commonly encountered with graph-based methods.



Fig. 2: Left: Effect of choosing nonstandard interaction potentials. The original image (left) is segmented into 12 regions corresponding to prototypical colors vectors. By modifying the interaction potential, the regularization strength is selectively adjusted to suppress foreground structures while allowing for fine details in the background. Such non-standard regularizers require special techniques in order to formulate them in a convex way.

Right: Mumford-Shah denoising of a grayscale image (left) using a nonconvex regularizer to remove fine structures while preserving hard edges (right). Using a lifting technique, many similar variational problems can be formulated and solved in the considered framework.

The quality of the segmentation can be further improved by employing tighter relaxations of the regularizer. These pose a problem for existing methods, as they require to iteratively solve inner problems at each step. In [2] we demonstrate how this can be avoided, increasing numerical robustness and speed at the same time. The proposed technique also works for a large class of general image processing problems that can be formulated in saddle-point form (Fig. 2).

Finally, we established *a priori* suboptimality bounds of combinatorial image labelings computed by our convex variational framework [3, 5].

### Outlook and Future Work

Image labeling provides a key subroutine for a range of increasingly sophisticated image analysis tasks. Two major directions of research concern the combination of image labeling with (i) shape prior information and (ii) with prior information in terms of empirical measures of either raw image data or coefficients of dictionaries, in order to cover incre-

asingly larger image classes without compromising mathematical rigor or provable performance of corresponding algorithms.

### References

[1] A. Chambolle, D. Cremers, and T. Pock. A convex approach for computing minimal partitions. Tech. Rep. 649, Ecole Polytechnique CMAP, 2008.

[2] J. Lellmann, D. Breitenreicher, and C. Schnörr. Fast and Exact Primal-Dual Iterations for Variational Problems in Computer Vision. In K. Daniilidis, P. Maragos, and N. Paragios, eds., European Conference on Computer Vision (ECCV), vol. 6312 of LNCS, pp. 494–505. Springer Berlin / Heidelberg, 2010.

[3] J. Lellmann, F. Lenzen, and C. Schnörr. Optimality Bounds for a Variational Relaxation of the Image Partitioning Problem, Dec 2011. <http://arxiv.org/abs/1112.0974>.

[4] J. Lellmann and C. Schnörr. Continuous Multiclass Labeling Approaches and Algorithms. SIAM J. Imag. Sci., 4(4):1049–1096, 2011.

[5] J. Lellmann and C. Schnörr. Continuous Multiclass Labeling Approaches and Algorithms. CoRR, abs/1102.5448, 2011. <http://arxiv.org/abs/1102.5448>.

## DISCRETE TOMOGRAPHY FOR PARTICLE IMAGE VELOCIMETRY

S. Petra, F. Becker, C. Schnörr

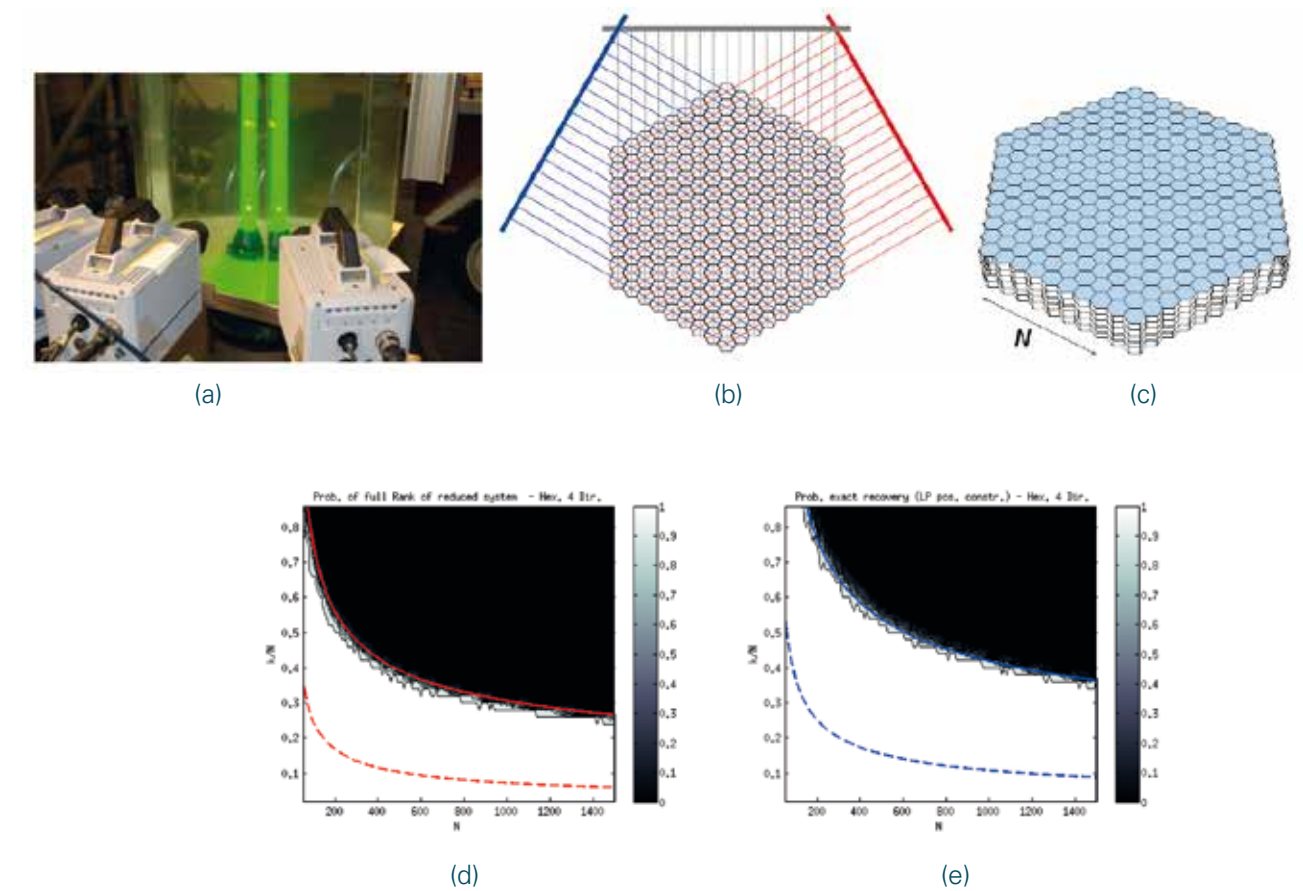


Fig. 1: (a) TomoPIV is based on a multiple camera-system, three-dimensional volume illumination and subsequent 3D reconstruction, and employs only few projections due to cost and complexity of the necessary measurement apparatus. The particle displacement (hence velocity) within the interrogation volume is then obtained by the 3D cross-correlation of the reconstructed particle distribution at the two exposures. In [1] a variational adaptive correlation method is developed.

(b) Sketch of a 3-camera setup in 2D. The corresponding 0 / 1 sensing matrix  $A^{3(2N+1) \times (3N^2+3N+1)}$  is underdetermined and marks in each row corresponding to a projection ray all incident discretization cells by the entry 1.

(c) This geometry can be easily extended to 3D by enhancing both cameras and volume by one dimension, thus representing scenarios of practical relevance as in (a), where a free jet inside an illuminated cylinder was imaged by cameras aligned on a line.

Recovery via (d) standard TomoPIV measurement system versus recovery via (e) the improved measurement system. (d) shows success and failure empirical phase transition for a 4-camera binary measurement system along with the analytical phase transition (dashed), see (2), for the binary 3-camera system from (b). (e) shows success and failure empirical phase transition for an improved 4-camera measurement system along with the analytical phase transition  $k(N)/N \approx 6N^{0.342-1+0.011 \log(N)}$  (dashed) for the improved 3-camera system corresponding to the geometry from (b). The results indicate that at least a 150% times better reconstruction performance may be obtained in practice within the considered range of image resolution.

We study the discrete tomography problem in Experimental Fluid Dynamics – Tomographic Particle Image Velocimetry (TomoPIV) – and focus on conditions for unique volume reconstruction in representative ill-posed scenarios. Illposedness is due to undersampling but also intimately connected to the particle density. Higher densities ease subsequent flow estimation but also aggravate ill-posedness of the reconstruction problem. A theoretical investigation of this trade-off is studied in the present work.

of the PIV volume reconstruction problem that is an essential prerequisite for any algorithm used to actually compute the reconstruction. Accordingly, we also investigate the role of various reconstruction algorithms currently used in PIV from the optimization point of view, see [2]. Finally, we outline connections to major developments in other disciplines (compressed sensing) and indicate how the imaging set-up may be further improved.

### Methods and Results

The reconstruction of particle volume functions from few projections can be modeled as finding the sparsest solution of an underdetermined linear system of equations, since the original particle distribution can be well approximated with only a very small number of active basis functions relative to the number of possible particle positions in a 3D domain. In general the search for the sparsest solution is intractable (NP-hard), however. In [3] it was shown that if the solution of  $\mathcal{A}$  is known to be sufficiently sparse and positive it is also the unique positive solution. If  $\mathcal{A}$  has only nonnegative entries, zero or negligible measurements can be eliminated along with the corresponding incident basis functions. This leads to an “equivalent” feasible set of reduced dimensionality. It can be shown that a binary matrix recovers *all*  $k$ -sparse binary vectors if and only if all these reduced

systems are overdetermined full-rank systems. The maximal such  $k$  is related to the minimal number of negative (or positive) entries in the sparsest null-space of  $\mathcal{A}$  and for the considered geometry, see Fig. 1 (c), equals 2. We estimated the critical  $k$  such that for *most* arbitrary  $k$ -sparse vectors the reduced systems are indeed overdetermined and obtained the relation

$$k(N) \approx 4N^{0.342 + 0.011 \log(N)} \quad (2)$$

depending on the problem size  $N$ . Additionally, we proved a tail bound entailing that for increasing large problem sizes  $N \rightarrow \infty$ , the critical  $k$  acts like a threshold that sharply discriminates successful reconstruction from failure. Our average case analysis of correct reconstruction revealed that by adding a fourth camera the critical  $k$  increases to

$$k(N) \approx 7.3N^{0.43 + 0.016 \log(N)} .$$

Fig. 1 illustrates this fact as well as results for sensing matrices that have been improved in a specific way.

### Outlook and Future Work

We currently study the tomographic problem of reconstructing particle volume functions from the general viewpoint of compressed sensing. In a nutshell, we show that the TomoPIV problem is quite degenerate from the viewpoint of compressed sensing, thus leading to poor performance guarantees. On the other hand, the probabilistic analysis of [4] yields average performance bounds that back up current rules of thumb of engineers for choosing particle densities in practice. Moreover, simulations demonstrate that slight random perturbations of the TomoPIV measurement matrix considerably boost both worst-case and expected reconstruction performance. This finding is interesting for CS

theory and for the design of TomoPIV measurement systems in practice. Our work aims at pointing out connections between the fields of compressed sensing and discrete tomography in order to stimulate further research.

*In cooperation with:*

B. Wienecke (LaVision, Göttingen),  
S. Gesemann, A. Schröder (DLR, Göttingen)

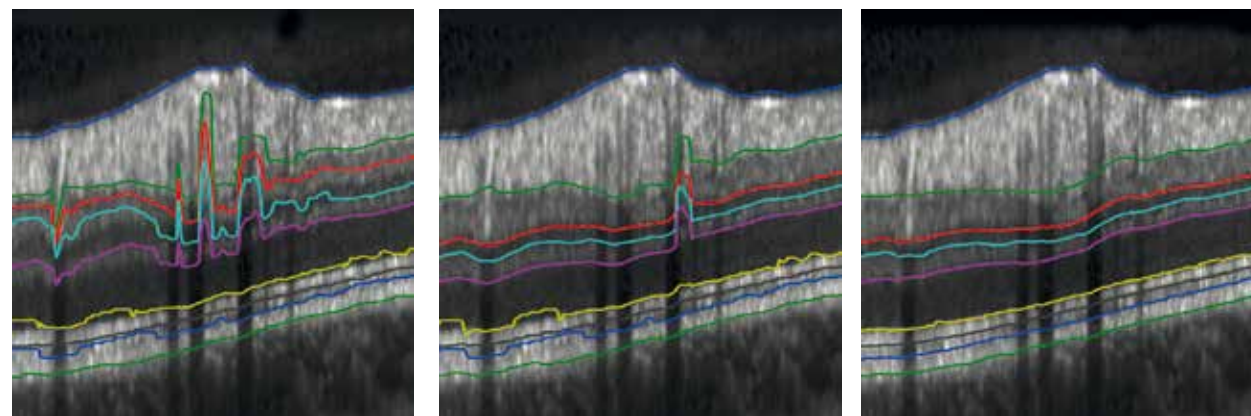
*Funding: DFG, grant SCHN457 / 11*

### References

- [1] F. Becker, B. Wienecke, S. Petra, A. Schröder, and C. Schnörr. Variational Adaptive Correlation Method for Flow Estimation. IEEE Transactions on Image Processing, 2011. accepted.
- [2] A. Nicola, S. Petra, C. Popa, and C. Schnörr. A general extending and constraining procedure for linear iterative methods. Int. J. Comp. Math., 2011. <http://dx.doi.org/10.1080/00207160.2011.634002>. in press.
- [3] S. Petra and C. Schnörr. TomoPIV meets Compressed Sensing. Pure Math. Appl., 20(1–2):49–76, 2009. [http://www.mat.unisi.it/newsito/puma/public\\_html/contents.php](http://www.mat.unisi.it/newsito/puma/public_html/contents.php).
- [4] S. Petra, C. Schnörr, and A. Schröder. Reconstruction Properties of Sensing Matrices in Tomographic Particle Imaging Velocimetry. In Volume Reconstruction Techniques Applied to 3D Fluid and Solid Mechanics, Proc. of FVR 2011, 2011.

## GENERATIVE MODELING OF APPEARANCE AND SHAPE FOR MEDICAL IMAGE ANALYSIS

F. Rathke, S. Schmidt, C. Schnörr



(a) Uniform Prior (b) Shape Prior (c) SP + Post-Processing

Fig.1: Close-up view of segmentation results for three models of increasing complexity.

Left (a): The model utilizes texture information only. Furthermore inference is performed for each column separately. For distinctive partition transitions this leads to accurate segmentation results, but fails for less well-defined ones.

Center (b): Shape information is added to the model column-wise. Although still lacking communication accross columns, the predicted segmentation improves in many image columns. For columns with strong texture artifacts, such as shadowing caused by blood vessels, the segmenation may still fail.

Right (c): The final model with added communication accross image columns, governed by the global shape prior. This leads to improved segmentations for difficult image regions as well.

The project focuses on classes of image data given by partitions with randomly varying geometry and fixed topology, and with class-specific appearance of each component of the partition. The application scenario concerns 2D OCT scans of retinal tissue. A probabilistic approach is presented, which combines discrete exact inference and a global shape prior, that produces accurate segmentations which preserve the physiological order of intra-retinal layers.

### Background and Goals

Over the last years Optical Coherence Tomography (OCT) has become a key technique for non-invasive diagnostic retina imaging. Quantitative measurement of the intra-retinal layers plays a central role for the early diagnosis of diseases like glaucoma or age-related macular degeneration. Since manual segmentation is tedious and time-consuming, there is a high demand for automated algorithms.

### Methods and Results

Our framework combines local appearance models with a global shape prior, all modeled probabilistically via Gaussian distributions and learned offline on a set of labeled training images.

To obtain segmentations, we rely on the following iterative procedure:

a) Exact inference is performed column-wise fusing appearance and shape information for the respective column.

b) In a regularization step, smoothness across image

columns is enforced utilizing the global shape prior, by altering the appearance terms. Both steps are iterated until convergence of the predicted segmentation.

For further details please refer to [1].

### Outlook and Future Work

Variational methods will be studied, that infer not segmentations but distributions over segmentations. This enables local assessment of predictions, i.e. locate potential weak spots in the segmentation. In an abnormality detection setting, these may correspond to pathological variations in the retina.

Funding: DFG RTG 1653

### References

[1] F. Rathke, S. Schmidt, and C. Schnörr. Order Preserving and Shape Prior Constrained Intra-retinal Layer Segmentation in Optical Coherence Tomography. In G. Fichtinger, A. L. Martel, and T. M. Peters, eds., MIC-CAI, vol. 6893 of Lecture Notes in Computer Science, pp. 370–377. Springer, 2011.

## globally optimal image segmentation by multicut

J. H. Kappes, M. Speth, B. Andres, F. Hamprecht, C. Schnörr

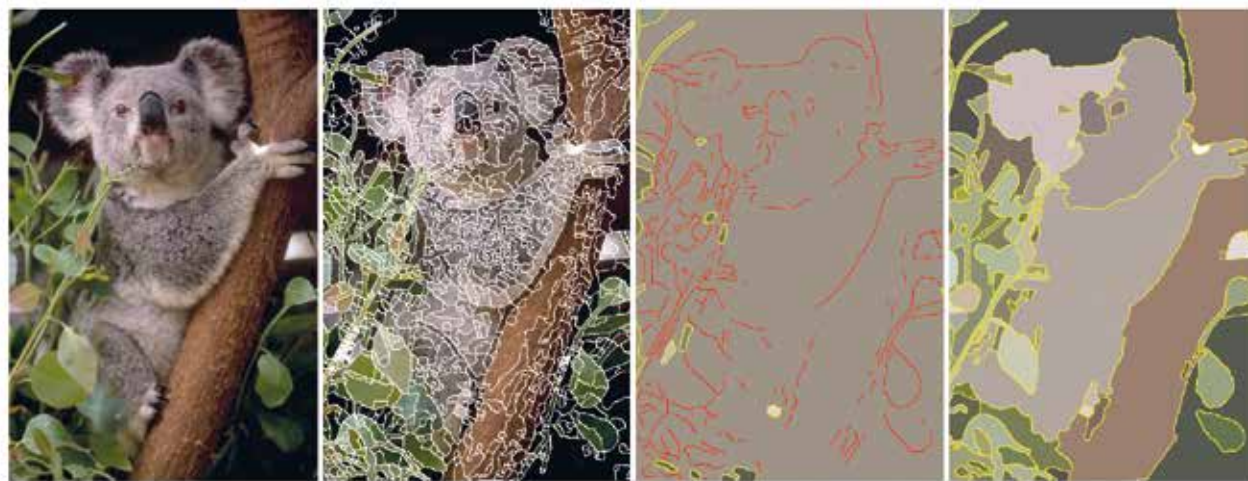


Fig.1: Example for segmenting an image in a priori unknown number of classes. The images above are taken from [1] and show from left to right: (1) the original image, (2) the over-segmentation that defines super-pixels, (3) a segmentation only based on decision-tree-classifiers trained on boundaries and (4) a segmentation using closeness constraints that enforce the edge-labeling to be in the multicut-polytope. Without this additional constraint, many edges (red) are inside a connected component and therefore ambiguous. Ignoring this ambiguity leads often to undesirable under-segmentation.

Segmentation of images into a given number of classes is an important problem for many computer vision applications. If the number of classes is unknown the problem renders much harder. We develop a branch-and-cut framework that solves these problems to global optimality. While the asymptotic run-time is in general exponential, we observe run-times on real world problems comparable or better than state-of-the-art methods. Furthermore the framework can be extended by using super-pixel for speed-up and to make it applicable to large-scale problems.

### Background and Goals

The overall goal of this project is to segment images into (i) a given number of predefined class (P1) or (ii) a unknown number of unknown classes (P2). Both problems can be formulated in terms of a Markov Random Field (MRF). Finding the most likely segmentation reduce to minimizing an objective function given by a sum of unary terms  $f_a(x_a)$ , which depend on local measurements on (super-)pixel  $a$ , and higher-order-terms  $f_C(x_C)$ , which depend on two or more (super-)pixels summarized by the sets

$C \in \mathcal{C}$ . In the simplest case  $\mathcal{C}$  includes all pairs of neighbored (super-)pixels. For the case when a predefined number of classes is given, the problem reads

$$\min_{x \in X} \sum_{v \in V} f_v(x_v) + \sum_{C \in \mathcal{C}} f_C(x_C). \quad (P1)$$

For the case a unknown number of classes, we assume w.l.o.g. that the number of classes is equal to the number of (super-)pixels, but includes no unary terms:

$$\min_{x \in X} \sum_{C \in \mathcal{C}} f_C(x_C), \quad \forall C \in \mathcal{C} : |C| \geq 2. \quad (P2)$$

A notable characteristic of the later problem is, that its objective function is invariant to a permutation of the state-space, i.e. the configurations  $x = (0, 1, 0, 2, 3, 1)$  have the same energy as  $x = (6, 0, 6, 1, 4, 0)$ , which renders the problems challenging for state-of-the-art methods, which try to assign a labeling to each variable/pixel.

### Methods and Results

We restrict the non-unary-terms of our objective function to be invariant to permutations of the state-space. While this is no restriction for (P2), for (P1) it is quite natural. Many common terms fall into this family, e.g. potts-functions. Let us number the set of valid partitions of a set with  $n$  elements<sup>1</sup> and let  $\alpha : \Omega^n \rightarrow \mathbb{N}$  be a mapping from a labeling to its

partition number. Then any real valued function that is invariant to permutations of the state-space can be written as:

$$f_C(x_C) = \beta_{C,\alpha(x_C)}, \quad \beta_{C,\alpha} \in \mathbb{R} \quad (1)$$

With this slightly restriction at hand we optimize no longer over the set of all node labelings. Instead we optimize over the set of all separating boundaries related to valid partitions, which is known as the multicut problem. While this does change nothing on the NP-hardness of our problem it has two major advantages: (i) it overcomes the ambiguity of optimal solutions in (P2), (ii) it provides a less memory consuming representation of both problems in form of an (integer) linear program.

We refer the reader to [2] to a general description for the second order case, i.e.  $\forall C \in \mathcal{C} : |C| \leq 2$ . In [1] we describe an application using also higher order terms. A description of the method for arbitrary order is in progress, we will give here a rough overview.

Problems (P1) and (P2) can be transformed into a linear program of moderate size together with a system of affine inequalities, defining the so called multicut polytope.

<sup>1</sup>The number of possible partitions is given by the bell number

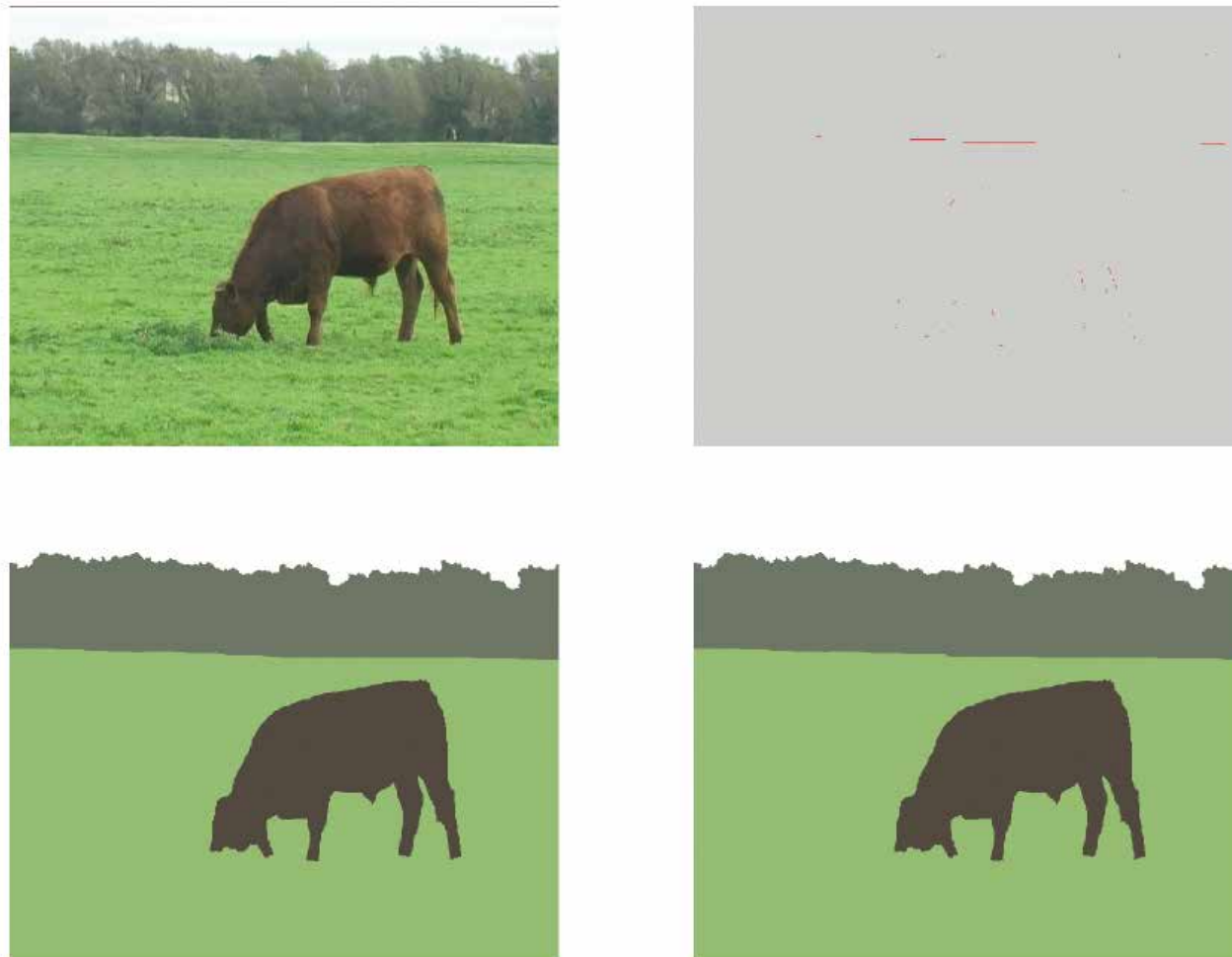


Fig. 2: The original image (top-left) is segmented in 4 predefined classes. The resulting segmentation is shown for our multicut method (bottom-left) and TRW-S (bottom-right). While our method guarantee for optimality, TRW-S found a suboptimal solution. The difference between these two segmentations (top-right) are located at object-boundaries.

While the number of inequalities is exponential we start with a polynomial subset of this system, apply separation procedures to find efficiently violated constraints out of this set and add those iteratively to our problem. If no more violated constraints can be found we apply branching techniques and proceed with detecting violated constraints as long as the optimal solution has been founded.

While for problems (P2) our methods outperform any method we compare with, for problems (P1) alternative state-of-the-art methods often provides

comparable but approximative results much faster. However, if one is interested in optimal solutions, our method seems to be currently the fastest one.

For the case of unknown classes Fig.1, we presegment the image-domain in the first step. This results in sets of pixels, also known as super-pixels. Working on super-pixels instead of the pixel level has two mayor advantages: (i) it drastically reduces the problem size and (ii) during the pre-segmentation it often makes inconsiderable decisions which

hardly determinable in the overall problem. Local classifiers give a prediction if a single boundary element between two super-pixels should belong to the overall boundary. A segmentation based only on this information leads to under-segmentation and active edges inside connected components (plotted in red). If we additionally enforce closeness constraints, *i.e.* solution have to be inside the multicut-polytope, we obtain accurate segmentations. Details how these models are learned and how the level of segmentation can be selected are reported in [1].

For the problem (P2), in which the set of classes is unknown, we compare our method with TRW-S, one of the state-of-the-art methods.

Fig. 2 shows the result for a four-class problem, without using super-pixels. While visually the results of our multicut method (bottom-left) and TRW-S (bottom-right) are comparable, a detailed look at the difference of labelings (top-right) shows that they differ on the object boundaries. Furthermore, TRW-S does not converge on this instance. We stop TRW-S after the same time, in which our method has found the global optimum.

#### Outlook and Future Work

We already extended our method do deal with higher order terms. For some types of functions we can deal up to orders of a view hundred. While for complex models we can not expect to find optimal solutions in reasonable time, we are looking for alternative cut defining procedures and better rounding schemes to obtain good solutions and bounds for earlier iterations.

#### References

- [1] B. Andres, J. H. Kappes, T. Beier, U. Köthe, and F. Hamprecht. Probabilistic Image Segmentation with Closedness Constraints. In Proceedings of ICCV, 2011. to appear.
- [2] J. H. Kappes, M. Speth, B. Andres, G. Reinelt, and C. Schnörr. Globally Optimal Image Partitioning by Multicuts. In EMMCVPR. Springer, 2011.

## IMAGE DENOISING WITH ADAPTIVE TOTAL VARIATION

F. Lenzen, F. Becker



Fig. 1: Comparison of data-dependent (middle) and solution-dependent (right) adaptive TV regularization for denoising a test image (left). We use a strong anisotropy to preserve as much edges as possible. For the data-dependent approach this leads to a significant preservation of noise structure in the image. The proposed solution-dependent approach does not show these artifacts. Decreasing the anisotropy to avoid artifacts for the data-dependent approach will, however, lead to an inferior preservation of true edge structures.

Adaptive total variation (TV) is a state-of-the-art approach to regularize inverse problems. We propose a generalization of this approach, where the adaptivity does not depend on the noisy input data, but on the unknown solution. The benefits of this generalization are demonstrated by means of image denoising. Compared to the classical approach of adaptivity, our method is able to much better preserve edge structures. In general our approach is applicable for arbitrary inverse problems.

### Background and Goals

Many image restoration methods are based on the idea of decomposing a given image into two or even more additive components, and, by this, dividing the original image content into a cartoon-like part, a texture part and a noisy part.

A prominent example is the method proposed by Rudin, Osher and Fatemi (ROF) [6], which utilizes Total Variation (TV) regularization. The ROF method deals with two image components, one for the noise-free cartoon content and one for both texture and noise. Fig. 2 shows a examples of decomposing a noisy test image into such parts. Interpreting both image parts as functions, they can be characterized as follows:

- The cartoon-like part, commonly denoted by  $u$ , is given as function of bounded total variation.
  - Due to the work of Meyer [4], the texture + noise part denoted by  $v$  can be described by introducing the so-called G-space, a space of functions, which are given as the divergence of some function  $p$ .
  - The sum of  $u$  and  $v$  gives the input data  $f$ .
- For the ROF approach, it turns out that function  $p$  has to lie in a certain convex set  $\mathcal{C}$ .

Therefore, we can find a smoothed version of noisy data  $f$  by projecting them onto the convex set  $\mathcal{C}$  given as  $\mathcal{C} = \text{div } \mathcal{D}$ , i.e. we have to find  $v$ , such that  $v = \text{div } p$  and  $p$  lies in the given set  $\mathcal{D}$ .

### Methods

The above geometrical formulation of TV regularization based on constraint set allows for an intuitive generalization. For the standard ROF model, the constraint set  $\mathcal{D}$  can be locally characterized as circles of fixed radius. An adaptive generalization then is to consider circles of locally varying size, or in view of anisotropic variants, to move from circles to other convex sets like rectangles, parallelograms or ellipses.

In each case adaptivity has to be steered by additional information obtained from the image structure, e.g. edge location and direction.

In order to obtain the required information, two concurrent strategies exist in literature. The first evaluates the noisy input data in a preprocessing step. Gaussian presmoothing is used to reduce the influence of noise. The second strategy is to estimate the required data parallel to the primary optimization problem.

In our work [2, 3] we propose a new strategy, where the adaptivity is defined directly depending on the unknown noise-free image. We refer to this approach as solution-dependent adaptivity. By this approach structural information is not influenced by the noise of the input data. As a result, adaptivity can be tuned in more effectively, see Sect. below.

Due to the proposed generalization we move from a convex optimization problem to a non-convex

one and thus theory of convex optimization can no longer be applied. In our theoretical work, we therefore reformulate the optimization problem as a quasi-variational inequality (QVI), which allows us to adapt existing theory from this field as well as suitable algorithms (cf. [1, 5]).

### Results

We compare our approach of solution-dependent adaptivity for TV regularization to two TV approaches from literature: the standard ROF model and an adaptive TV approach, where the adaptivity is determined by examining the noisy input image (we refer to this as data-dependent adaptivity). Fig. 1 and Fig. 2 show the different results for denoising a test image (left image). Smoothing with the standard ROF model (Fig. 2 middle) removes the noise but also some of the image structures, which become part of the noise component  $v$  (cf. Fig. 2 right).

For both TV variants with data- and solution-dependent adaptivity, we use the same parameters providing a weak presmoothing and a relatively strong anisotropy, which in both cases results in a good preservation of image structures. With the data-dependent adaptivity (Fig. 1 middle), however, a part of the noise is regarded as image structures and thus is also preserved. This is due to the fact that the adaptivity is defined based on the noisy input data. In contrast, the result of the solution-dependent approach (Fig. 1 right) shows a good denoising capability while preserving most of the edges and without producing artifacts from noise. Increasing the presmoothing parameters or decreasing the anisotropy would prevent noise artifacts in the data-adaptive approach but also the preservation of weak image structures and



Fig. 2: Decomposition of a noisy image  $f$  into a geometric component  $u$  and a noise component  $v$ . Here we used the ROF model [6]. The noise component contains unwanted structures from the original noise-free data.

thus lead to a inferior quality of the denoised image. To sum up, solution-dependent adaptivity allows us to refrain from a strong presmoothing and to use a strong anisotropy to preserve and regularize image edges.

We successfully applied our approach to various applications within the HCI research projects, e.g. for regularizing depth maps or optical flow.

Funding: HCI

### References

[1] D. Chan and T. Pang. The Generalized Quasi-Variational Inequality Problem. *Math. Operat. Res.*, 7(2):211–222, 1982.

[2] F. Lenzen, F. Becker, J. Lellmann, S. Petra, and C. Schnörr. A class of quasi-variational inequalities for adaptive image denoising and decomposition. *Computational Optimization and Applications*, 2012.

[3] F. Lenzen, F. Becker, J. Lellmann, S. Petra, and C. Schnörr. Variational Image Denoising with Adaptive Constraint Sets. In *Proceedings of the 3rd International Conference on Scale Space and Variational Methods in Computer Vision 2011*. Springer, 2012.

[4] Y. Meyer. *Oscillating Patterns in Image Processing and Nonlinear Evolution Equations*, vol. 22 of *Univ. Lect. Series*. Amer. Math. Soc., 2001.

[5] Y. Nesterov and L. Scriali. Solving strongly monotone variational and quasi-variational inequalities. *Core Discussion Paper 2006/107* [http://www.core.ucl.ac.be/services/psfiles/dp06/dp2006\\_107.pdf](http://www.core.ucl.ac.be/services/psfiles/dp06/dp2006_107.pdf), Nov 2006.

[6] L. I. Rudin, S. Osher, and E. Fatemi. Nonlinear Total Variation Based Noise Removal Algorithms. *Physica D*, 60(1-4):259–268, 1992.

## INFERENCE IN MARKOV RANDOM FIELDS BASED ON PRIMAL-DUAL CONVEX OPTIMIZATION

B. Savchynskyy, S. Schmidt, J. H. Kappes

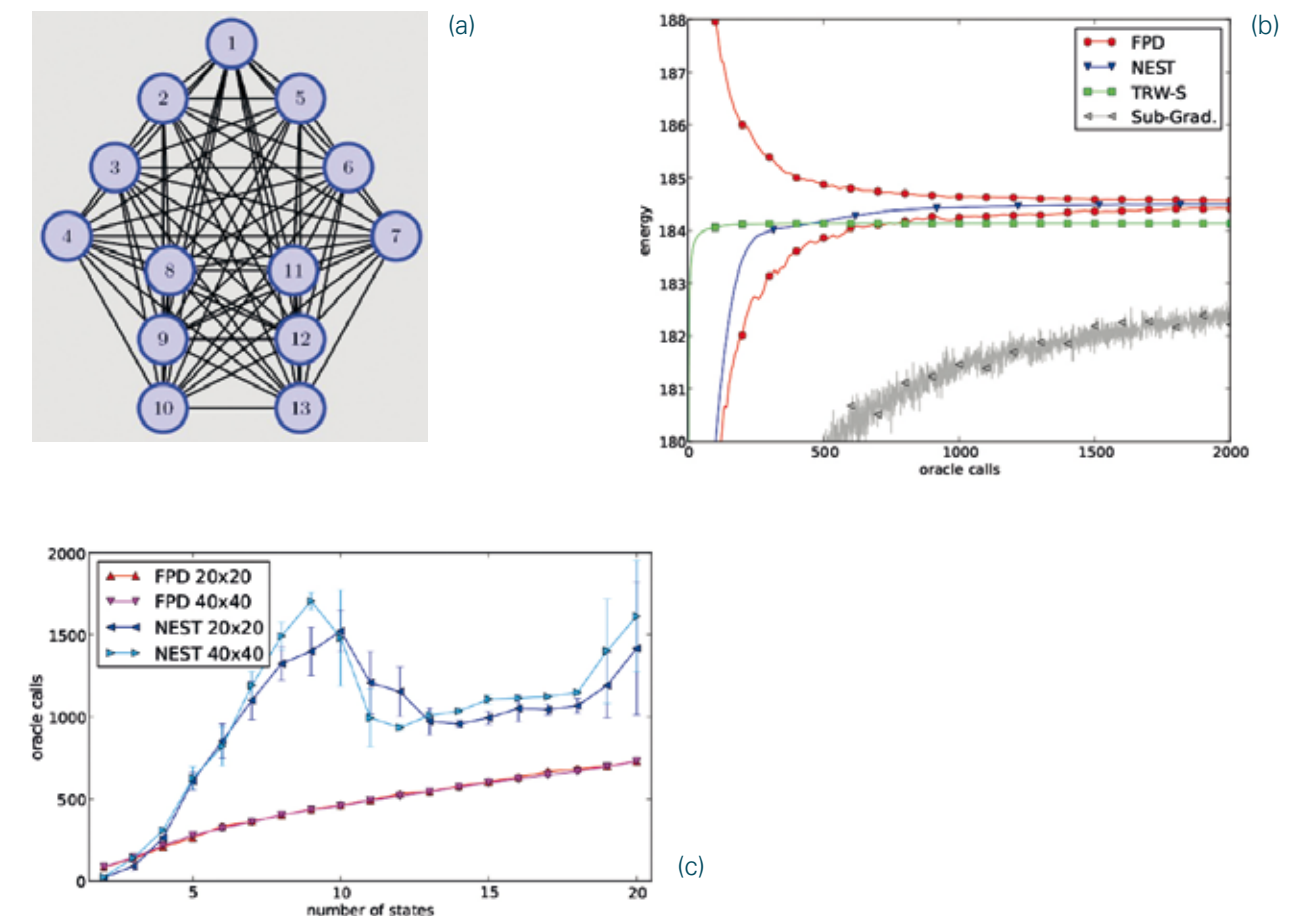


Fig. 1: Top left (a): an example of a graphical model. Nodes correspond to random variables, edges describe conditional statistical dependence between variables.

Top right (b): Plot shows convergence of objective function value (the vertical axis) with respect to the time (measured in oracle calls) for different methods. The decreasing curve correspond to a primal objective, increasing curves - to dual ones. Red curves correspond to the investigated FPD method [3], other colors - to competing methods. The only visible curve for a primal objective belongs to FPD. Other primal objectives are incomparably worse - they even do not fit into the plot. However the fastest convergence w.r.t. the dual objective is demonstrated by our competing method NEST [2].

Bottom (c): Plot shows how the time (measured in oracle calls) needed to achieve a certain precision depends on the number of possible random variables' states (the horizontal axis). Red curves - the investigated FPD method, blue curves - our competing NEST method. The plot shows that as the number of labels increases, FPD performs better than others.

We investigate a novel primal-dual optimization algorithm for maximum a posteriori inference for graphical models. Such models became an important tool for image analysis nowadays. In its turn the inference problem is the central for in many applications.

### Background and Goals

Markov random fields and graphical models associated to them play an important role for image processing. In the last years they became a modeling tool widely used in nearly all subfields from medical imaging to 3D scenes reconstruction. One bottleneck of this framework, which we treat in this project, is associated to the inference problem, i.e. estimating values of hidden variables of the field. Since the problem is NP-hard in general one has to consider either its special cases or solvable relaxations.

There is a family of methods based on so called *Graph Cuts*. They are quite efficient, but can be applied only when the prior probability distribution (decoded in edges of the graph) has a certain form, i.e. they consider special cases of the problem.

Alternative class of methods, addressing convex relaxations of the problem does not have this restriction. However it turns out that even the simplest linear programming relaxation constitutes a convex problem with billions of variables and out-of-the-shelf solvers either can not be used at all or are restricted to specific scenarios. Hence specialized solvers have to be developed. This fact was recognized by the community and a series of methods were proposed in the recent past years. These methods however operate either in primal or in a dual space of the corresponding linear programming problem.

The dual objective is easier and thus can be easier optimized, however reconstructing a primal solution out of the dual one is not easy and could require significant computational efforts. Contrary, primal methods deal with more difficult optimization and thus are less efficient. They operate however with primal variables directly and getting an approximate primal solution in this case is quite straightforward.

Our goal is to combine advantages of both approaches (primal and dual) in a primal-dual framework.

### Methods and Results

As the first step we considered (see [3] for details) the First-Order Primal-Dual (FPD) algorithm proposed in [1] and widely used in the related field of variational image processing. It has several advantages comparing to others:

- (i) its iterate converge to the optimum of the relaxed primal and dual problems, i.e. it recovers both solutions at once;
- (ii) it has a good and theoretically substantiated convergence rate;
- (iii) it can be easily modified to compute a duality gap, which leads to a clear stopping condition.

The method is very general and, what is very important, has a very high degree of possible parallelization. We compared its performance to a series of state-of-the-art dual solvers (see Fig.1) and found that

- as expected, it significantly speeds-up convergence of the primal bound to the optimum comparing to purely dual methods;
- its convergence does not slow down rapidly as the number of variable states increases, as it is typical for dual methods;

However this algorithm has also several drawbacks:

- the method splits the initial problem into a collection of very small (and thus simple) subproblems. Specialized dual methods (like e.g. NEST proposed in our work [2]) treat larger subproblems and thus require less iterations to converge;
- it has to keep and operate directly all primal variables. This requires a lot of memory and purely dual methods does not have this drawback.

### Outlook and Future Work

The investigated primal-dual method

- is highly parallelizable;
- is guaranteed to converge to the optimum of the relaxed problem, moreover its convergence rate is optimal in a certain sense;
- demonstrates faster convergence of the primal objective, which indeed is of the interest for applications (not the dual one).

Our future work will address its further specialization to the problem structure to obtain advantages of other existing methods while preserving its own positive properties

*Funding: HCI / IPA*

### References

[1] A. Chambolle and T. Pock. A first-order primal-dual algorithm for convex problems with applications to imaging. *Journal of Math. Imaging and Vision*, 2011.  
 [2] B. Savchynskyy, J. Kappes, S. Schmidt, and C. Schnörr. A Study of Nesterov's Scheme for Lagrangian Decomposition and MAP Labeling. In *CVPR*, 2011.

[3] S. Schmidt, B. Savchynskyy, J. H. Kappes, and C. Schnörr. Evaluation of a First-Order Primal-Dual Algorithm for MRF Energy Minimization. In *EMM-CVPR*, vol. 5681 of LNCS, pp. 89–103. Springer, 2011.

## PEDESTRIAN PATH PREDICTION USING LEARNED MOTION MODELS

C. Keller, C. Schnörr

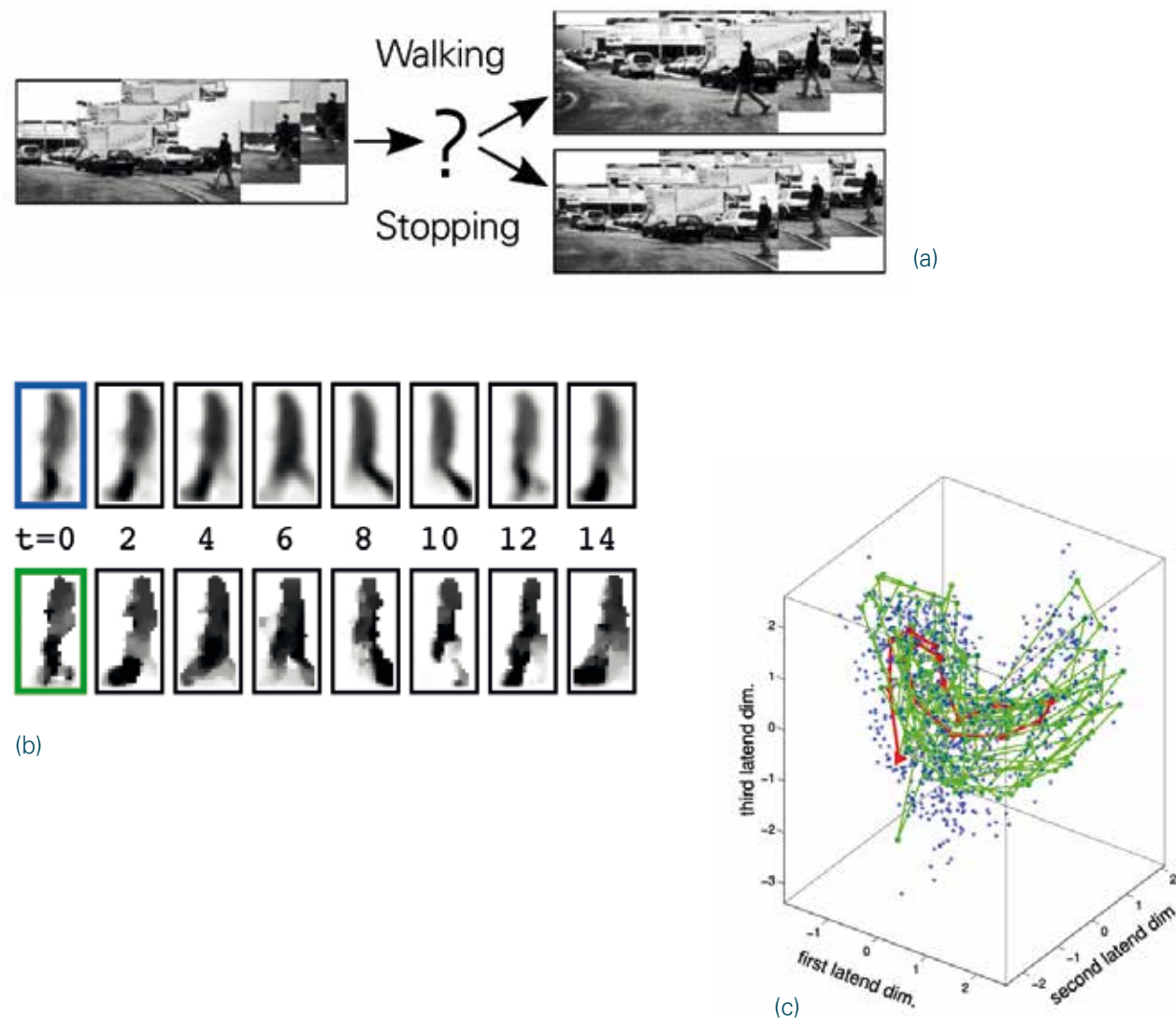


Fig.1: (a) Will the pedestrian stop or walk. (right) Low dimensional representation of dense optical flow features. (b) Learning the dynamics from pedestrian trajectory data allows the prediction of motion patterns. Observed optical flow feature (green box) and corresponding reconstructed feature (blue box). Reconstruction of the latent space prediction of a feature for different prediction time-steps (top). Features that will be measured at the corresponding time-steps (c).

Future vehicle systems for active pedestrian safety will not only require a high recognition performance, but also an accurate analysis of the developing traffic situation. In this work a system for pedestrian path prediction at short time intervals ( $< 1s$ ) is presented. Features extracted from dense optical flow are used to learn a low dimensional feature representation. These low dimensional features are integrated in a probabilistic filtering framework.

### Background and Goals

Strong gains have been made over the years in improving pedestrian recognition performance. However, the initiation of an emergency vehicle maneuver requires a precise estimation of the current and future position of the pedestrian with respect to the moving vehicle. One major challenge is the highly dynamic behavior of pedestrians, which can change their walking direction in an instance, or start / stop walking abruptly. As a consequence, prediction horizons for active pedestrian systems are typical short; even so, small performance improvements can produce tangible benefits. Accident analysis shows that being able to initiate emergency braking 0.16 s (4 frames @ 25 Hz) earlier, at a

Time-to-Collision of 0.66 s, reduces the chance of incurring injury requiring hospital stay from 50% to 35%, given an initial vehicle speed of 50 km/h.

### Methods and Results

We present a system for accurate pedestrian path prediction from a moving vehicle, at short time intervals. Features are extracted from dense stereo and dense optical flow data computed over the bounding box returned by a pedestrian detector. Lateral and longitudinal position of the pedestrian is obtained from disparity values on the pedestrian upper body. A low dimensional representation of optical flow features that captures motion patterns of moving pedestrians is learned from a set of training trajectories. Integrating the learned pedestrian motion model into a particle filter framework allows the prediction of future optical flow features. Speed changes in the pedestrian motion are derived from the predicted features. For larger prediction horizons (17 frames into the future) the proposed system outperforms state of the art Kalman Filter based systems with respect to localization errors.

Funding: Daimler AG

### References

[1] C. G. Keller, M. Enzweiler, and D. M. Gavrila. A new benchmark for stereo-based pedestrian detection. Intelligent Vehicles Symposium (IV), 2011 IEEE, pp. 691–696, 2011.  
 [2] C. G. Keller, C. Hermes, and D. M. Gavrila. Will the Pedestrian Cross? Probabilistic Path Prediction Based on Learned Motion Features. Proc. of the DAGM Symposium on Pattern Recognition, pp. 386–395, 2011.

## VARIATIONAL METHODS FOR IMAGE SEGMENTATION WITH SHAPE PRIORS

B. Schmitzer, C. Schnörr



Fig.1: A toy example. Left: a template shape represents the prior knowledge, middle: a given distorted input shape, right: output shape restored with our shape prior functional and a simple data fidelity term. Due to the metric-space representation the relative position and orientation of template and input does not play a role and the shape prior works completely isometry invariant.

Prior knowledge about the shape of objects constitutes an important cue for image segmentation. Constructing shape prior functionals entails a delicate trade-off between descriptive power and mathematical and computational feasibility. Simple approaches are often unsatisfying in properly describing the set of allowed shapes, while sophisticated techniques usually yield highly non-convex functionals that are difficult to handle from the optimization point-of-view.

In this project we try to develop efficient approximations to powerful but computationally intractable shape-similarity measures and to combine them with recent progress concerning convex variational relaxations of the segmentation problem.

### Background and Goals

Image labeling is one of the central problems in image processing and computer vision. One wants to assign a label to each point in the image domain based on local affinities and subject to regularity conditions for the transitions between regions of different assignments. Convex relaxation methods can today approximately solve such initially combinatorial problems with high accuracy.

However more complex criteria such as the shape of the labeled regions cannot be taken into account within this framework yet.

The question of how to mathematically describe and compare shapes has been raised in the context of the shape registration and classification tasks on 3D meshes. Representing shapes as metric spaces abstracts them from their embedding into the surrounding space. The resulting metric spaces are then compared by the Gromov-Hausdorff and the related Gromov-Wasserstein distance.

While this yields promising results there are some obstacles for direct application to image segmentation: the underlying optimization problems are combinatorial and non-convex and thus expensive to solve. In addition noisy data requires that one must not only compute the distance between fixed shapes but one needs to optimize over the shape itself as well.

We seek to overcome these problems by means of convex relaxation, yielding feasible models, while trying to preserve as much of the initial descriptive power of the Gromov-Wasserstein distance as possible.

### Methods and Results

By two subsequent approximation steps the initial Gromov-Wasserstein distance is converted into an optimal transport problem with a problem specific cost function. Hence, at all steps standard linear solvers can be used. In contrast to conventional optimal transport problems with cost functions based on mere distances our approach can correctly establish correspondences between objects after Euclidean transformations. Optimizing over a joint functional with a data fidelity and a shape prior term can reveal the sought-after shape regardless of its position and orientation (see Fig.1).

Although some additional difficulties arise, this in principle extends to a geodesic framework.

### Outlook and Future Work

Currently the prior functional consists only of linear terms thus having only limited descriptive power. Future work will include investigating the potential of higher order terms.

Funding: DFG, grant GRK 1653

## VARIATIONAL RECURSIVE JOINT ESTIMATION OF SCENE STRUCTURE AND EGOMOTION FROM MONOCULAR IMAGE SEQUENCES

F. Becker, F. Lenzen, C. Schnörr



Fig.1: Left: One frame of a monocular traffic image sequence with large displacements (arrows) up to 35 pixels induced by a fast moving camera. Our approach jointly estimates camera motion and (middle) a dense depth map (colour-encoded, superimposed on the frame).

Right: Reconstruction of dense scene structure based on the depth maps from the camera's viewpoint (green), and the corresponding camera track (red).

For driver-assistance systems it is essential to have a reliable representation of the surrounding scene. In this project we consider a monocular camera setup and develop an approach to jointly estimate the camera motion and a dense scene representation. Our formulation balances the model expressiveness and computational efficiency.

### Background and Goals

In this project we consider image sequences recorded by a single fast moving camera, e.g. mounted in a car. We exploit the apparent motion of the static scene induced by the camera movement – known as optical flow – to jointly estimate both the (unknown) camera trajectory as well as a scene

representation. In contrast to feature-based methods we estimate a dense depth map which provides distance information together with a reliability measure at any image position. Furthermore, we allow the camera to move freely (i.e. full translation and rotation) and not constrained to e.g. yaw and horizontal translation.

### Methods and Results

In view of an implementation in dedicated hardware, we chose a recursive formulation of the highly involved chicken-and-egg problem of jointly estimating egomotion and the depth map. This ansatz reduces data storage to a minimum as it requires only the two most recently recorded image frames

for computation. At the same time it allows to efficiently incorporate information from previous frames and thus increases robustness and temporal consistency.

We make use of established mathematical methods to solve the underlying optimisation problems arising from a variational formulation. Second-order Newton-like methods speed up convergence, especially for the high-dimensional depth map estimation. Accurate camera pose estimation is performed on the Euclidean manifold. For details we refer to [1].

The approach is evaluated by means of real traffic image sequences. The results compare favourably with two alternative settings that require more input data: The depth map estimated by our approach is verified by comparing to stereo methods which are based on image pairs recorded by stereo setups with much better motion parallax than the monocular scenario. The computed egomotion is compared to the camera tracks provided by a bundle adjustment implementation which have access to all image frames simultaneously.

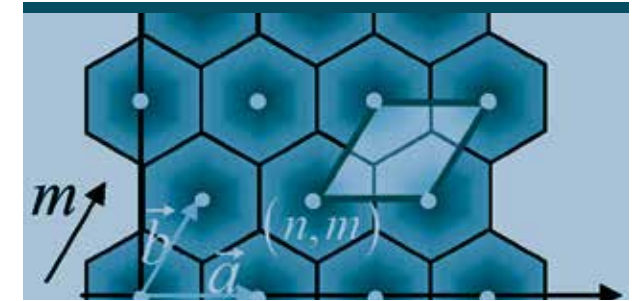
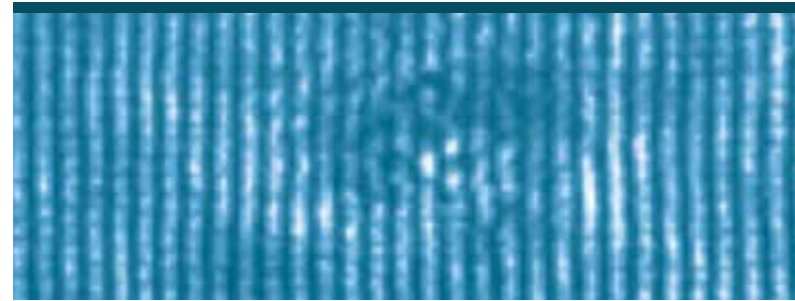
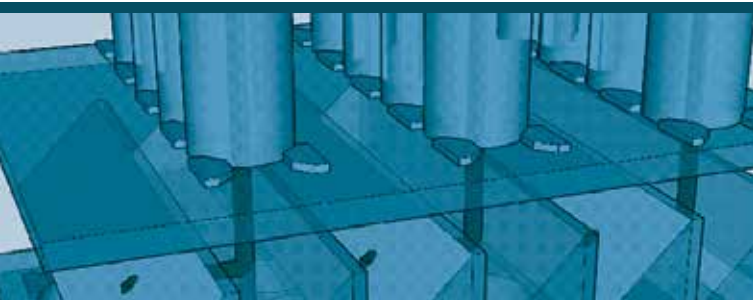
### Outlook and Future Work

Our current research concentrates at further refining the theoretical foundations of this approach. Future work involves verification of the accuracy and robustness as well as extension to motion-based segmentation of the scene.

*Funding: HCI*

### References

- [1] F. Becker, F. Lenzen, J. H. Kappes, and C. Schnörr. Variational Recursive Joint Estimation of Dense Scene Structure and Camera Motion from Monocular High Speed Traffic Sequences. In 2011 IEEE International Conference on Computer Vision (ICCV), pp. 1692–1699, 2011.



## CHAIR OF OPTOELECTRONICS PROJECT OVERVIEW

Prof. Dr. Karl-Heinz Brenner

ANALYSIS OF THE IMAGE ABERRATIONS PRODUCED BY SLIGHTLY SPHERICAL DICHROIC BEAM SPLITTERS IN THE IMAGING PATH .....	88
E. Slognat, P. Fischer, K.-H. Brenner	
ASPECTS FOR CALCULATING LOCAL ABSORPTION WITH THE RIGOROUS COUPLED-WAVE METHOD .....	90
M. Auer, K.-H. Brenner	
DESIGN OF THE ILLUMINATION PATH IN A MINIATURIZED PARALLEL FLUORESCENCE-MICROSCOPE .....	92
E. Slognat, K.-H. Brenner	
DETERMINATION OF THE JONES-MATRIX OF A SLM BY A MACH-ZEHNDER INTERFEROMETER WITH AN OFF-AXIS REFERENCE WAVE .....	94
X. Liu, K.-H. Brenner	
IMPLEMENTATION OF AN EFFICIENT FINITE DIFFERENCE METHOD FOR THE E-FIELD TO CALCULATE LIGHT PROPAGATION IN THE TIME DOMAIN .....	96
E. Treiber, K.-H. Brenner	
MONOLITHIC FABRICATION OF OPTICAL MICRO SYSTEMS .....	98
F. Merchán, K.-H. Brenner	

NUMERICAL LIGHT PROPAGATION BETWEEN TILTED PLANES .....	100
K.-H. Brenner	
RIGOROUS SIMULATION OF THE IMAGING PROPERTIES OF MAXWELL'S FISHEYE LENS .....	102
K.-H. Brenner	
TALBOT LENGTH OF RECTANGULAR AND HEXAGONAL GRATINGS .....	104
X. Liu, K.-H. Brenner	
THEORETICAL, NUMERICAL AND EXPERIMENTAL ANALYSIS OF A NEW CONCEPT FOR PARALLEL SCANNING MICROSCOPY .....	106
T. Stenau	

## ANALYSIS OF THE IMAGE ABERRATIONS PRODUCED BY SLIGHTLY SPHERICAL DI-CHROIC BEAM SPLITTERS IN THE IMAGING PATH

E. Slognat, P. Fischer, K.-H. Brenner

In a concept of a parallel multi-spectral fluorescence microscope, the excitation light and the emission light have to pass several dichroic beam splitters (Fig.1).

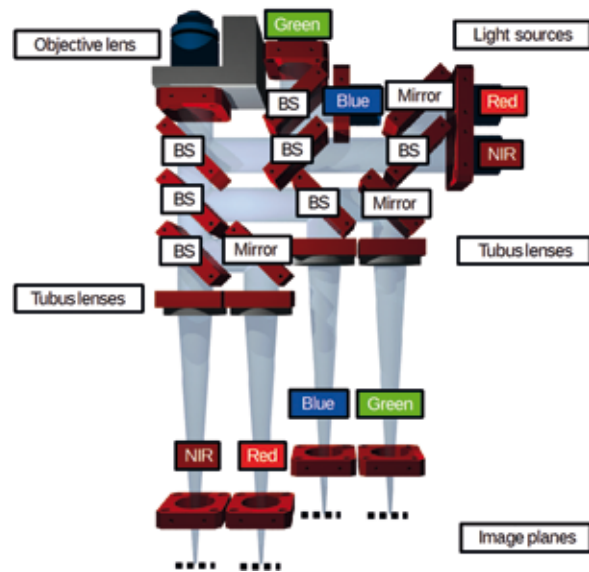


Fig.1: Schematic setup of a parallel multi-spectral fluorescence microscope

The system is infinity corrected and all beam splitters are located in the pupil plane. Thus the light beams passing through the beam splitters are almost collimated. The objective lens has a magnification of 10 and a NA of 0.45. The focal length of all tubus lenses is 164.5 mm and the diameter of the light beams is 20 mm.

Due to the fabrication process, all beam splitters in this project have a slight, primarily spherical surface (Fig. 2).

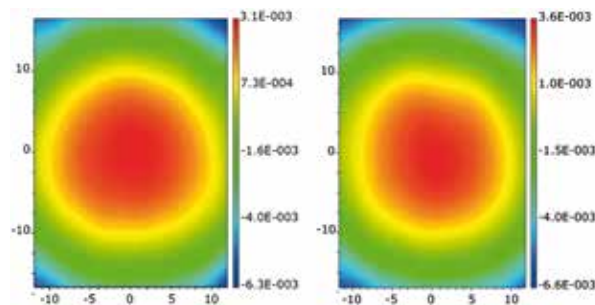


Fig.2: Measured surface profile of two different dichroic beam splitters (units: mm)

The spherical shape would be tolerable, if the incident angle of the light was orthogonal to the beam splitter surface. In this case the spherical part of the deformation could be compensated by refocusing (Fig.3). In this set-up, however, the beam splitters are at an angle of 45 degree with respect to the optical axis.

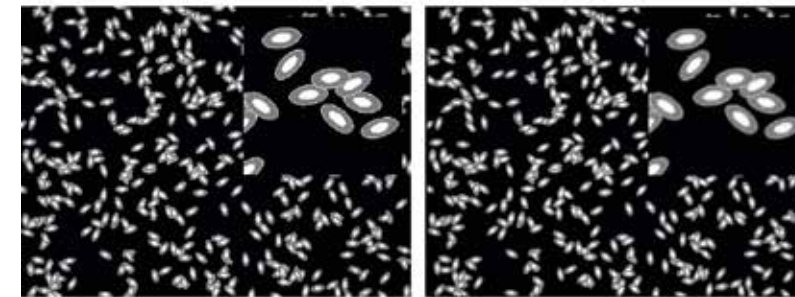


Fig.3: Simulated images (left: perfect mirror; right: with measured surface data of beam splitter as mirror and refocusing)

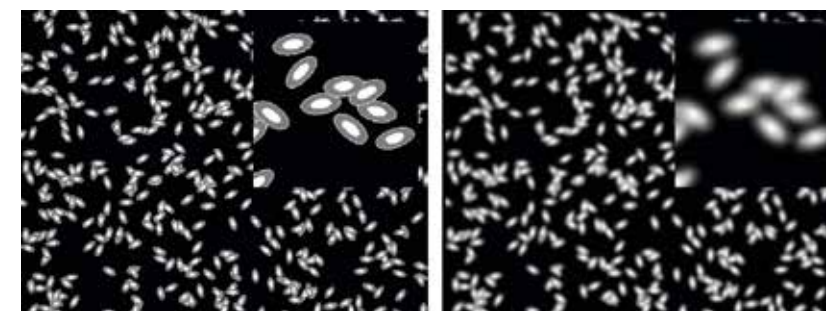


Fig.4: Simulated images (left: perfect mirror; right: with measured surface data of beam splitter as mirror)

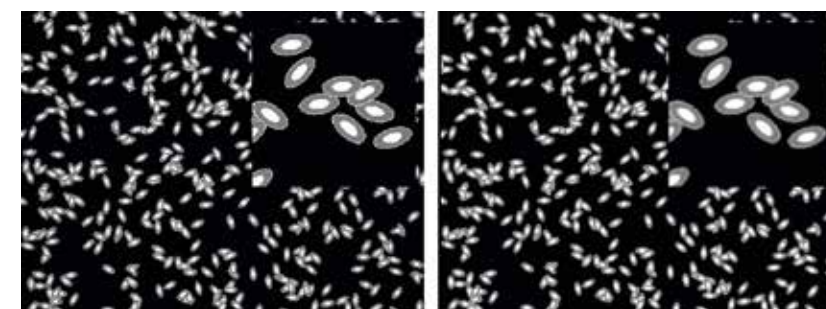


Fig.5: Simulated images (left: perfect mirror; right: with measured surface data of beam splitter as mirror and aperture behind tubus lens)

In the excitation path the deformations do not play a significant role. In the imaging path there are two different scenarios: When used in transmission, they mainly produce a phase shift, which does not affect image quality. When used in reflection, the deformations produce a position-dependent defo-

cus. Due to this local dependency the image is blurred (Fig.4). If an aperture is inserted behind the tubus lens, a sharper image is achieved again (Fig.5), but this improvement is accompanied by a loss of intensity.

## ASPECTS FOR CALCULATING LOCAL ABSORPTION WITH THE RIGOROUS COUPLED-WAVE METHOD

M. Auer and K.-H. Brenner

The Rigorous Coupled Wave Analysis (RCWA) is a method for the rigorous solution of the Maxwell's equations. It can be used to calculate the interaction between electromagnetic fields and periodic nanostructures, like optical gratings.

In most applications only the diffraction coefficients and efficiencies are the relevant quantities. Using the law of energy conservation, one can easily determine the *Global Absorption* from these quantities:

$$\text{Global Absorption} = 1 - \text{Transmission} - \text{Reflection} \quad (1)$$

The reasons for calculating the electromagnetic near fields on the other hand are mostly for visual display. In some newer applications though, like in the design and optimization of solar cells and extremely compact detectors, the *Local Absorption*, which is directly connected to the local fields, plays an important role. The relative absorbed and integrated power [1] is:

$$\frac{P_a}{P_{inc}} = \frac{k_0^2}{k_{inc,z}} \frac{1}{A} \iiint_V \text{Im}(\epsilon(\mathbf{r})) |\mathbf{E}_1(\mathbf{r})|^2 dV \quad (2)$$

The characteristics of the fields, however, strongly depend on a calculation time critical factor, which is the number of modes (or resolution of the frequency domain). In order to be able to calculate realistic fields even with a small mode count, different methods of field calculation were presented in the past. But this way the EM-fields, which are derived

from the RCWA, are not unique anymore. Here the theory of *Local Absorption* [1] provides a quantitative reference criterion as the following law must apply:

$$\text{Global Absorption} - \iiint_V \text{Local Absorption}(\mathbf{r}) dV = 0 \quad (3)$$

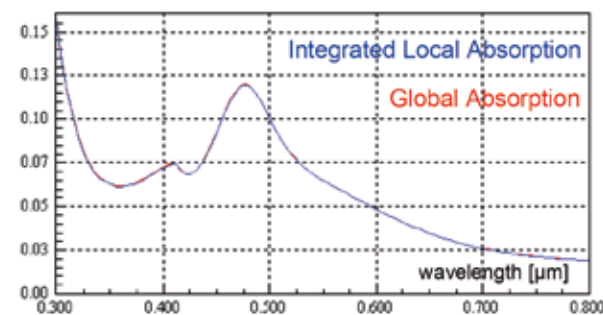


Fig.1: Integrated Local and Global Absorption for different wavelengths

For a homogeneous absorbing medium, *Global Absorption* and integrated *Local Absorption* are perfectly consistent, when calculating the local fields with the standard method (cf. fig1).

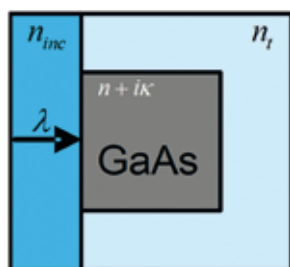


Fig.2: Geometry of a unit cell

For a structured absorbing medium (cf. fig2) though the two quantities agree only roughly (cf. fig3a/b). While in case of TE polarization the deviation can still be explained by the discretization of the simulation area, in the TM-case there is a systematic error.

A closer look on how the 2D-RCWA calculates the fields by default (4) shows that in all equations material parameters only occur as mode-limited and thereby continuous quantities. However, for the x-component of the electric field at a boundary surface, Maxwell only demands the continuity of the tangential components. But due to the material discontinuity at the boundaries one would also expect discontinuity of the electric field in normal direction.

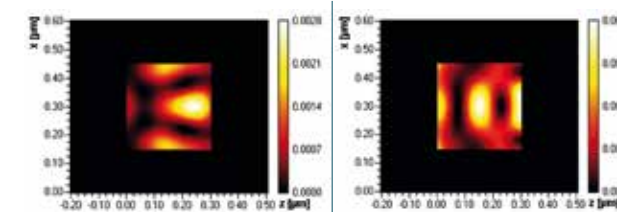


Fig. 3a:  
Local. Abs., TE-Pol.  
Global Abs.: 3.540%  
Integr. Loc. Abs.: 3.535%  
Error: 0.14%

Fig. 3b:  
Local. Abs., TM-Pol.  
Global Abs.: 1.389%  
Integr. Loc. Abs.: 1.479%  
Error: 6.48%

Therefore Lalanne & Jurek (5) derived the x-component from the continuous D-field and then multiplied with the local permittivity  $\epsilon(\mathbf{r})$ , in order to obtain the desired discontinuity. A method by Brenner (6) likewise derives the x-component from the continuous D-field, but then multiplies with the mode-limited permittivity.

$$E_x(x, z) = \sum_m e_m(z) \exp(ik_{x,m}x) \quad \mathbf{e}(z) = -i \cdot \mathbf{E}_a \mathbf{W} \mathbf{Q} \mathbf{D}(z) \quad (4)$$

$$E_x(x, z) = \frac{1}{\epsilon(x)} \sum_m d_m(z) \exp(ik_{x,m}x) \quad \mathbf{d}(z) = -i \cdot \mathbf{W} \mathbf{Q} \mathbf{D}(z) \quad (5)$$

$$E_x(x, z) = \sum_m e_m(z) \exp(ik_{x,m}x) \quad \mathbf{e}(z) = -i \cdot \mathbf{E}^{-1} \mathbf{W} \mathbf{Q} \mathbf{D}(z) \quad (6)$$

(4): Standard method, (5): Lalanne & Jurek, (6): Brenner

Using (3) as a target function, now the different approaches can be compared. Fig.4 shows that both improvements lead to significantly more consistent results.

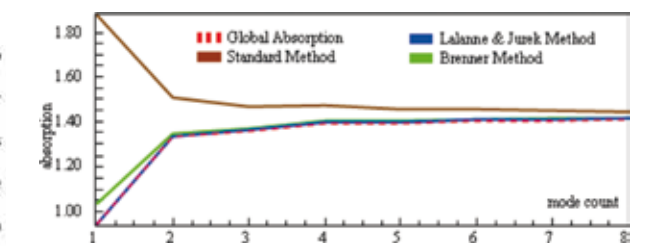


Fig. 4: convergence behavior of different field calculation methods

### Publications

[1] Brenner, K.-H. "Aspects for calculating local absorption with the rigorous coupled-wave method" *Optics Express*, Vol. 18, Issue 10, pp. 10369-10376 (2010).

## DESIGN OF THE ILLUMINATION PATH IN A MINIATURIZED PARALLEL FLUORESCENCE-MICROSCOPE

E. Slognat, K.-H. Brenner

To accelerate image acquisition in systems biology, a concept of a miniaturized parallel fluorescence-microscope was designed (Fig. 1). The imaging path was characterized by simulations and an experimental setup [1].

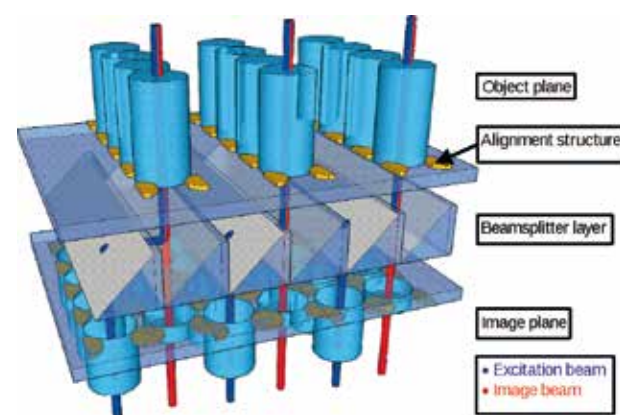


Fig. 1: Integration scheme of the miniaturized parallel fluorescence-microscope

Here a simulation of the illumination path is presented, which is designed for the fluorophore eGFP (Excitation maximum: 488 nm; Emission maximum: 507 nm). The field of view, which has to be illuminated, has a diameter of 400  $\mu\text{m}$ .

Fig. 2 shows the illumination path from the light source to the object plane.

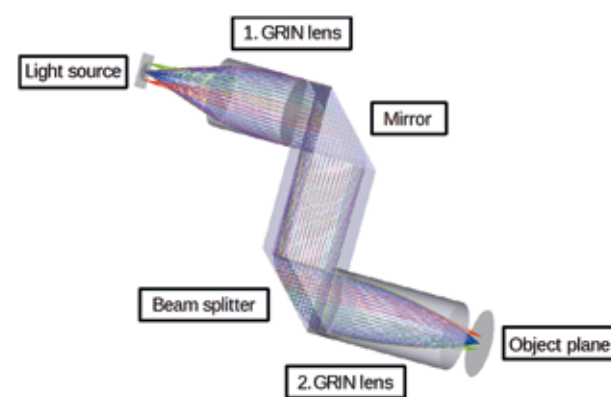


Fig. 2: Ray-trace of the illumination path of the micro-system

Since the second GRIN lens is also used in the imaging path, the only part which can be optimized is the first GRIN lens.

As light source a square Lambertian radiator with a length of the edge of 0.5 mm, a wavelength of 488 nm and a power of 1 mW is used.

The optimization goals are homogeneous illumination and low energy loss. An additional constraint was, that the light had to be almost collimated in the beam splitter layer. The optimization parameters are the length of the first GRIN lens, two fabrication parameter of the lens and the distance of the light source.

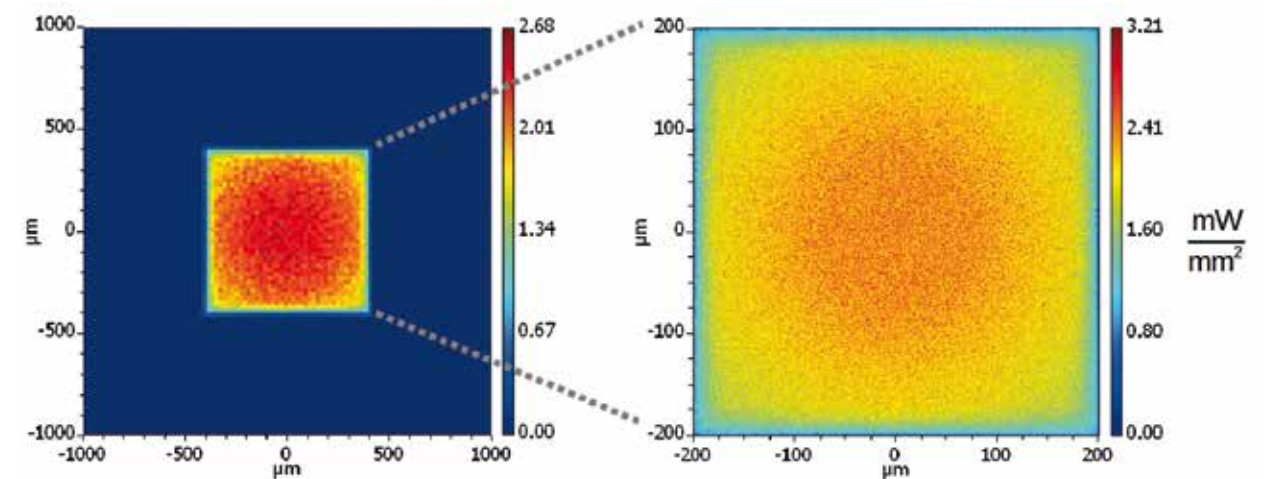


Fig. 3: Intensity distribution inside the field of view

Fig. 3 shows the simulated intensity distribution in the object plane. Considering the reflexion and transmission loss, the energy efficiency is about 33 %.

Due to the light source's characteristics, a homogenous illumination of the Field of View can only be reached by using additional optical components. The main part of the energy loss is produced by the beam splitter, which is essential for combining the illumination and imaging paths. Nevertheless an energy efficiency of about 33 % could be reached, which was enough to realize an illumination system using LEDs with high optical output power. Using GRIN-rods with a diameter of 2 mm, the total system size is smaller than a cube of 1 cm length.

### References

- [1] E. Slognat, R. Buschlinger, K.-H. Brenner, „Miniaturisierte parallele Mikroskopie in der Systembiologie“, DGaO-Proceedings (Online-Zeitschrift der Deutschen Gesellschaft für angewandte Optik e. V.), ISSN: 1614-8436, 111. Jahrestagung in Wetzlar (2010)
- [2] E. Slognat, K.-H. Brenner, „Design des Beleuchtungspfad für ein miniaturisiertes paralleles Fluoreszenz-Mikroskop“, (Online-Zeitschrift der Deutschen Gesellschaft für angewandte Optik e. V.), ISSN: 1614-8436-urn:nbn:de:0287-2011-P00x-x, 112. Jahrestagung in Ilmenau (2011)

## DETERMINATION OF THE JONES-MATRIX OF A SLM BY A MACH-ZEHNDER INTERFEROMETER WITH AN OFF-AXIS REFERENCE WAVE

X. Liu, K.-H. Brenner

The spatial light modulator (SLM) to be characterized was HOLOEYE's LC 2002, based on a translucent liquid crystal micro display with  $832 \times 624$  pixel and a pixel pitch of  $32 \mu\text{m}$ . The device modulates light spatially in amplitude and phase by addressing each pixel with an 8 bit grey value.

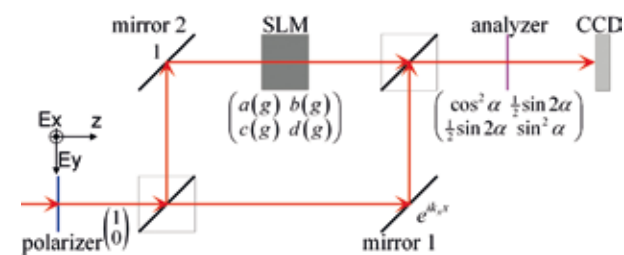


Fig. 1: Measurement setup: off-axis Mach-Zehnder interferometer

A Mach-Zehnder interferometer with an off-axis reference wave  $e^{ik_x x}$  (Fig. 1) is proposed to characterize the complex modulation of the SLM by a Jones matrix, which is dependent on the given grey value  $g$

$$\mathbf{J}(g) = \begin{pmatrix} a(g) & b(g) \\ c(g) & d(g) \end{pmatrix}, \quad a, b, c, d \in \mathbb{C} \quad (1)$$

The off-axis reference wave is set in such a manner that without any test object in the object path, the interference pattern on CCD shows vertical fringes (Fig. 2).

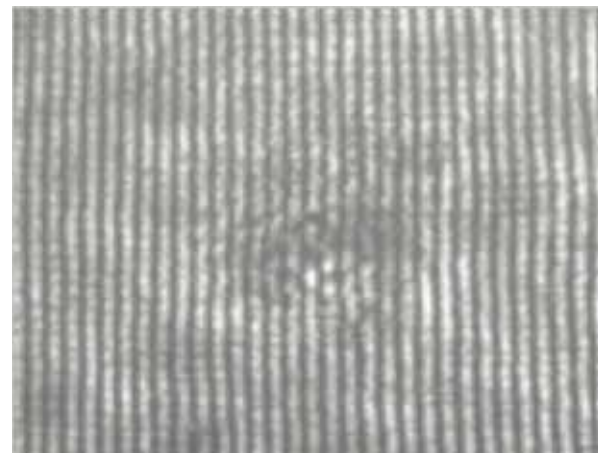


Fig. 2: Interferogram without SLM

If the SLM in the object path, is set by a grey value distribution as shown in Fig. 3 left, the contrast of interference fringes on the CCD will change and the fringe position will be shifted as shown in Fig. 3, right.

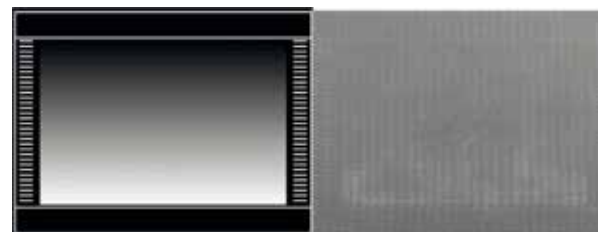


Fig. 3: Left: grey values distribution, right: interferogram on CCD

The complex Jones matrix for each grey value can then be derived from the contrast and the interference stripe shift by comparing them with the in-

itial situation of figure 2. For each grey value, the determination of all the 4 unknown complex parameters  $a, b, c, d$  requires at least 4 independent measurements of the contrast and the fringe shift. The independent measurements are realized here by adjusting the proper polarization states of the analyzer (Fig. 1). The polarizer is set in x-direction all the time.

To determine the complex parameters  $a, c$  the polarization state of the analyzer is set to x-direction firstly and then to  $\alpha=45^\circ$  with respect to the x-axis. The relationship of the measured contrast values and fringe shifts to  $a$  and  $c$  can then be represented by

$$\begin{aligned} \text{contrast}_{\alpha=0} &= |a|, & \text{shift}_{\alpha=0} &= -\arg(a), \\ \text{contrast}_{\alpha=45^\circ} &= \frac{1}{2}|a+c|, & \text{shift}_{\alpha=45^\circ} &= -\arg(a+c) \end{aligned} \quad (2)$$

To determine the complex parameters  $b, d$ , the SLM is rotated by  $90^\circ$  around the optical axis to swap the x- and y-axis of the SLM. Now in the coordinate system of the interferometer, the Jones matrix of SLM is transformed to

$$\mathbf{J}_{90^\circ}(g) = \begin{pmatrix} d(g) & -c(g) \\ -b(g) & a(g) \end{pmatrix}, \quad a, b, c, d \in \mathbb{C} \quad (3)$$

After the rotation of the SLM, the polarization state of analyzer is set to x-direction and then to  $\alpha=45^\circ$  with respect to the x-axis too.

The relationship between the measured parameters and the parameters to be determined are now expressed by

$$\begin{aligned} \text{contrast}_{\alpha=0} &= |d|, & \text{shift}_{\alpha=0} &= -\arg(d), \\ \text{contrast}_{\alpha=45^\circ} &= \frac{1}{2}|d-b|, & \text{shift}_{\alpha=45^\circ} &= -\arg(d-b) \end{aligned} \quad (4)$$

The evaluated 4 complex parameters  $a, b, c, d$  are shown in the following graphics in dependence of the grey value.

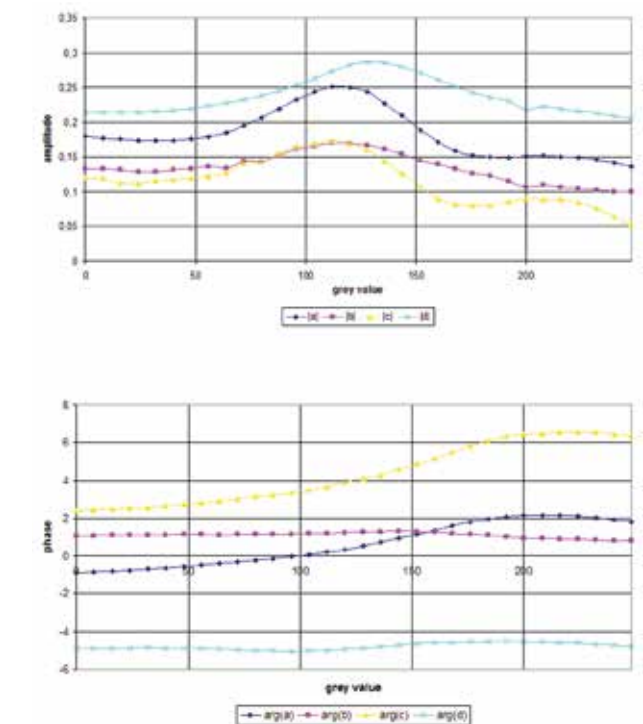


Fig. 4: Amplitude (top) and phase (bottom) of  $a, b, c, d$ .

## IMPLEMENTATION OF AN EFFICIENT FINITE DIFFERENCE METHOD FOR THE E-FIELD TO CALCULATE LIGHT PROPAGATION IN THE TIME DOMAIN

E. Treiber, K.-H. Brenner

In the thesis of my academic studies, I am dealing with a fast and rigorous method for the numerical simulation of the propagation of light. The aim is to calculate light propagation in different systems with only real electric fields in the time domain, so there is no need for any complex treatment or the introduction of magnetic fields. This reduction is possible without loss of accuracy for monochromatic light fields.

Starting with Maxwell's equations, for isotropic and linear media we expressed the magnetic field in terms of the electric field, resulting in a differential equation only for the real part of the electric field. A discretisation of this differential equation yielded a method to directly calculate the electric field in every inner point of the discretisation region with the knowledge of the field at two previous time steps.

What was (and is) more challenging than getting the finite difference equation is the implementation of

the source and the boundaries as they should represent physical reality; for example a source may be transparent or absorbing. Boundaries should indeed act as ideal absorbers and not reflect any unphysical wave back into the simulation region.

The aim of the work was to enable a user to construct any system he wants from a set of elementary layers like gratings or homogeneous regions, then set the parameters of the system, the source, choose the parameters for observation and, if he wishes to, the user can watch the light propagating through the system. Fig.1 shows the user interface. The elementary components are assembled as a tree structure in the top left corner of the window. Each component can be edited in the bottom left corner. The result of the simulation is displayed as electric field in the diagram tab of the window. The graphic- and the table-tab provide quantitative data such as transmission and reflection curves.

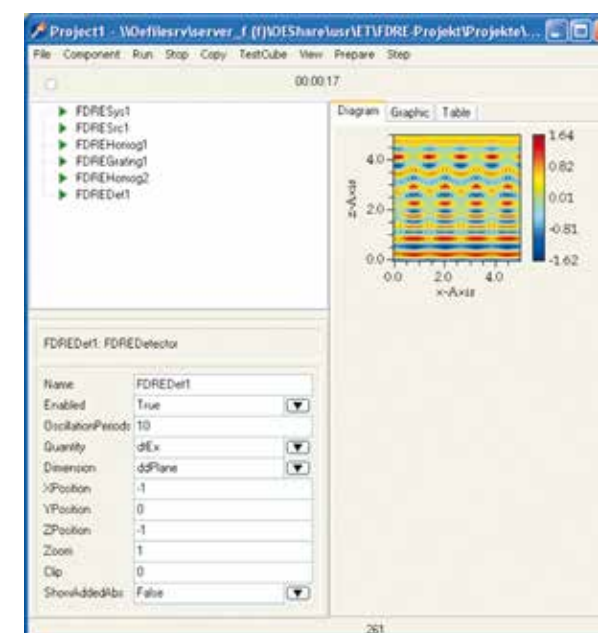


Fig.1: User interface of the finite difference time domain simulation tool.

For verification of the software, we used a simple interface between two different media, because the result is also known analytically. The result agreed very well with the theoretical results.

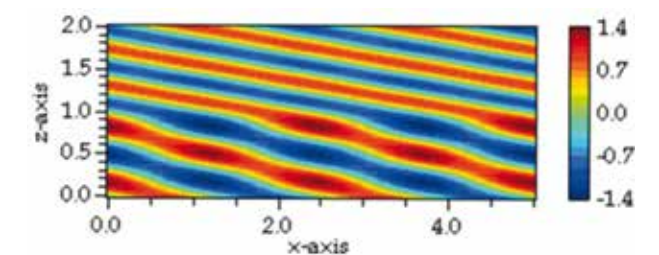


Fig.2: Verification of the software using a known problem, the reflection and transmission at a single interface

### References

- [1] A. Unger, K.-H. Brenner, "Vergleich exakter optischer Lösungsmethoden im Zeitbereich in Hinblick auf Genauigkeit und Effizienz," DGaO-Proceedings 2008, <http://www.dgao-proceedings.de>, ISSN 1614-8436, 109. Jahrestagung in Esslingen am Neckar/Deutschland (2008).

## MONOLITHIC FABRICATION OF OPTICAL MICRO SYSTEMS

F. Merchán, K.-H. Brenner

Recent works have confirmed the replication of metal masters as a very accurate and cost effective method for the fabrication of optical micro-devices. In fig.1 the fabricated metal master for a modern multi-channel system is shown. In this application we use the direct replication of metal masters for the fabrication of an optical coupler. The applicability of this method in micro-integrated systems makes it attractive for the development of new concepts as we present in the following.

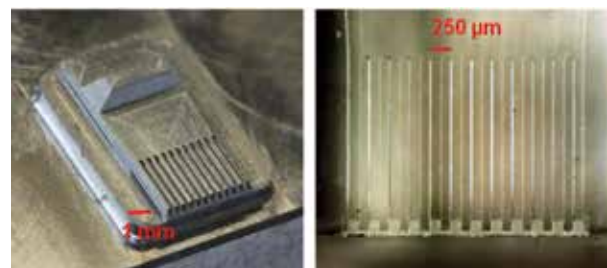


Fig.1: Metal master for the multi-channel system (left) and optical coupler (right)

According to Moore's law, the number of transistors that can be placed in a volume unit and thus the performance doubles every two years. Modern supercomputers achieve some Peta-FLOPS ( $10^{15}$  Floating point operations per second). The requirements for data transfer between devices grow correspondingly. At bandwidths above 1 GHz, electrical trans-

mission lines show high losses, therefore electrical signals can be transmitted only over very short distances (some cm) with an acceptable quality.

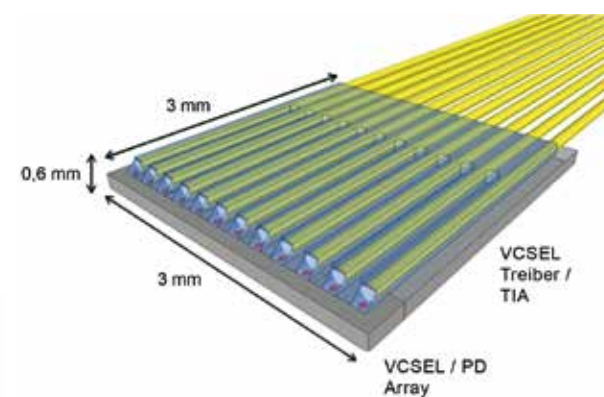


Fig.2: Optical systems fabricated directly on the arrayed electronics

This problem can be overcome by converting the electrical signal into an optical one. Independent of the application, the development of an integrated solution is nowadays unavoidable, in order to transmit high data rates over distances up to 100 meters.

In our concept, which is based on the coupling of a laser beam to a fiber using a mirror that redirects the beam by  $90^\circ$  [1], it is possible to integrate high speed microelectronics and micro-optical systems in a very small volume as shown in fig.2.

A solution that is suitable for industrial use requires a high reproducibility and cost effectiveness of the fabrication process. A PDMS (Polydimethylsiloxan) negative master fabricated from a metal positive master is UV-transparent enabling the replication of its shape on microchips, that are connected using e.g. a BGA (Ball Grid Array) package.

VCSELs and laser drivers for the sender or photodiodes and transimpedance amplifiers for the receiver are embedded in a single chip. Modern systems reach transmission rates of 12,5 Gigabits per second. A 12 channel system would have a data rate of 300 Gbps duplex.

New developments in the area of chip packaging make an effort for integrating several functional blocks like electrical connections, memory units, a processor unit, a logic device and the optoelectronic devices in a single package.

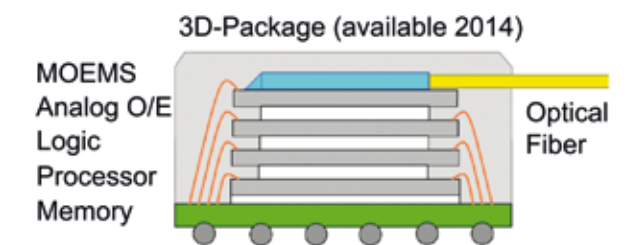


Fig.3: Possible future developments

A sketch of the concept is shown in the fig.3, in which additionally, the optical system is integrated in the package. As result, a compact computing unit working at very high speeds is no longer limited by the bandwidth of electrical transmission lines.

### References

- [1] F. Merchán, K.-H. Brenner, "Neuartiges Integrationskonzept für kostengünstige Herstellung optischer Mikrosysteme," DGaO-Proceedings (Online-Zeitschrift der Deutschen Gesellschaft für angewandte Optik e. V.), ISSN: 1614-8436, 112. Jahrestagung in Ilmenau, (2011).

## NUMERICAL LIGHT PROPAGATION BETWEEN TILTED PLANES

K.-H. Brenner

The numerical treatment of light propagation usually occurs between two planes perpendicular to the optical axis. Examples include the Fresnel propagation, the angular spectrum of plane waves (AS) or the Sommerfeld diffraction formula. Consequently the source plane and the destination plane are parallel. There are many situations, where one requires a propagation between non-parallel or tilted planes. For example, in tolerance analysis, one needs to know how much tilt of a lens or a detector plane is allowable for a given system configuration. Another very old example is the Scheimpflug condition, applied to reduce distortion in recording situations, where the camera looks at a tilted source plane. But also in micro optics there are several examples, where numerical light propagation between tilted planes is needed. One natural candidate is the parallel integration of optical components on a substrate surface (PIFSO) where the light propagation occurs at a 45° angle to the plane parallel surfaces. In one of our projects, the micro-integration of an optical fiber connector, we also required a numerical light propagation between tilted planes. In this project, light from a semiconductor laser falls on a 45°-mirror and is reflected towards the fiber. In order to analyse the sensitivity of this arrangement to mirror imperfections, the mirror plane had to be tilted.

The problem of light propagation has been reported by several authors, most recently in [1]. In all of these publications, the coordinate transformation from the source plane to the destination plane is treated as a single rotation around an axis - typically an elementary axis like the x- or y-axis. For a general tilt, the transformation has to be synthesized by a series of rotations around orthogonal axes, which complicates the treatment significantly.

In order to simplify this problem, we have taken a different approach. We assume, that there is a global coordinate system with the orthogonal unit vectors  $\mathbf{e}_x$ ,  $\mathbf{e}_y$  and  $\mathbf{e}_z$  and we define the source and the destination coordinate system in terms of this global system. Assume, the source coordinate system is defined by the three orthogonal unit vectors  $\mathbf{x}$ ,  $\mathbf{y}$  and  $\mathbf{z}$  and an origin vector  $\mathbf{o}$  and likewise the destination coordinate system is defined by the three orthogonal unit vectors  $\mathbf{X}$ ,  $\mathbf{Y}$  and  $\mathbf{Z}$  and an origin vector  $\mathbf{O}$ .

Then, the mapping of a point from the source coordinate system to the destination coordinate system can be described as

$$\begin{pmatrix} X \\ Y \\ Z \end{pmatrix} = \begin{pmatrix} \mathbf{xX} & \mathbf{yX} & \mathbf{zX} \\ \mathbf{xY} & \mathbf{yY} & \mathbf{zY} \\ \mathbf{xZ} & \mathbf{yZ} & \mathbf{zZ} \end{pmatrix} \begin{pmatrix} x \\ y \\ z \end{pmatrix} + \begin{pmatrix} (\mathbf{o}-\mathbf{O})\mathbf{X} \\ (\mathbf{o}-\mathbf{O})\mathbf{Y} \\ (\mathbf{o}-\mathbf{O})\mathbf{Z} \end{pmatrix} \quad (1)$$

The inverse operation can be determined in a similar way. The important difference to previous approaches is that no rotation matrix has to be constructed. All the quantities required for the transformation are available in the description of the unit vectors and the origins. Applying this transformation to the angular spectrum of plane waves method, we obtain

$$u(\mathbf{R}) = \frac{1}{(2\pi)^2} \iint \tilde{u}_0((\mathbf{t} \cdot \mathbf{K})_{\perp}) e^{i\mathbf{K} \cdot \mathbf{T} \cdot \Delta \mathbf{O}} e^{i\mathbf{K} \cdot \mathbf{R}} |\mathbf{J}_{t,K}| d^2 K_{\perp} \quad (2)$$

with  $\mathbf{T}=\mathbf{t}^{-1}$  as the transformation matrix and  $\Delta \mathbf{O}$  as the origin difference from eq. 1. All the contributions like the propagation phase shift and the Jacobian of the transformation follow naturally from the coordinate replacement. The most important aspect of eq. 2 is that tilted light propagation can also be treated by a standard Fourier transform, which enables a calculation which is almost as fast as the classical calculation.

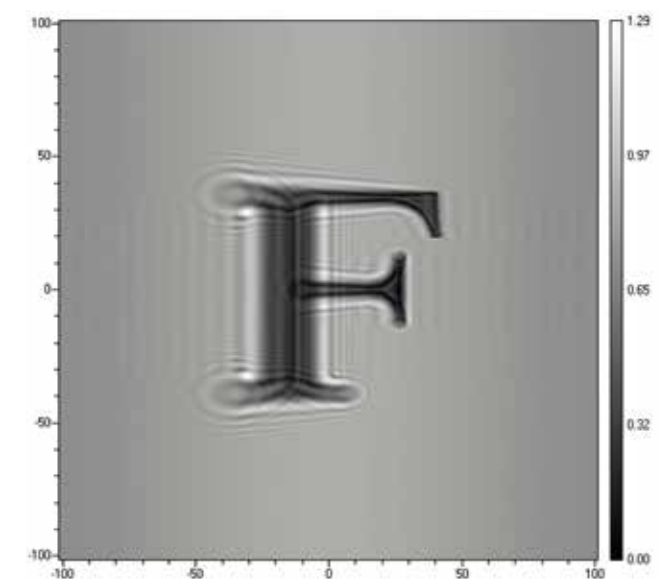


Fig.1: Numerical light propagation of a black letter F on white background to a plane separated by 30 μm and tilted by 45°

### References

- [1] K. Matsushima, H. Schimmel, F. Wyrowski - J. Opt. Soc. Am A, Vol. 20, No. 9, 1755 (2003).
- [2] K.-H. Brenner, „Aspekte der Lichtausbreitung zwischen verkippten Ebenen“, Jahrestagung der Deutschen Gesellschaft für angewandte Optik e. V. in Wetzlar (2010).

## RIGOROUS SIMULATION OF THE IMAGING PROPERTIES OF MAXWELL'S FISHEYE LENS

K.-H. Brenner

Recently, there has been considerable interest in the possibility of perfect imaging of Maxwell's fish-eye lens. Perfect imaging has been reported before by Zhang, Pendry and others [1] for the case of double negative index materials, where the negative index material performs as an amplifier for the evanescent waves. The new interest has been stimulated though a publication [2] by Ulf Leonhardt from St. Andrews university, where he claimed, that a Maxwell's fish-eye, well known from ray optics as a perfect imaging instrument, also performs perfect in the wave optical treatment. Perfect imaging in this context means that an arbitrarily small (sub-wavelength) light source will be imaged to the same size, thus breaking the Abbe resolution limit. This would be especially surprising since Maxwell's fish eye is composed of conventional gradient index material without any negative index effects.

The possibility of perfect focusing has been debated by a number of authors [3]. At the same time it appears to have been confirmed by microwave experiments.

Although it may not seem very practical to use tiny spheres for high resolution imaging, the understanding of the mechanisms could lead to new and unconventional imaging systems. Therefore we looked into this subject in a very straight forward way. Because we have all the simulation tools for

analysing this question readily available, we performed a simulation based on the rigorous coupled wave analysis.

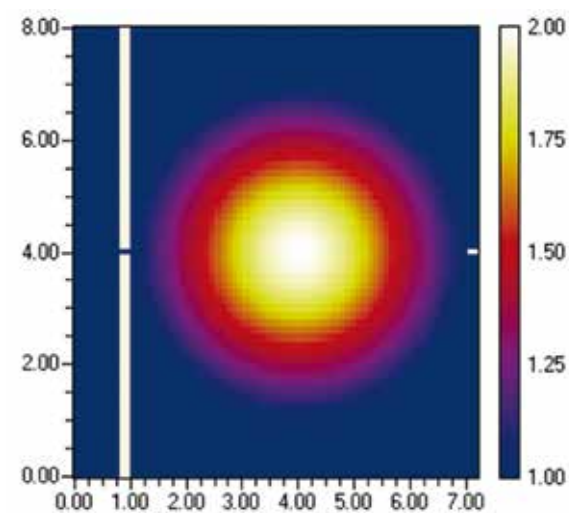


Fig.1: Index distribution of the model geometry of the fisheye lens used in the simulation

The model geometry is shown in fig.1. To generate a subwavelength sized source, we added a metal aperture of 100 nm, using 1000 nm wavelength for the source. The result of the simulation is shown in fig.2. At first, we notice, that it is very difficult to generate a source with a diameter of  $\lambda/10$ . Although we used TM-polarization, the transmitted amplitude has decreased considerably compared to the incident field. The other thing to note is that

the fisheye lens indeed generates an image spot, but the resolution is not below the Abbe resolution limit since the smallest features in the intensity according to Abbe should be  $\lambda/2$ , which agrees with the observation.

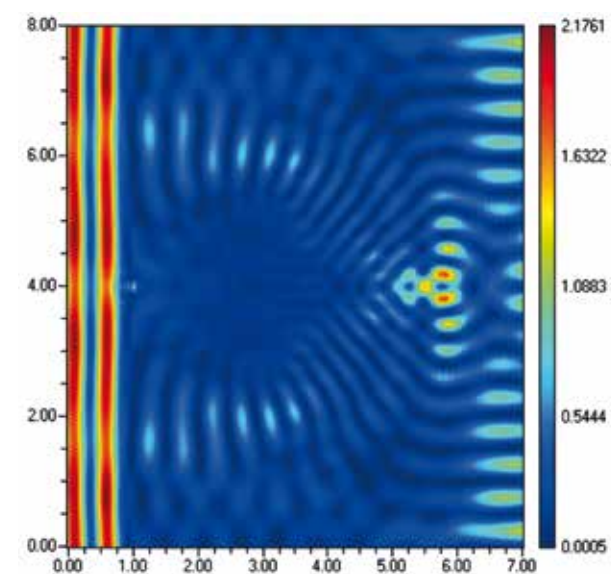


Fig.2: RCWA simulation of light propagation in a Maxwell fisheye lens using a 100 nm aperture and a 100 nm drain

lic drain of 100 nm diameter (fig.1, right side). The result of this simulation (fig.2) showed no notable difference to the case without a drain.

### References

- [1] K.-H: Brenner, „Plane Wave Decomposition in Layered Materials and Meta-materials“, 6th International Workshop on Information Optics, ed. J.A. Benediktsson, B. Javidi, K.S. Gudmundsson, American Institute of Physics (AIP), ISBN 978-0-7354-0463-2/07, pp 59–66, (2007).
- [2] U. Leonhardt „Perfect imaging without negative refraction“, New Journal of Physics 11 (2009) 093040.
- [3] R. J. Blaikie, „Perfect imaging without refraction? New Journal of Physics 13 (2011) 125006, 1367-2630.

In the discussion mentioned before, Leonhardt argued that a drain in the image plane is essential for the performance. Therefore we added a metal-

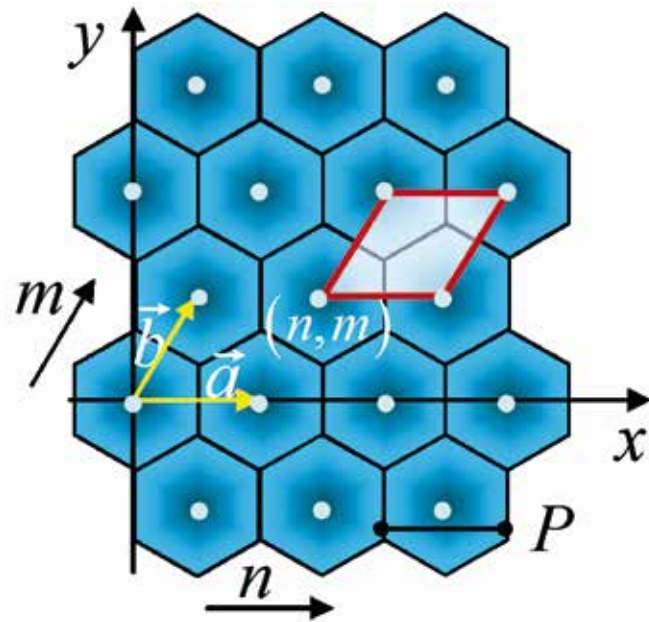


Fig.1: A hexagonal grating and its elementary cell

## TALBOT LENGTH OF RECTANGULAR AND HEXAGONAL GRATINGS

X. Liu, K.-H. Brenner

The Talbot effect is a well-known optical phenomenon: self-imaging effect. When a plane wave is transmitted through a periodic structure, the propagating wave replicates its amplitude distribution at multiples of a defined distance away from the periodic structure. This distance is named the Talbot length. It is well-defined for one-dimensional (1d) periodic structures:

$$z_{\text{Talbot}} = 2P^2/\lambda \quad (1)$$

where  $P$  is the period and  $\lambda$  the wavelength. For the two-dimensional case the derivation is not as straightforward as in the 1d case. In the context of a parallel scanning microscope, we have investigated the Talbot length of rectangular and also hexagonal gratings.

Since the Talbot effect is a near field diffraction effect in the paraxial approximation, it is a natural consequence of Fresnel diffraction. To determine the

Talbot length, we compare the grating amplitude  $|u_0|$  and its propagated amplitude  $|u_z|$ . It is clear, that a necessary condition of  $|u_z| = |u_0|$  leads to:

$$e^{-i\pi\lambda z \left( \frac{k^2}{P_x^2} + \frac{l^2}{P_y^2} \right)} = 1 \Rightarrow e^{-i2\pi z \left( \frac{k^2}{2P_x^2/\lambda} + \frac{l^2}{2P_y^2/\lambda} \right)} = 1 \quad (2)$$

Since  $k, l$  are integers, the condition above is fulfilled if and only if the smallest common multiple (LCM) of two real numbers exists:

$$z_{\text{Talbot}} = \text{LCM} \left( \frac{2P_x^2}{\lambda}, \frac{2P_y^2}{\lambda} \right) \quad (3)$$

The LCM of two integers or rational numbers is well-defined. Here, LCM is extended to any two real numbers and if existing, LCM is the smallest real number that is an integer multiple of both of two real numbers. However, the LCM of any two real numbers may not exist. For example, one can not find a real number, which is an integer multiple of

$\sqrt{3}$  and at the same time also an integer multiple of  $\sqrt{5}$ , therefore LCM of  $\sqrt{3}$  and  $\sqrt{5}$  does not exist. Hence, for an arbitrary rectangular grating, Talbot effect may or may not occur. For a square shaped 2d-grating ( $P_x = P_y = P$ ), the Talbot length is well-defined according to eq. 1

For a hexagonal grating with a period  $P$ , shown in Figure 1, the necessary condition to satisfy  $|u_z| = |u_0|$  is now

$$e^{-i\pi\lambda z \left( \frac{k^2}{P^2} + \left( \frac{2}{\sqrt{3}} \frac{l}{P} - \frac{1}{\sqrt{3}} \frac{k}{P} \right)^2 \right)} = e^{-i2\pi \frac{z}{3P^2/2\lambda} (k^2 + l^2 - lk)} = 1 \quad (4)$$

Since  $k, l$  are integers, this condition can be fulfilled if

$$z_{\text{Talbot}} = 3P^2/2\lambda \quad (5)$$

Thus, for a hexagonal grating, self imaging always exists and the Talbot length in a hexagonal geometry is well-defined by multiples of  $3P^2/2\lambda$  [1,2].

### Publications

- [1] John T. Winthrop and C. R. Worthington, „Theory of Fresnel Images. I. Plane Periodic Objects in Monochromatic Light“, JOSA, vol. 55, pp 373–380, (1965).
- [2] Peng Xi, Changhe Zhou, Enwen Dai and Liren Liu, „Generation of near-field hexagonal array illumination with a phase grating“, Opt. Lett. Vol. 27, pp 228–230 (2002).

## THEORETICAL, NUMERICAL AND EXPERIMENTAL ANALYSIS OF A NEW CONCEPT FOR PARALLEL SCANNING MICROSCOPY

T. Stenau

A new parallel scanning microscope as a non-imaging technology, which contains micro and macro optical components, is developed in a diploma thesis and was presented at the annual general meeting of the DGaO 2011 [1]. The concept is shown in figure 1.

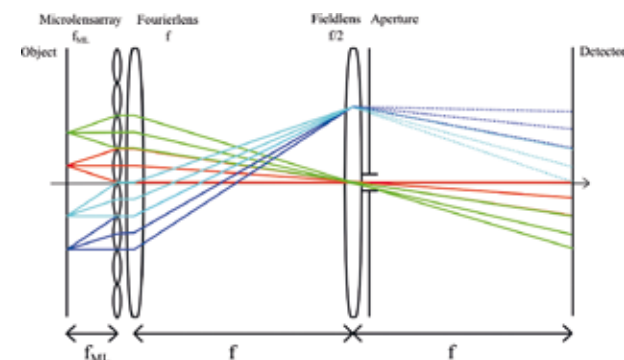


Fig.1: Path of rays of the concept

A micro lens array combined with a movable aperture images objects in the focus of the micro lenses on a detector. The image on the detector without the aperture is a superposition of all object points in front of the micro lenses, the aperture filters which points of the focal plane of the micro lens array are detected.

The system is analysed with scalar optical simulation tools and in an optical experiment. Different illuminations are compared and it is discussed whether the micro lens array can be replaced by a phase-step array.

The experiment showed that best results are achieved by using a spatially incoherent source such as an OLED instead of an LED or a coherent light source as the illuminating system, see figure 2.

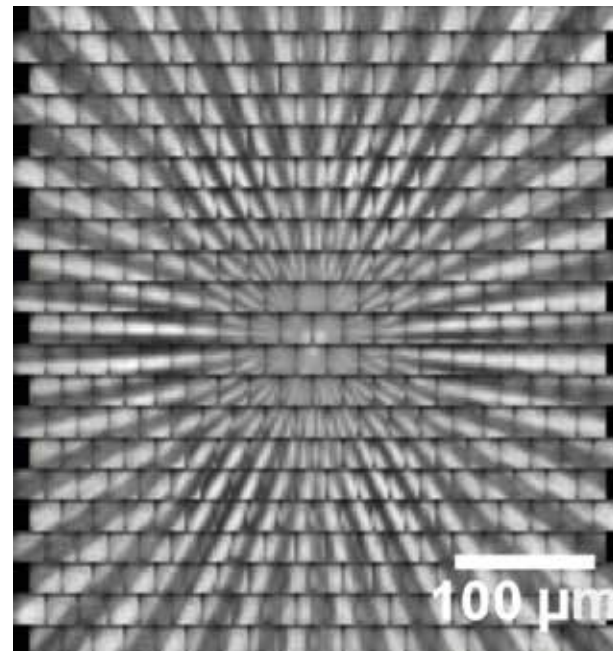


Fig.2: Result of the experiment with an OLED as illuminating source

The experimentally achieved resolution using a micro lens array was measured as  $3.4 \pm 0,2 \mu\text{m}$ . This resolution is close to the Rayleigh limit of  $3.0 \pm 0,2 \mu\text{m}$  and confirms the theoretical values, so the capabilities of this new system are validated.

### Publications

[1] T. Stenau, X. Liu, K.-H. Brenner, „Analyse eines neuen Systemkonzepts zur parallel scannenden Mikroskopie“, DGaO-Proceedings (Online-Zeitschrift der Deutschen Gesellschaft für angewandte Optik), ISSN 1614-8436-urn:nbn:de:0287-2011-P005-9, 112. Jahrestagung, 14.-18. Juni 2011, Ilmenau, (2011)

## RESEARCH GROUP ADVANCED COMPUTER ARCHITECTURE

Holger Fröning<sup>1</sup>, Heiner Litz<sup>1</sup>, Sven Kapferer<sup>1</sup>, Alexander Giese<sup>1</sup>, Christian Leber<sup>1</sup>, Maximilian Thürmer<sup>1</sup>, Federico Silla<sup>2</sup>

<sup>1</sup>University of Heidelberg, Germany

<sup>2</sup>Technical University of Valencia, Spain

Today's computing landscape is driven by the demand for more computing power together with a trend towards data-intensive computing. Despite the fact that technological advances and architectural improvements steadily increase the amount of computing power, the demands of many applications still cannot be satisfied. Data-intensive applications are not primary dependent on computing power, but rather on storage and memory solutions to handle a vast amount of data. The complete computing landscape will become more data-centric and the sheer amount of data demands new techniques to handle this trend.

This research group focuses on new and innovative techniques to provide solutions for both compute- and data-intensive applications. In particular we have identified that global address spaces might improve state-of-the-art technologies significantly. However, today architectures either completely aggregate or disaggregate all resources, in particular resources like computing cores and main memory. Message passing systems are prominent examples for overall disaggregation, and coherent shared memory architectures for overall aggregation. Instead, we propose to decouple resources aggregation in a way that the kind of aggregation can be chosen depending on the application. For instance, data-intensive applications might choose to aggregate only main memory, and not computational cores. Another aspect of current research is relaxing consistency in a way that the overhead for coherency

protocols can be reduced. This allows to replace current message-passing programming paradigms with shared-memory ones, for an easier programming and more efficient use of parallel computers. The research areas this year include in-memory databases, data-intensive calculations, relaxed consistency models and high performance and scalable synchronization primitives. This research has been conducted in close collaboration with the Technical University of Valencia, represented in this research group by Prof. Dr. Federico Silla.

In detail, we have used our proposal of globally non-coherent, but locally coherent global address spaces (called MEMSCALE) in order to evaluate the execution of data-intensive calculations on remote memory resources. Using MEMSCALE, the vast memory requirements of such applications can be addressed by leveraging distributed memory resources, but providing a binary-compatible interface to the applications [2]. Applications benefit from avoiding secondary storage and their run-time decreases dramatically.

Compared to this execution which is constraint to the scope of a single node, we have developed a suitable task and consistency model for parallel execution [1] [5]. A new relaxation allows avoiding continuous coherency, and only makes guarantees about visibility and consistency at synchronization points like locks or barriers. An evaluation shows that the scalability of message passing can now be reached with shared memory programming. Rela-

ted to this work is our main focus of 2011: using MEMSCALE for distributed in-memory databases [3][4]. We rely on distributed memory resources for in-memory databases, and can avoid the slow secondary storage while still benefitting from the low access latency of DRAM. Preliminary evaluations show a speed up of up to 77x, motivating us to continue with this research line: further research will

include more sophisticated data placement, write support and improved integration into local coherency domains.

*Supported by grants: Spanish MEC and MICINN, European Commission FEDER funds (CSD2006-00046, TIN2009-14475-C04), Cooperation: Technical University of Valencia*

### References

- [1] Holger Fröning, Hector Montaner, Federico Silla, Jose Duato, On Memory Relaxations for Extreme Manycore System Scalability, 2nd Workshop on New Directions in Computer Architecture (NDCA-2), held in conjunction with the 38th International Symposium on Computer Architecture (ISCA-38), June 2011, San Jose, California.
- [2] Hector Montaner, Federico Silla, Holger Fröning, Jose Duato, Unleash your Memory-Constrained Applications: a 32-node Non-coherent Distributed-memory Prototype Cluster, 13th IEEE International Conference on High Performance Computing and Communications (HPCC-2011), Sept. 2–4, 2011, Banff, Canada.
- [3] Hector Montaner, Federico Silla, Holger Fröning, Jose Duato, MEMSCALE: a Scalable Environment for Databases, 13th IEEE International Conference on High Performance Computing and Communications (HPCC-2011), Sept. 2–4, 2011, Banff, Canada.

- [4] Hector Montaner, Federico Silla, Holger Fröning, Jose Duato, MEMSCALE: In-Cluster-Memory Databases, 20th ACM Conference on Information and Knowledge Management (CIKM2011), demo session, Oct. 24–28, 2011, Glasgow, UK.

- [5] Holger Fröning, Alexander Giese, Hector Montaner, Federico Silla, Jose Duato, Highly Scalable Barriers for Future High-Performance Computing Clusters, 18th annual IEEE International Conference on High Performance Computing (HiPC 2011), Dec. 18–21, 2011, Bangalore, India.

## RESEARCH GROUP ADVANCED DETECTORS FOR SCIENTIFIC AND MEDICAL APPLICATIONS

### I. Peric

#### Introduction

Design of active pixel sensors in commercial IC-technologies is the main research field of our group. The sensors we develop employ very sophisticated pixel- and readout electronics, which makes them able to detect the single elementary particles, to measure their arrival time with nanosecond time resolution or to operate in a harsh radiation environment.

The aimed applications of our sensors are particle physics, synchrotron radiation experiments and medical imaging. Until recently, only non-commercial sensor technologies had the required properties for such applications. In last decade, several research groups (and among them ours) started investigating the possibility to use the commercial IC technologies for the development of the scientific-grade pixel sensors. This could make the research in the above mentioned field less expensive.

In 2011, we have focused our work to the development of sensors for two particle physics experiments.

In collaboration with Faculty for Physics and Astronomy, University of Heidelberg, we are developing a pixel sensor for a muon decay experiment (Mu3e) at Paul Scherrer Institute (PSI) in Switzerland.

In collaboration with several groups involved in ATLAS experiment at CERN (Bonn, Berkeley, CERN, Marseille) we are investigating the possibility to use our sensors as the particle tracker in ATLAS-upgrade.

We are also developing the sensors in SOI technology for synchrotron radiation experiments within SOI collaboration.

Another smaller research theme is the sensor for transmission electron microscopy. Application in PANDA experiment at GSI is also planned, our partner is Mainz University.

The key point of our research was so far the development of the novel "smart diode array" (SDA) detector structure. We are developing such sensors since 2006.

#### SDA Technology

SDAs are detector family that allows implementation of low-cost and thin radiation-tolerant detectors with good time resolution. Beside charge collection by drift, the unique property of these detectors is that the CMOS processing electronic is embedded inside sensor diodes.

In the R&D phase of the development (2006-2011), we have demonstrated a radiation tolerance of 1015 neq/cm<sup>2</sup>, nearly 100% detection efficiency and a spatial resolution of about 3 micrometers. As already mentioned; since 2011, the smart diode arrays have first applications: The technology is presently the main option for the pixel detector of the planned Mu3e experiment. Two 50-micrometer thin detector layers with 200 million pixels are planned.

Thanks to its high radiation tolerance, the SDA technology is also seen at CERN as a promising alternative to standard options for ATLAS upgrade and CLIC. In order to test the concept, within ATLAS upgrade R&D, we are currently exploring an active pixel detector demonstrator HV2FEI4 in the standard AMS 180nm HV CMOS process. The contacts between the detector- and readout chip can be established either capacitively or by bump-bonding.

#### Accomplished working packages

In the period April 2011 – April 2012 we have designed four pixel chips:

1. Hpixel chip – type: SDA, application: transmission electron microscopy.
2. HV2FEI4 chip – type: SDA, application: particle physics, ATLAS detector at CERN.
3. MuPixel2 chip – type: SDA, application: particle physics, Mu3e experiment at PSI.
4. SUSOKI2 chip – type SOI, application: synchrotron radiation experiments.

We have designed six test systems, particularly, the firmware code for the existing FPGA boards, the sensor chip PCBs and the readout software:

1. SUSOKI1 – software Linux C++ (new code), Hardware: SUSIBO board, PCB.
2. SDS Chip – software Linux C++ (new code) and Windows C++ and C# under Visual Studio (new code), hardware: SUSIBO board, PCB.
3. Hpixel Chip – software Linux C++ (new code), hardware: SUSIBO board, PCB.
4. HVPixelM – software Borland C++ for Windows (update), hardware SUSIBO board, PCB.
5. MuPixel2 – software Borland C++ for Windows (update), hardware: UXIBO board, PCB.
6. HV2FEI4 – two PCBs (for single chip and hybrid-module tests).

We have tested the following five chips – all successfully:

1. SUSOKI1 chip (SOI detector for synchrotron experiments).
2. SDS chip (Pixel sensor prototype with 2.5 micrometer pixels in 65nm CMOS technology).
3. Hpixel chip (SDA detector for transmission electron microscopy).
4. HVPixelM chip (SDA detector for transmission electron microscopy).
5. MuPixel1/2 chips (SDA detector for Mu3e experiment).

#### Publications and funding

In the period April 2011 – April 2012, one reviewed- and one proceeding paper were published in scientific journals.

The SDS chip in 65nm technology was described in the Europractice Activity Report.

SDA technology was introduced as an option for the ATLAS and CLIC experiments in the "ATLAS letter of intent" and "CLIC conceptual design report".

Our research results were presented by 11 talks on international conferences, workshops and collaboration meetings.

Last but not least, two students finished their bachelor and diploma work in our group.

We have applied together with Prof. Andre Schöning (Faculty for Physics and Astronomy, University of Heidelberg) for BMBF funding.

Design of HV2FEI4 chip was supported by CERN groups with 13k€.

#### Publications:

- [1] I. Peric, at all. „Particle pixel detectors in high-voltage CMOS technology - New achievements," Nucl. Inst. Meth. A 650, Issue 1, pp. 158 – 162, (2011).
- [2] I. Peric, F. Mandl; „Monolithic SOI Pixel Detector for x-Ray Imaging Applications with high Dynamic Range and MHz Frame-Rate," IEEE Nucl. Sci. Symposium Conference Record, pp. 1051 – 1056, (2011).
- [3] I. Peric; "Pixel Sensor ASIC in 65nm UMC Technology," Europractice Activity Report 2011, pp. 34 (2012).
- [4] F. Mandl; „Characterisierung eines SOI Pixelchips" Diploma Thesis, University of Heidelberg, 2011.
- [5] T. H. H. Nguyen; „Design und Untersuchung eines Sensor Chips in 65nm Technologie," Bachelor Thesis, University of Heidelberg and University of Applied Sciences Mannheim, 2012.

## RESEARCH GROUP APPLICATION SPECIFIC COMPUTING

W. Gao, T. Gerlach, M. Kretz, A. Kugel, N. Schroer, A. Wurz

Within the context of application specific computers the research group focuses on the following primary topics:

High-performance readout systems for physics experiments. This includes hardware development and production of electronic modules, development of FPGA firmware and software for microcontrollers, standard PCs and GPUs.

Applications and frameworks for reconfigurable computing platforms, including novel debugging tools and embedded operating systems, for example Linux on FPGAs.

There is a broad overlap between the activities of the research group and the activities of the "Chair of computer science V", in particular concerning the projects XFEL and ATLAS.

ATLAS is one of four high-energy physics experiments that are operated at the LHC at CERN. Besides the continuous work in the areas TDAQ and IBL [2] a major activity in 2011 was the preparation of the new BMBF funding application for the period of mid 2012 to mid 2015. The aim of the proposal is to seamlessly continue the ATLAS activities within the context of the research group from mid 2012.

The main research topics for the three-year period are the development of a PC-based readout-architecture for the upgrade of the LHC and PC-based detector calibration software, potentially accelerated with GPUs. A part of the calibration routines for the ATLAS pixel detector have been ported from the current DSP-based implementation to a distributed architecture with FPGA-based histogramming and

subsequent processing on CPU or GPU. Preliminary results indicate that a standard PC (Fig. 1, middle) and a GPU (Fig. 1, right) can achieve about the same performance as the optimized DSP implementation (Fig. 1, left), while providing more flexibility for the algorithm and a more convenient development environment. Direct porting of the look-up-table-based (LUT) DSP algorithm achieves a significant speed-up (Fig. 1, smallest column), however at the expense of less flexibility.

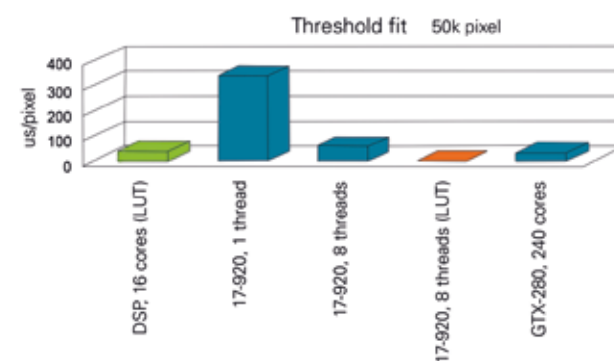


Fig. 1: Pixel Calibration Execution Times

For the DSSC readout system an FPGA based local DAQ controller has been designed, which will be implemented with the latest (series-7) FPGA family in 2012/2013. The goal is to take advantage from the high density and communication capabilities of those devices by implementing all control software on an FPGA-based Linux platform, with direct attachment of four 10GE data links.

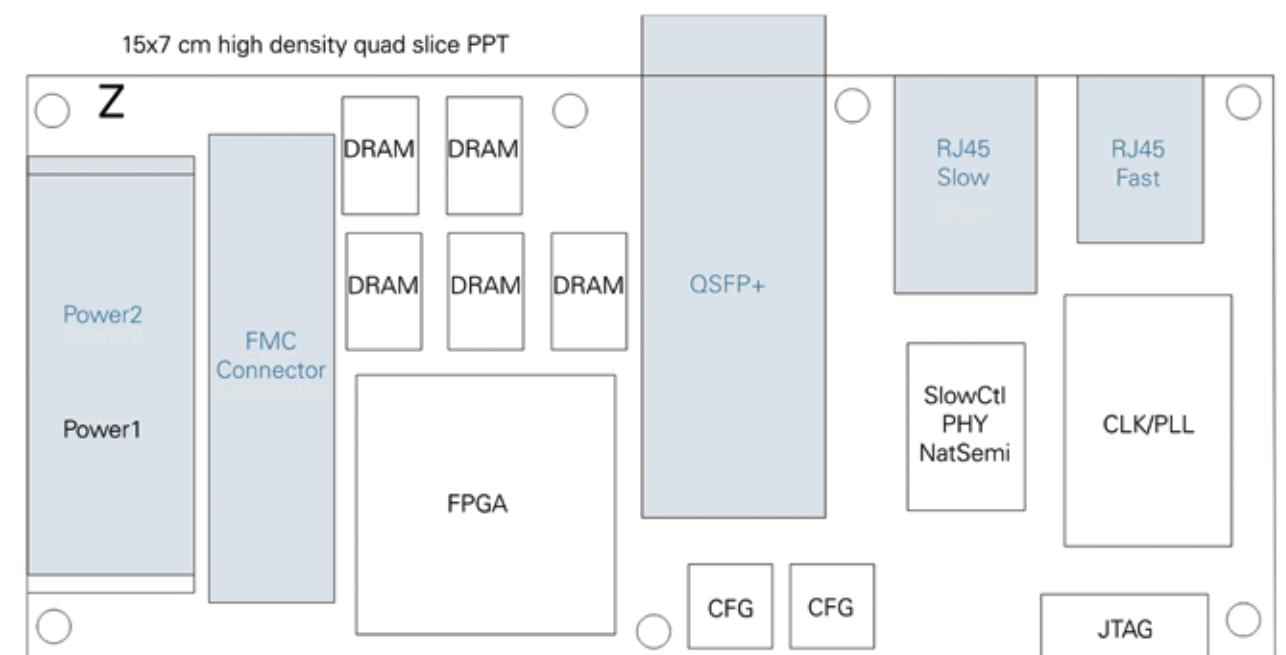


Fig. 2: DSSC Quad PPT

A sketch of the intended, very compact layout (15\*7cm) is shown in Fig. 2

Linux on reconfigurable platforms [1] facilitates the integration of application specific computers into a standard software framework, The ATLAS and XFEL readout systems are typical such scenarios. In contrast to the state-of-the-art approaches in this area which are most commonly based on special kernel versions (uClinux, commercial or vendor supplied) the research group is aiming at using a regular Linux kernel, which provides a more portable and flexible solution. Initial performance evaluations of a typical Microblaze FPGA system-on-chip architecture implemented on different hardware platforms have been performed in order to assess for example interrupt latencies, memory/peripheral bandwidth and network performance.

ATLAS is supported by: BMBF (05H09VHA), Cooperations: CERN, Wuppertal University, NIKHEF (NL), RHUL (UK), INFN Bologna (I)

### References

- [1] A. Kugel, Linux on reconfigurable platforms, proceedings of "1st Embed With Linux" workshop at RenPar'20 / SympA'14, Saint-Malo, France, May 10–13, 2011.
- [2] J. Anzu et al., The ATLAS IBL BOC Demonstrator, Proceedings of 2011 IEEE Nuclear Science Symposium and Medical Imaging Conference, Valencia, Spain, 23–29 Oct 2011, <https://cdsweb.cern.ch/record/1401224/files/ATL-INDET-PROC-2011-038.pdf>

## RESEARCH GROUP ACCELERATED SCIENTIFIC COMPUTING

**Astrophysical Simulations with Special Hardware**  
G. Marcus, D. Razmyslovich, R. Männer

We presented several contributions to astrophysical simulations using diverse hardware platforms. Several aspects of the work are covered in the dissertation for Marcus [1], and expanded in subsequent papers, including the following.

We introduced the MPRACE framework [2], a collection of libraries and linux drivers to facilitate the development of FPGA-based accelerators. The framework provides linux drivers, a DMA Engine for the FPGA, buffer management libraries and high-level transfer operations.

As part of the collaborations within the GRACE project, several simulations were run using GPUs in multiple clusters located in Germany, China and the US to demonstrate the scalability and feasibility of astrophysical algorithms in heterogeneous platforms. Figure 1 shows the scalability up to 144 GPUs running in the Laohu cluster in Beijing. This work received the prestigious PRACE Award 2011 at the ISC [3] in Hamburg in June 2011.

We also presented the raceSPH library with support for CPUs, FPGAs, GPUs and Cell processors, and showed its performance inside a particle simulation in [4]. The library abstracts the SPH computations, providing an accelerator-agnostic interface to the application, facilitating the task of using different platforms and removing the application from the complexities of each target system. Figure 2 shows the performance of the GPU cores against CPU implementations.

*Supported by: VW Foundation*

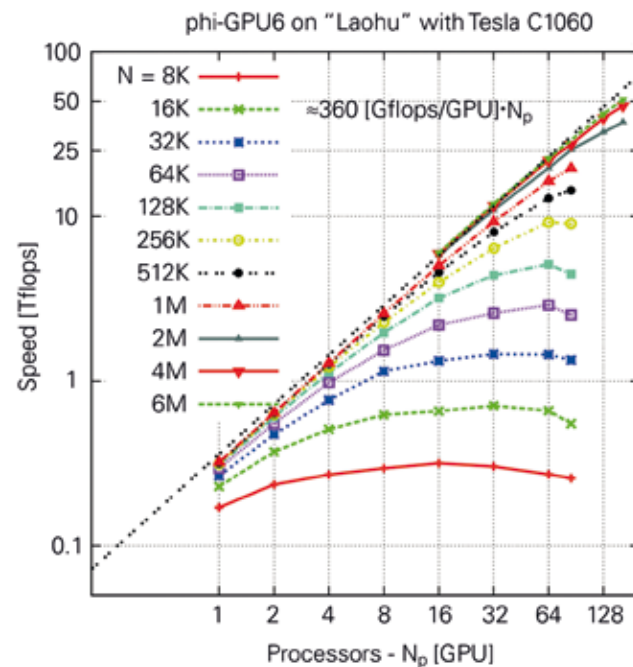


Fig.1: Scaling up to 144 GPUs in the Laohu cluster (NOC, Beijing)

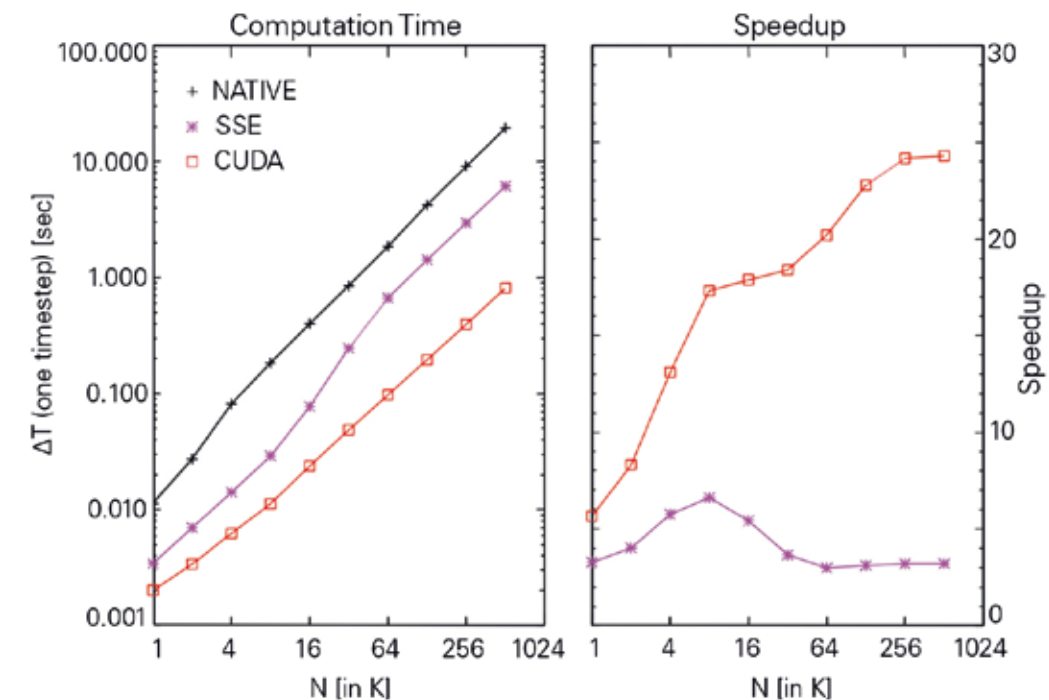


Fig.2: SPH speedup using CUDA with the raceSPH library.

### References

- [1] Marcus, G. „Astrophysical Simulations with Special Hardware.“ Dissertation, Heidelberg (2011).
- [2] Marcus et al, „The MPRACE framework: An open source stack for communication with custom FPGA-based accelerators.“ SPL 2011.
- [3] Spurzem et al, „Astrophysical particle simulations with large custom GPU clusters on three continents.“ ISC 2011.
- [4] Liu et al, „Astrophysical SPH Simulations with raceSPH Library.“ Frontier of GPU Computing, 2011.

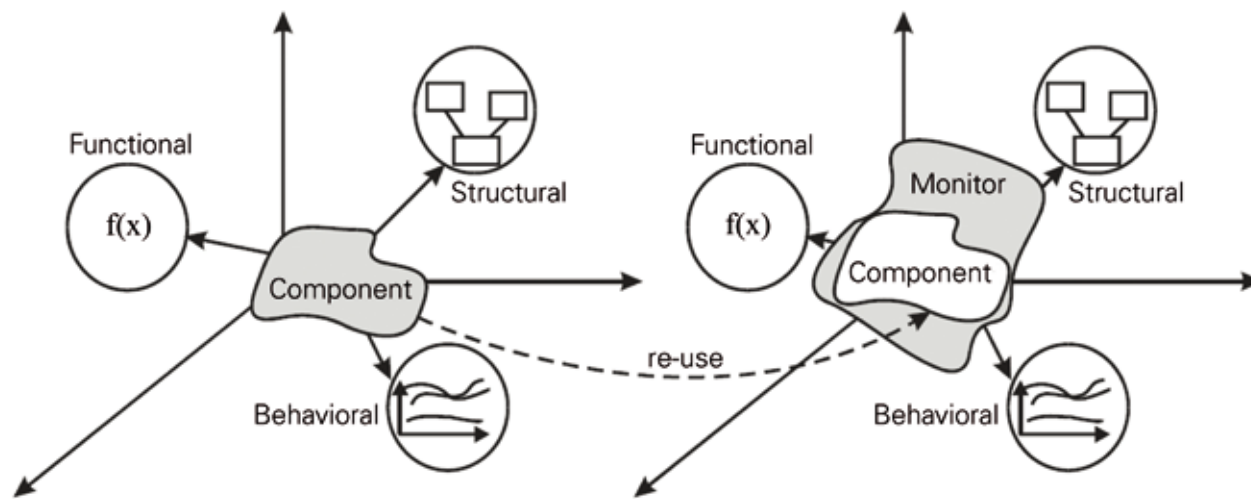


Fig.1: Reuse of component specifications for system monitoring

## RESEARCH GROUP DEPENDABLE ROBOTICS (DeBot)

### Design of Dependable Mobile and Medical Robots

A. Wagner, E. Nordheimer, S. Rady, L. Zouaghi, E. Badreddin

The goal of the “Dependable Robotics” group is the development of methods for the modeling, design and realization of dependable systems in the robotics area. Design concepts are founded on a fundamental modeling of basic structural and dynamical system properties and the generalization of automatic control and information theoretical methods. The research in the year 2011 focused on hybrid monitoring, navigation and motion control of mobile and medical robots as well as human-machine-interaction concepts.

Hybrid monitoring of control systems is based on the mixed continuous/discrete modelling of system dynamics, which are tackled on three levels:

- Development of new algorithms for the Petri nets-based hybrid system monitoring and a definition of a new class of Petri nets called Modified Particle

Petri Nets (MPPN) with specific firing rules dealing with the hybrid nature of systems and the modeling of uncertainties. A fault Diagnosis module based on Reachability tests of Petri nets and decision-making algorithms have been developed [1].

- An MPPN simulation tool and an XML-generator for automatic code generation and adaptation of the monitoring models to the available mission while the system is running has been implemented and applied to Robot navigation.

- A generic model for component monitoring has been integrated within a component-based design process, which utilizes abstractions of the component description and the reuse of the original component’s realization (Fig.1) [2]. In such development processes two steps were worked out: observer modeling and generic monitoring specification.

Hybrid frameworks for navigation have been investigated in [3]. Compact hybrid maps have been generated for large-scale indoor environments. A map for a given environment preserves information set at two different abstractions and resolutions, and possesses both geometric and non-geometric properties. The coarse-resolution information enables global topological localization for a robot through place matching, while the higher-resolution information enables local metric localization through triangulation. The topological and metric navigation have been thoroughly tested and validated through a high-resolution Tracking reference system (Krypton-K600).

A real-time level of autonomy adaptation method for Human-Machine-Interaction was developed based on hierarchical control system topology in [4]. The technical system and its operator are modelled as dynamical system components in a symmetrical way according to their reaction times. Based on control system decomposition methods, the human behaviour can be partitioned into behavioural levels. By comparing the user’s and the technical system’s time constants, a reference system can be defined, which allows the monitoring of user activities and system adaptation in real-time. As a result, guide-lines are provided for the dependable design of interfaces between the human operator and the technical system.

Together with external partners dependable motion control methods for medical and rehabilitation systems have been developed. The C3P-project paid attention to the stability analysis of a modular mobile robot platform based on the Lyapunov direct method [5]. The results demonstrate that, the used Lyapunov function candidate leads to regions

with guaranteed stability and regions with potential instable control behaviour, which should be avoided. The description and the avoidance of critical singular positions based on kinematic control methods was also a subject within the medical robot project CYCLOBOT<sup>1</sup>.

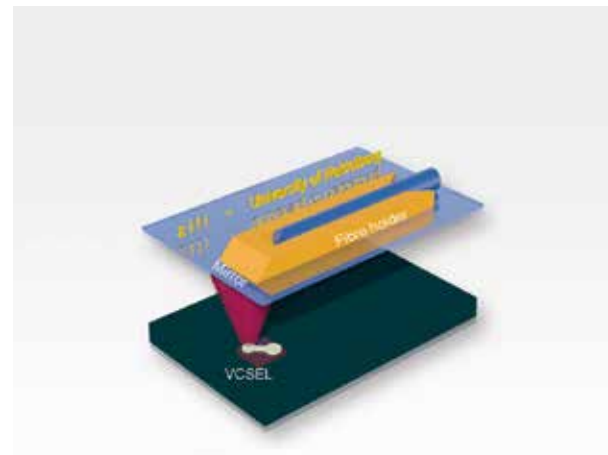
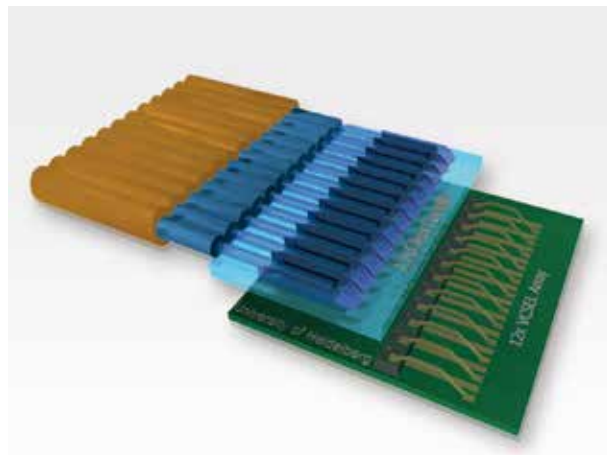
<sup>1</sup> Project CYCLOBOT – Funded by the German Research Foundation.

### References

- [1] L. Zouaghi, A. Alexopoulos, A. Wagner, E. Badreddin, “Modified Particle Petri Nets for Hybrid Dynamical Systems Monitoring Under Environmental Uncertainties”, IEEE/SICE International Symposium on System Integration (SII), 2011, pp. 497–502.
- [2] A. Wagner, L. Zouaghi, F. Barth, C. Atkinson, E. Badreddin, “A Unified Design Approach for Component-Based Dynamic Systems Monitoring”, IEEE/SICE International Symposium on System Integration (SII), 2011, pp.1137–1142.
- [3] S. Rady, A. Wagner, E. Badreddin, “Hierarchical Localization using Compact Hybrid Mapping for Large-Scale Unstructured Environments”, Proceedings of the IEEE International Conference on System, Man and Cybernetics (SMC11), pp. 2375–2380, Alaska, 2011.
- [4] E. Badreddin, A. Wagner, “Real-Time Level of Autonomy Adaptation for Human-Machine-Interaction Based on the Reaction Time”, 18th IFAC World Congress, Milano, Italy, 2011.
- [5] A. El-Shenawy, A. Wagner, A. Kandil, E. Badreddin, “Lyapunov Stability Study for a Special Actuated Holonomic Wheeled Mobile Robot”, IEEE International Conference on System, Man and Cybernetics: 2011, pp. 1962–1967.

## RESEARCH GROUP HIGH SPEED SHORT RANGE INTERCONNECTS

D. Wohlfeld, F. Lemke, S. Schenk, H. Fröning, F. Merchán, K.-H. Brenner, U. Brüning



Parallel VCSEL to fiber coupling principle based on total internal deflection

There is a continuously growing demand for optical high-speed, short-range interconnects in applications like networking for high performance computing (HPC) and data centers. One example is the Active Optical Cable (AOC), which combines the advantages of optical transmission and electric connection, encapsulating the electrical-optical conversion inside the connector housing.

The research project focuses on two new methods to couple light from active components into fibers including optimization of the complete fabrication chain to enable low-cost high-volume production. Both methods are based on an integrated 45° mirror and a fiber guide, which is positioned directly above the active component. Figure 1 shows the principle of light coupling: light coming from the VCSEL is deflected from the mirror and coupled into a multi-mode fiber (Fig.1).

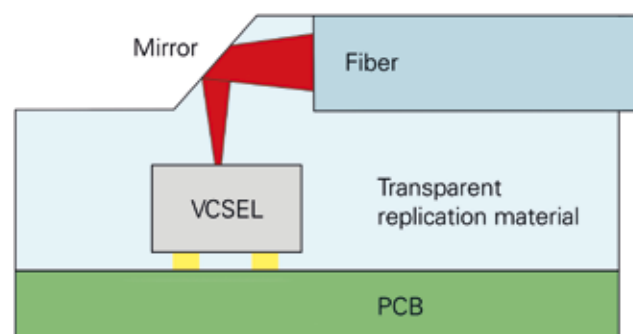


Fig.1: Light deflection using total internal deflection to couple light from a VCSEL into a multi-mode fiber.

Based on the milestone of 2010 where 3.25Gbps were measured in our early prototype we continued to improve the electrical design of the PCB and the manufacturing process. While the first PCB designs used flip chip versions of the VCSEL driver and TIA chip we encountered several problems. The reliability of the flip chip process on a standard FR4 PCB is

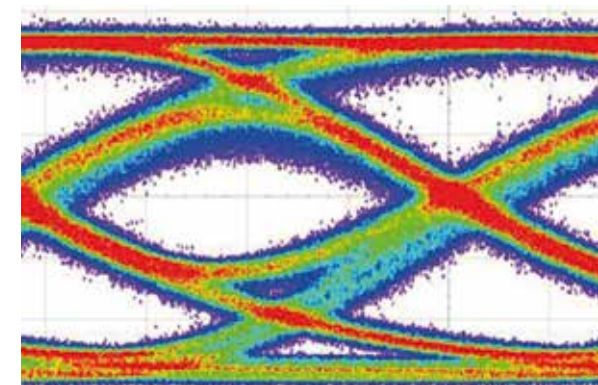


Fig.2(a): Optical Eye diagram with 1 mm wire bonds at 4.5 Gbps

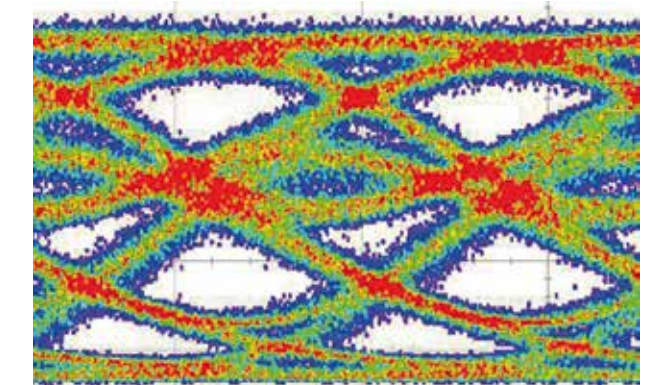


Fig.2(b): Optical Eye diagram with 1 mm wire bonds at 6.4 Gbps

not sufficient for a high yield production due to the very small feature size of the chip pads and the two row design. Since the flip chip process swaps the differential driver pins of the chip, the laser arrays and PD arrays have to be cross wire bonded which increases the bond wires and thus decreases signal integrity. Measurements of 6.4 Gbps signals showed the strong influence of bond wires with a length of 1mm on signal integrity. The optical eye is almost closed at 6.4 Gbps. While the TIA is still capable to recover the signal with a BER of 10E-13 higher speeds require shorter bond wires. Figure 2 shows the optical eye diagram at 4.5Gbps and 6.4 Gbps.

The next generation of our HD-AOC will include an all wire bond version with minimal bond wire length, < 0.5mm, for improved signal integrity.

Cooperation: KIT Thomas Blank

### References

- [1] Invited: D. Wohlfeld, K.-H. Brenner Aspects of short-range interconnect packaging SPIE Photonics West Conference Optoelectronic Interconnects XII, 8267-26, Jan. 2012, San Francisco, USA.
- [2] Merchán, F.; Brenner, K.-H.; "A concept for the assembly and alignment of arrayed microelectronic and micro-optical systems for Optical Multi-Gigabit Communication," SPIE Conference Optoelectronic Interconnects and Component Integration XI OE112, 7944-12, Jan. 2011.



Fig.1: Galibier PCIe Board

## RESEARCH GROUP NEXT GENERATION NETWORK INTERFACES

M. Nüssle, N. Burkhardt, B. Geib, B. Kalisch, A. Giese, C. Leber

In modern computing an increasing amount of parallelisation on all levels from chips to clusters can be observed. The bi-annual list of the 500 fastest computers of the world ([www.top500.org](http://www.top500.org)) illustrates this. Because of this development, interconnection networks and network interface architectures become increasingly important for modern parallel computer architectures.

The research group "Next Generation Network Interfaces" focuses on a holistic approach to advance the architecture of interconnect solutions in the HPC space. Several activities were conducted within the

year 2011, mainly for the EXTOLL network architecture, which has been developed at the Computer Architecture Group of the ZITI.

Building on earlier results, the next revision of EXTOLL called EXTOLL R2 was implemented. This involved all stages of the hardware design. All of the network controller units were revisited and optimized, similar to the work that had been done to the RMA unit previously. Also, the whole network layer including the link and network layer protocols, the crossbar switch and the link modules have been improved.

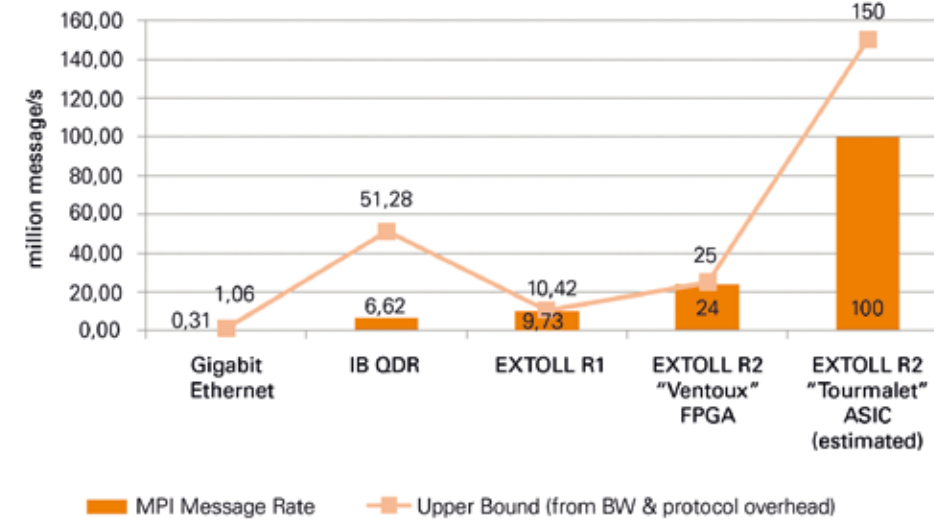


Fig. 2: Message rate comparison of different networks

Prior to 2011, the EXTOLL hardware was attached to the host using a HyperTransport interface (for example on the "Ventoux" board). Starting in 2011, EXTOLL hardware was also ported and optimized to work with industry standard PCI Express interfaces. To this end, the "Galibier" board developed within the institute was used as the first PCIe platform for EXTOLL (Figure 1).

The adaption of EXTOLL for an ASIC version was started. To this end, the data path width had to be increased to 128bit. The higher data path width will enable higher peak bandwidth performance on a future ASIC version of EXTOLL. The implementation of this feature was started.

The verification environment for EXTOLL was vastly improved. Many new UVM components for the EXTOLL hardware components were developed and added to the nightly regression runs.

Also, the first test machines running EXTOLL R2 on the "Ventoux" board were phased in and some of the PEAC cluster machines were updated with the new hardware. On the software side, the whole stack was ported to run on the new hardware revision and take advantage of the new possibilities added. As a result of this work, it was shown that the ping-pong latency between two nodes running EXTOLL R2 on "Ventoux" is well below one microsecond. An analysis of attainable message rates showed performance numbers that excelled EXTOLL R1. This is especially interesting when compared to other commercially available network solutions (Fi-

gure 2). EXTOLL R2 on Ventoux handles more than 24 million messages a second, more than 3.5 times the number of Infiniband QDR.

As an on-going project, the group continued its work in the area of High Frequency Trading (HFT).

The EXTOLL technology was featured on a booth both at the International Supercomputing Conference in Hamburg and the SC'11 in Seattle. In December the EU-project DEEP was kicked-off, where the EXTOLL technology will provide the network technology for the so called booster part of the machine. The booster in DEEP is a novel concept for a parallel machine built from many-core accelerators. The BMWI project continued throughout 2011.

*In part supported by: BMWI (03EFT5BW24), EU Project DEEP (ICT-287530)*

### References

- [1] Leber, C.; Geib, B.; Litz, H.; „High Frequency Trading Acceleration using FPGAs“, 21st International Conference on Field Programmable Logic and Applications (FPL 2011), September 5–7, 2011, Chania, Greece.
- [2] Litz, H.; Leber, C.; Geib, B.; „DSL Programmable Engine for High Frequency Trading Acceleration“, 4th Workshop on High Performance Computational Finance at SC11 (WHPCF 2011), co-located with SC11, November 13th, 2011, Seattle, USA.



Fig.1: Reverse osmosis pilot plant

## RESEARCH GROUP PROCESS CONTROL (ProCon)

### Reverse Osmosis Desalination Plant powered by Renewable Energy Sources A. Gambier, R. Staudt, A. Kandil, E. Badreddin

The use of reverse osmosis (RO) plants for water desalination is becoming more popular, especially in remote arid areas, where grid electricity might be unavailable. In this case, hybrid energy sources, such as wind and solar energy, are used to generate the necessary electricity for running the RO-plant and for domestic use.

Based on outcomes and experience gained from the EU project OPEN-GAIN [1, 2, 3], research in this area has been continued on a RO-pilot plant powered by renewable energy with battery storage at the Automation Laboratory (fig.1).

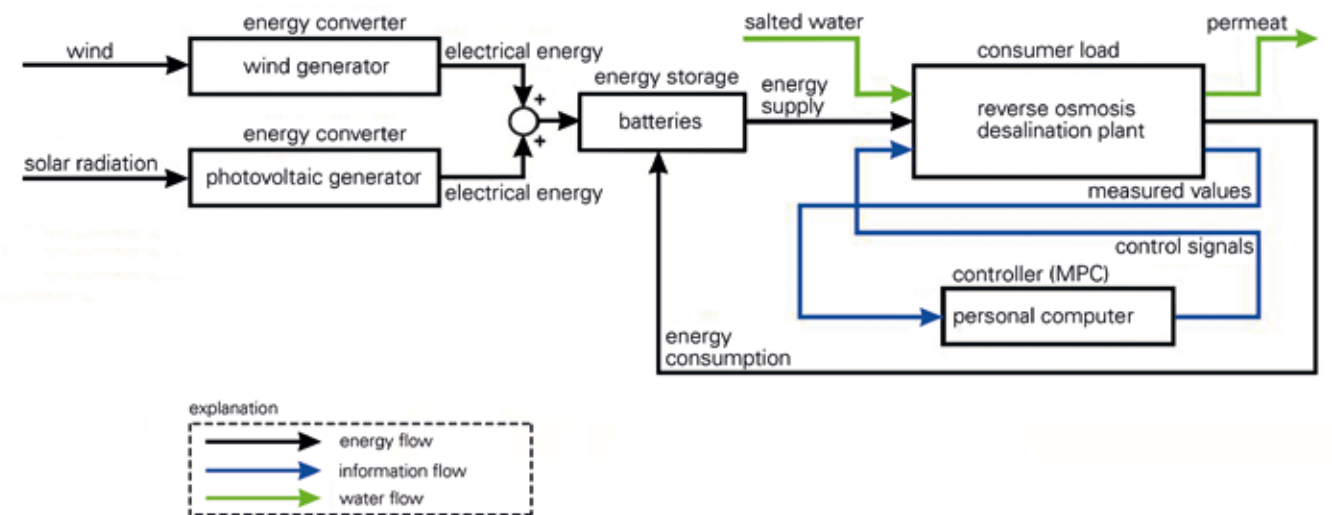


Fig. 2: Schematic structure of the entire system

A very important aspect when operating in arid areas is that the RO-plant keeps on producing water as long as possible under varying weather conditions. To realize this goal, a control strategy is developed to operate the RO-plant at different operating points, so that the RO-plant consumes less energy. The availability of wind or solar energy is also considered [4].

given by flow rate and conductivity, respectively. Switching between the predefined operating points is performed when the state-of-charge of the batteries decreases to a specified value by applying an automaton.

A schematic structure of the entire system with its main components is shown in Fig. 2.

The mathematical models for the wind and the photovoltaic generators as well as the batteries are derived from first principles. The reverse osmosis desalination plant is modelled as a black-box model of fourth order using the algorithm N4SID. According to experience, several suitable operating points were chosen, at which the RO-plant does not consume much energy when producing water. At each operating point the corresponding linearised model parameters are identified.

A model predictive controller (MPC) is utilized to guarantee, according to a predefined energy consumption level, permeate quantity and quality

#### References

- [1] OPEN-GAIN Project Group: OPEN-GAIN. <http://www.open-gain.org/>
- [2] Kandil, A.; Badreddin, E.: Optimal design of off-grid reverse osmosis desalination unit operated by hybrid PV/Wind/Diesel power plant. In: 12th Inter. Conference on Environmental Science and Technology (CEST2011), Greece, 2011.
- [3] Gambier, A.; Miksch, T.; Badreddin, E.: Fault-Tolerant Control of a Small Reverse Osmosis Desalination Plant with Feed Water Bypass. In: American Control Conference (2010), pp. 3611–3616.
- [4] Staudt, R.: Regelung mit Arbeitspunktanpassung zum optimalen Energieverbrauch einer Umkehrosmoseanlage. Mannheim, University of Heidelberg, Automation Laboratory, diploma thesis, 2011.



Fig.1: Autonomous Helicopter from Aeroscout type Scout B1-100.

## RESEARCH GROUP UNMANNED AERIAL VEHICLES

A. Kandil, M. Koslowski, S. Rady, A. Alexopoulos, E. Badreddin

The integration of Unmanned Aerial Vehicles (UAVs) into civil application fields is growing every day. Fixed-wing aircraft and vertical take-off and landing unmanned vehicles are being increasingly used for surveillance, search and rescue missions, aerial mapping, inspection, and agricultural imaging, to name

just few applications domains. Unlike fixed-wing aircrafts, helicopters are distinguished by their maneuverability and hovering ability, which makes them suitable for performing a wide variety of tasks. The autonomous helicopter at the Automation Laboratory is of the type Scout B1-100.

The research on this project started mainly with two topics. The first topic concerns developing a dynamic model of the autonomous helicopter derived from first principles using the Newton-Euler equations. The linearised model of thirteenth order captures the rotor flapping dynamics and the yaw damping system. Several identification methods are utilized to determine the unknown parameters of the state space model so that the model fits to the measured flight data [1]. The developed model will be used for design and test of different control strategies.

The second topic focuses on the localization of autonomous UAV in GPS denied areas signal. The idea is described in fig. 2, where a standby localization technique is integrated onboard to support emergency localization. The localization method detects some pre-extracted features in images and hence calculates the position of the UAV when the signal of the GPS is lost. A Kalman filter can additionally fuse the signals from the inertial sensors with the position sensor (GPS or the vision system in case the GPS is not available).

This idea has been introduced in [2], where a vision-based solution approach is proposed for the purposes of homing and mission execution. The approach is a hybrid design, which is capable of localizing the UAV on topological and metric levels. The approach consists of two phases. In the first phase, features are extracted and reduced using an information-theoretic analysis. The analysis helps maintaining only the informative features that provide recognition accuracy with less computational overhead to match real-time operation. The reduced features are represented by local descriptors and are additionally tagged with their metric position. In the second phase, the UAV is located using the map. A fast and coarse topological location is identified based on using a compressed form of the local descriptor

data. This guides the UAV in a fast and safe emergency homing. A second precise metric position is estimated in extension according to a previously identified topological location and with the aid of the features' metric position data. This assists the UAV navigation in case the mission should be completed without interruption despite the GPS signal loss.

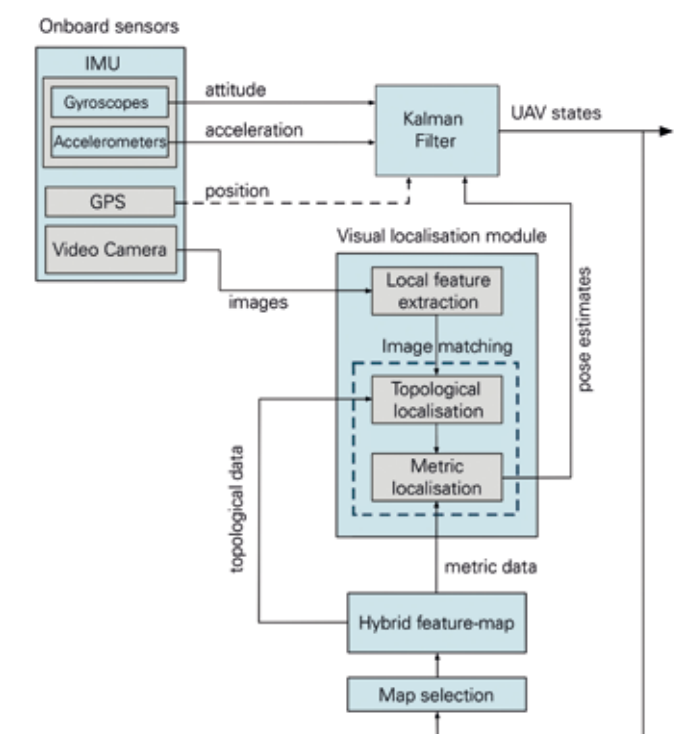


Fig. 2: UAV Localisation Architecture

### References

- [1] Koslowski, M. "Modeling, Identification and Control of an Autonomous Helicopter," diploma theses.
- [2] Rady, S. , Kandil, A.A. and Badreddin, E. , "A hybrid localization approach for UAV in GPS denied areas," IEEE/SICE International Symposium on System Integration (SII), pp. 1269–1274, December 2011, Kyoto, Japan.



Fig. 1: NeuroSim module

## RESEARCH GROUP VIRTUAL PATIENT ANALYSIS (ViPa)

### Medical Training Simulators Based on Virtual Reality F. Beier, N. Hüsken, O. Schuppe, E. Sismanidis

Surgical operations are often complex and potentially dangerous procedures. Only well trained and experienced surgeons are able to perform these interventions successfully. Surgical skills are usually acquired by assisting and by operating under the supervision of more experienced surgeons. Another possibility to improve surgical skills is the

training on plastic models, on animals, or cadaver preparation. However, these methods lack realism or endanger patients' lives. Consequently, there is an urgent need for an efficient training environment that is realistic but does not depend on human beings or animals.

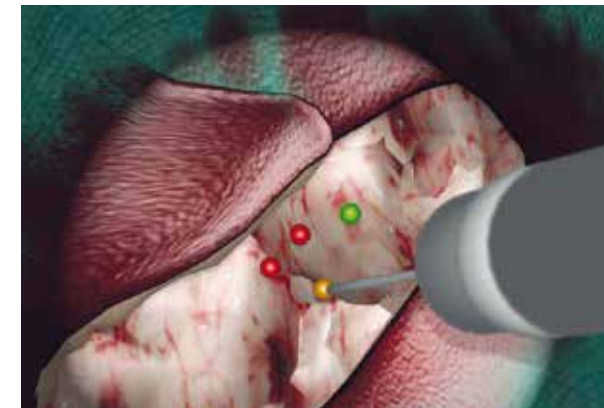


Fig. 2: Abstract training

Virtual reality (VR) can be used in order to implement such a training system. Apart from the fact that VR simulators do not involve human beings, they offer several advantages: Surgical tasks are reproducible and can be trained at any time, even if the medical case is rare. The surgeons' skills are measured objectively and the result can be compared to other users.

In order to implement a medical training simulator, several requirements have to be met: The interface between the user and the simulator has to be as native as possible in order to generate immersion.

The simulation of biological tissue and medical instruments has to be realistic. Everything has to be done in realtime, leading to huge demands on the hardware as well as on the algorithms.

Current research of the ViPA group focuses on two simulators: NeuroSim for intracranial surgery and MicroSim for microsurgical interventions.

NeuroSim uses original instruments and a real surgical microscope (see figure 1). The microscope is tracked by an optical tracking system. For the tracking of the instruments, a sensorfusion between inertial and optical tracking methods is used. The simulator features several abstract tasks in order to train basic skills (see figure 2). The first medical training module focuses on the clipping of an aneurysm. [1,2,3]



Fig. 3: Tracking system

MicroSim is a simulator for microsurgical tasks that are done using a microscope. Original instruments are used and tracked by an optical tracking system (see figure 3). A marker-based setup is implemented [5], a markerless approach is in development.

The simulation of virtual tissue and vessels uses realtime mass-spring algorithms and is based on tetrahedron models. Methods for tearing and cutting as well as algorithms for the simulation of suture material (see figure 4) have been developed [4,5]. As a first training module, the preparation and the suturing of blood vessels is currently being developed.



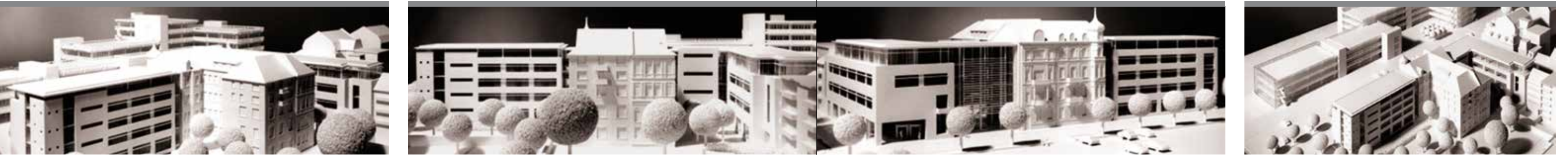
Fig. 4: Simulated thread

*Both simulators are developed in cooperation with the VRmagic GmbH in Mannheim. NeuroSim is supported by Leica Microsystems GmbH and developed in cooperation with the Department of Neurosurgery (Medical Faculty Mannheim, University of Heidelberg). MicroSim is supported by the BMWI (2351202SS9).*

---

#### References

- [1] F. Beier, S. Diederich, K. Schmieder, R. Männer. NeuroSim - The Prototype of a Neurosurgical Training Simulator. *Studies in Health Technology and Informatics*, 163:51-56, 2011.
- [2] F. Beier, E. Sismanidis, A. Stadie, K. Schmieder, R. Männer. An Aneurysm Clipping Training Module for the Neurosurgical Training Simulator NeuroSim. *Studies in Health Technology and Informatics*, 173:42-47, 2012.
- [3] F. Beier. The Integration of a Neurosurgical Microscope as an Interface to a Medical Training Simulator. *Virtual Reality Conference (VR)*, 2012 IEEE, 2012.
- [4] N. Hüsken. Realtime Simulation of Stiff Threads Using Large Timesteps. *Workshop in Virtual Reality Interactions and Physical Simulation „VRIPHYS“*, pp. 1-9, 2011.
- [5] O. Schuppe. An Optical Tracking System for a Microsurgical Training Simulator. *Studies in Health Technology and Informatics*, 173:445-9, 2012
- [6] E. Sismanidis. Real-time Simulation of Blood Vessels and Connective Tissue for Microvascular Anastomosis Training. *Virtual Reality Conference (VR)*, 2012 IEEE, 2012.



## MEMBERS AND STAFF

### Professors

Last Name	Name	Chair
Badreddin	Essameddin	Automation
Brenner	Karl-Heinz	Optoelectronics
Brüning	Ulrich	Computer Architecture
Fischer	Peter	Circuit Design
Fröning (Juniorprofessor)	Holger	Computer Engineering (since Oct 1, 2011)
Männer	Reinhard	Computer Science
Schnörr	Christoph	Computer Vision, Graphics and Pattern Recognition

### Secretaries

Last Name	Name	Chair
Feldmann	Marlis	Computer Architecture (until Oct 4, 2011)
Fischer	Ursula	Automation
Seeger	Andrea	Computer Science V
Volk	Sabine	Optoelectronics
Wilhelm	Evelyn	Computer Vision, Graphics and Pattern Recognition
Wunsch	Beate	Circuit Design

### Ph. D. Candidates and Research Assistants

Last Name	Name	Chair
Alexopoulos	Alexander	Automation
Armbruster	Tim	Circuit Design
Auer	Max	Optoelectronics
Bakulina	Alena	Computer Science V
Bartolein	Christian	Automation
Beier	Florian	Computer Science V
Binder	Michaela	ZITI
Breitenreicher	Dirk	Computer Vision, Graphics and Pattern Recognition
Brock	Alexander	Automation
Burkhardt	Niels	Computer Architecture
Enzweiler	Markus	Computer Vision, Graphics and Pattern Recognition
Erdinger	Florian	Circuit Design
Fertig	Matthias	Optoelectronics
Fröning	Holger	Computer Architecture
Gambier	Adrian	Automation
Geib	Benjamin	Computer Architecture
Geppert	Dina	ZITI
Gerlach	Thomas	Computer Science V
Giese	Alexander	Computer Architecture
Gipp	Markus	Computer Science V
Groß	Dominik	Circuit Design
Hlindzich	Dzmitry	Computer Science V
Hüsken	Nathan	Computer Science V
Kalisch	Benjamin	Computer Architecture



Last Name	Name	Chair
Kandil	Amr	Automation
Kapferer	Sven	Computer Architecture
Kappes	Jörg	Computer Vision, Graphics and Pattern Recognition
Keller	Christoph	Computer Vision, Graphics and Pattern Recognition
Kirchgessner	Manfred	Circuit Design
Knopf	Jochen	Circuit Design
Köpfle	Andreas	Computer Science V
Koslowski	Markus	Automation
Krackhardt	Ulrich	Computer Architecture
Krasnopevtsev	Pavel	Computer Science V
Kreidl	Christian	Circuit Design
Krieger	Michael	Circuit Design
Krivosos	Oleg	Computer Science V
Kugel	Andreas	Computer Science V
Leber	Christian	Computer Architecture
Lehmann	Lars	Circuit Design
Leibig	Christian	Computer Architecture
Lellmann	Jan	Computer Vision, Graphics and Pattern Recognition
Lemke	Frank	Computer Architecture
Leys	Richard	Computer Architecture
Litz	Heiner	Computer Architecture
Liu	Xiyuan	Optoelectronics
Marcus Martinez	Guillermo	Computer Science V
Merchán Alba	Fernando	Optoelectronics
Miksch	Tobias	Automation
Mlotok	Viacheslav	Circuit Design

Last Name	Name	Chair
Nguyen	Thi Hong Hanh	Circuit Design
Nüssle	Mondrian	Computer Architecture
Peric	Ivan	Circuit Design
Petra	Stefania	Computer Vision, Graphics and Pattern Recognition
Pommrenke	Christopher	Computer Vision, Graphics and Pattern Recognition
Rady ElAsmar	Sherine	Automation
Rathke	Fabian	Computer Vision, Graphics and Pattern Recognition
Razmyslovich	Dzmitry	Computer Science V
Richter	Andrea	Automation
Rittmeyer	Daniel	Automation
Ritzert	Michael	Circuit Design
Rüdiger	Jan	Automation
Rukletsov	Alexander	Computer Science V
Sacco	Ilaria	Circuit Design
Schenk	Sven	Computer Architecture
Schmidlin Fajardo Silva	Raul	Computer Science V
Schmidt	Stefan	Computer Vision, Graphics and Pattern Recognition
Schmitzer	Bernhard	Computer Vision, Graphics and Pattern Recognition
Schroer	Nicolai	Computer Science V
Schuppe	Oliver	Computer Science V
Schulte-Wieking	Kay	Computer Science V
Sismanidis	Evangelos	Computer Science V
Slogsnat	Eike	Optoelectronics
Staudt	Ralph	Automation
Steinle	Christian	Computer Science V



Last Name	Name	Chair
Stumpfs	Wolfgang	Optoelectronics
Stolzenberger	Frank	Automation
Swoboda	Paul	Computer Vision, Graphics and Pattern Recognition
Thil	Christophe	Circuit Design
Thürmer	Maximilian	Computer Architecture; Circuit Design
Wagner	Achim	Automation
Watson	Myles	Computer Architecture
Wohlfeld	Denis	Computer Architecture
Wolf	Martin	Automation
Wurz	Andreas	Computer Science V
Yu	Maoyuan	Computer Science V
Yuning	Yang	Computer Science V
Yuan	Jing	Computer Vision, Graphics and Pattern Recognition
Zouaghi	Leila	Automation

## THIRD-PARTY-FUNDED PROJECTS

Research at ZITI is funded by various national and international programs and sponsors.

Funding by	Project Title	Project Funding Amount	Project Funding Period	Chair
AiF	Entwicklung eines kardiologischen klinischen PAC (Patient Archiving and Communication)	175.000 €	07.2010 – 04.2012	Computer Science V
BMBF	ATLAS: Betrieb, Wartung und Entwicklung von HLT/DAQ-Komponenten	338.722 €	07.2009 – 06.2012	Computer Science V
BMBF	ViroQuant	187.121 €	01.2007 – 12.2011	Optoelectronics
BMBF	CBM Data Acquisition at FAIR	258.500 €	07.2009 – 06.2012	Computer Architecture
BMBF	FORSYS-VIROQUANT – Systembiologie von Virus-Zell-Interaktionen	296.240 €	01.2007 – 12.2011	Circuit Design
BMBF / PT DESY	SUPER BELLE – Auslesechips und Bumping für den DEPFET Vertexdetektor bei SuperBelle	290.360 €	07.2009 – 06.2012	Circuit Design
BMBF / PT GSI	FAIR-CBM II – Front End Elektronik	260.000 €	07.2009 – 06.2012	Circuit Design
BMW	HD-Active-Optical-Cable	38.979 €	07.2010 – 02.2011	Computer Architecture
BMW	Entwicklung eines auf Virtueller Realität basierenden Trainingssimulators für mikrochirurgische Eingriffe (MicroSim)	175.000 €	12.2009 – 10.2011	Computer Science V
BMW	EXIST Forschungstransfer: EXTOLL – Innovative skalierbare Hochleistungs-Rechnersysteme	383.856 €	09.2010 – 02.2012	Computer Architecture
Daimler AG	FAS für Fußgängererkennung	112.500 €	01.2011 – 06.2012	Computer Vision, Graphics and Pattern Recognition



Funding by	Project Title	Project Funding Amount	Project Funding Period	Chair
DESY / ESRF	XNAP - Development of an APD 2D Pixel Array Detector	315.200 €	01.2009 – 12.2012	Circuit Design
DESY / MPE	XFEL-Projekt DESY/DAQ	310 150 €	04.2009 – 03.2013	Computer Science V
DFG	Cyclobot	171.000 €	08.2009 – 08.2012	Automation
DFG	Mercator	123.146 €	09.2010 – 09.2011	Automation
DFG	3D-Tomographie mit wenigen Projektoren in der experimentellen 3D-Strömungsmessung	1 BAT IIa/E13 (100 % pos.) 25.900 €	04.2010 – 03.2012	Computer Vision, Graphics and Pattern Recognition
DFG	Graduiertenkolleg 1653/1 Spatio/Temporal Graphical Models and Applications in Image Analysis	585.000 €	04.2010 – 09.2014	Computer Vision, Graphics and Pattern Recognition
DFG + Industrie	Heidelberg Collaboratory for Image Processing (HCI)	1.675.589 €	01.2008 – 10.2012	Computer Vision, Graphics and Pattern Recognition
EU	DEEP Dynamical Exascale Entry Platform	507.350 €	12.2011 – 11.2014	Computer Architecture
EU	HYPERImage - Hybrid PET-MR system for concurrent ultra-sensitive imaging	645.185 €	04.2008 – 09.2011	Circuit Design
EU	SUBLIMA - SUB nanosecond Leverage In PET/MR Imaging	1.000.250 €	09.2010 – 08.2014	Circuit Design
Google Inc.	Efficient high speed flash memory without flash translation layer overhead	41.747 €	05.2010 – 05.2011	Computer Architecture
GSI	Front End Elektronik, schnelles Kommunikationsnetzwerk	182.148 €	01.2008 – 06.2011	Computer Science V
IMC Trading B.V.	Accelerated Computing using FPGAs	264.803 €	10.2009 ongoing	Computer Architecture

Funding by	Project Title	Project Funding Amount	Project Funding Period	Chair
Jäger, MSC, Kuroda	Test und Inbetriebnahme von HTX-Boards (Anwendung gesicherter Erkenntnisse - AgE)	51.105 €	03.2009 ongoing	Computer Architecture
VW	GRACE II	60.000 €	04.2010 – 12.2012	Computer Science V
XFEL GmbH	XFEL - Development of a Large Format X-ray Imager with Mega-Frame Readout Capability based on the DEPFET Active Pixel Sensor	1.024.600 €	04.2009 – 09.2012	Circuit Design



## SELECTED PROJECT PARTNERS

Company/Institution	Location	Chair
AAST (Arab Academy of Science and Technology)	Alexandria, Egypt	Automation
AGH University of Science and Technology	Krakow, Poland	Computer Architecture
American University of Beirut (AUB)	Beirut, Lebanon	Automation
ATLAS Collaboration CERN	Geneva, Switzerland	Computer Science V
CBM Collaboration GSI	Darmstadt, Germany	Computer Science V
Daimler AG	Sindelfingen, Germany	Automation
Delft University of Technology	Delft, The Netherlands	Circuit Design
DLR (Deutsches Zentrum für Luft- und Raumfahrt/German Aerospace Center) location Goettingen	Goettingen, Germany	Computer Vision, Graphics and Pattern Recognition
École polytechnique fédérale de Lausanne (EPFL)	Lausanne, Switzerland	Circuit Design
Fraunhofer ITWM	Kaiserslautern, Germany	Computer Architecture
Ghent University	Ghent, Belgium	Circuit Design
Goethe University Frankfurt/Main	Frankfurt/Main, Germany	Circuit Design
GSI	Darmstadt, Germany	Computer Architecture
Heinrich-Hertz-Institut, Fraunhofer Institut	Berlin, Germany	Optoelectronics
Honda Research Institute Europe GmbH	Offenbach, Germany	Automation
IBM	Böblingen, Germany Zurich, Switzerland	Optoelectronics
Indian Institute of Technology Kharagpur iitkgp	Kharagpur, India	Computer Architecture
Jagiellonian University	Krakow, Poland	Circuit Design
Johann Wolfgang Goethe-Universität	Frankfurt, Germany	Computer Architecture
King's College	London, United Kingdom	Circuit Design

Company/Institution	Location	Chair
Klinikum Mannheim	Mannheim, Germany	Computer Science V
KSB AG	Frankenthal, Germany	Automation
Kyoto University	Kyoto, Japan	Automation
La Vision GmbH	Goettingen, Germany	Computer Vision, Graphics and Pattern Recognition
Leica Microsystems AG	Heerbrugg, Switzerland	Computer Science V
MPI Semiconductor Laboratory	Munich, Germany	Circuit Design
MWM GmbH	Mannheim, Germany	Automation
National Astronomical Observatories, Chinese Academy of Sciences	Peking, China	Computer Science V
Otto Bock Mobility Solutions GmbH	Königsee, Germany	Automation
Philips Research	Eindhoven, The Netherlands	Circuit Design
Polytechnico di Milano	Milano, Italy	Circuit Design
RWTH Aachen University	Aachen, Germany	Computer Architecture
RWTH Aachen University	Aachen, Germany	Circuit Design
Siemens AG	Nürnberg/Karlsruhe, Germany	Automation
SMOS	Walldorf, Germany	Optoelectronics
Technolution B. V.	Gouda, The Netherlands	Circuit Design
Technical University of Chemnitz	Chemnitz, Germany	Computer Architecture
Technical University of Dresden	Dresden, Germany	Computer Architecture
Technical University of Valencia	Valencia, Spain	Computer Architecture
Universitat Politècnica de València	Valencia, Spain	Circuit Design
Universitat de Barcelona	Barcelona, Spain	Circuit Design
University Hospital Aachen	Aachen, Germany	Circuit Design
University of Bergamo	Bergamo, Italy	Circuit Design
University of Bonn	Bonn, Germany	Circuit Design



Company/Institution	Location	Chair
University of Castilla-La Mancha	Castilla-La Mancha, Spain	Computer Architecture
University of Muenster	Muenster, Germany	Circuit Design
University of Siegen	Siegen, Germany	Circuit Design
Various European Universities in conjunction with EU-Project IntelliCIS	Europe	Automation
Vrmagic GmbH	Mannheim, Germany	Computer Science V
XFEL Collaboration DESY	Hamburg, Germany	Computer Science V

## PUBLICATIONS

### Chair of Automation

- Badreddin, E. and Wagner, A.,  
Real-Time Level of Autonomy Adaptation for Human-Machine-Interaction Based on the Reaction Time, accepted by 18th IFAC World Congress, Milano, Italy, 2011.
- El-Shenawy, A., Wagner, A., Kandil, A. and Badreddin, E.,  
Lyapunov stability study for a special actuated holonomic wheeled mobile robot, IEEE International Conference on System, Man and Cybernetics (IEEE SMC 2011), pp.1962–1967, Anchorage, Alaska, 2011.
- Kandil, A. and Badreddin, E.,  
Optimal design of off-grid reverse osmosis desalination unit operated by hybrid PV/Wind/Diesel power plant, 12th International Conference on Environmental Science and Technology (CEST2011), Rhodes island, Greece, Sept 8–10, 2011.
- Pott, P., Wagner, A., Badreddin, E., Weiser, H.P. and Schwarz, M.L.R.,  
Inverse Dynamic Model and a Control Application of a Novel 6-DOF Hybrid Kinematics Manipulator, Journal of Intelligent and Robotic Systems 63(1): 3–23, 2011.
- Rady, S., Kandil, A. and Badreddin, E.,  
A hybrid localization approach for UAV in GPS denied areas., IEEE/SICE International Symposium on System Integration (SII), pp.1269–1274, Kyoto, Japan, 2011.
- Rady, S., Wagner, A. and Badreddin, E.,  
Hierarchical Localization using Compact Hybrid Mapping for Large-Scale Unstructured Environments, IEEE International Conference on System, Man and Cybernetics (IEEE SMC 2011), Anchorage, Alaska, 2011.
- Wagner, A., Nordheimer, E., Merscher, M., Heute, S., Weiser, H.P., Pott, P., Badreddin, E. and Schwarz, M.L.R.,  
Kinematics-based position control of the 6-DOF surgical robot epizactor, 11th Annual Meeting of CAOS-International, London, UK, June 15–18, 2011.



- Wagner, A., Zouaghi, L., Barth, F., Atkinson, C. and Badreddin, E.,  
A Unified Design Approach for Component-Based Dynamic Systems Monitoring (2011),  
IEEE/SICE International Symposium on System Integration (SII), pp.1137–1142, 2011.
- Wolf, A., Jipp, M., Kloess, S. and Badreddin, E.,  
An Overview over Recent Advances and Future Directions of the Theory of Structured Intelligence,  
IEEE International Conference on Systems, Man, and Cybernetics (IEEE SMC 2011), pp. 2139–2144,  
Anchorage, Alaska, 2011.
- Zouaghi, L., Alexopoulos, A., Wagner A. and Badreddin, E.,  
Modified Particle Petri Nets for Hybrid Dynamical Systems Monitoring Under Environmental  
Uncertainties (2011),  
IEEE/SICE International Symposium on System Integration (SII), pp. 497–502, 2011.
- Zouaghi, L., Alexopoulos, A., Wagner, A. and Badreddin, E.,  
Probabilistic Online-Generated Monitoring Models for Mobile Robot Navigation using Modified Petri net,  
15th International Conference on Advanced Robotics, Tallinn, Estonia, 2011.
- Zouaghi, L., Wagner, A. and Badreddin, E.,  
Monitoring of Hybrid Systems using Behavioural System Specification,  
accepted by 18th IFAC World Congress, Milano, Italy, 2011.

#### Chair of Circuit Design

- Andricek, L., Caride, J., Doležal, Z., Drásal, Z., Kriedl, C., Knopf, J. et al. (DEPFET Collaboration),  
Intrinsic resolutions of DEPFET detector prototypes measured at beam tests,  
NIMA, Vol. 638, Issue 1, 11 May 2011, pp. 24–32.
- ATLAS Collaboration (from P. Fischer's ATLAS membership when in Bonn),  
Measurement of the differential cross-sections of inclusive, prompt and non-prompt J/Psi production in  
proton-proton collisions at  $\sqrt{s} = 7$  TeV, Nuclear Physics B, Volume 850, Issue 3, 21 September 2011,  
pp. 387–444.
- Facchinetti, S., Bombelli, L., Fiorini, C., Porro, M., De Vita, G. and Erdinger, F.,  
Characterization of the Flip Capacitor Filter for the XFEL-DSSC Project,  
IEEE Transactions on Nuclear Science 2011, Volume: 58 , Issue: 4, pp. 2032–2038.

- Facchinetti, S., Bombelli, L., Castoldi, A., Fiorini, C., Guazzoni, C. and Erdinger, F.,  
Fast, low-noise, low-power electronics for the analog readout of non-linear DEPFET pixels,  
Nuclear Science Symposium and Medical Imaging Conference (NSS/MIC), 2011, pp. 1846–1851.
- Gerlach, T., Kugel, A., Wurz, A., Hansen, K., Klär, H., Müntefering, D. and Fischer, P.,  
The DAQ Readout Chain of the DSSC Detector at the European XFEL,  
Nuclear Science Symposium and Medical Imaging Conference (NSS/MIC), 2011, pp. 156–162.
- Knopf, J., Fischer, P., Kreidl, C. and Peric, I.,  
256 Channel 8-Bit Current Digitizer ASIC for the Belle II PXD,  
JISNT 6 (2011) C01085 (Volume 6, January 2011).
- Mlotok, V., Ritzert, M., Fischer, P., Peric, I., Solf, T. and Schulz, V.,  
Floodmap measurement of a pixellated gamma scintillation detector module using fully integrated readout,  
Nuclear Science Symposium and Medical Imaging Conference (NSS/MIC), 2011, pp. 1980–1981.
- Peric, I., Fischer, P., Knopf, J. and Nguyen, T. H. H.,  
DCDB and SWITCHERB, the Readout ASICs for Belle II DEPFET Pixel Detector,  
Nuclear Science Symposium and Medical Imaging Conference (NSS/MIC), 2011, pp. 1536–1539.
- Peric, I., Kreidl, C. and Fischer, P.,  
Hybrid pixel detector based on capacitive chip to chip signal-transmission Original Research Article,  
NIMA, Vol. 617, Issues 1–3, 11–21 May 2010, pp. 576–581.
- Peric, I., Kreidl, C. and Fischer, P.,  
Particle pixel detectors in high-voltage CMOS technology – New achievements  
NIMA, Vol. 650, Issue 1, 11 September 2011, pp. 158–162.
- Peric, I. and Takacs, C.,  
Large monolithic particle pixel-detector in high-voltage CMOS technology,  
NIMA, Vol. 624, Issue 2, 11 December 2010, pp. 504–508.
- Peric, I., Takacs, C., Behr, J., Wagner, F.M. and Fischer, P.,  
The first beam test of a monolithic particle pixel detector in high-voltage CMOS technology,  
NIMA, Vol. 628, Issue 1, 1 February 2011, pp. 287–291.



- Porro, M., Andricek, L., Bombelli, L., De Vita, G., Fiorini, C., Fischer, P. et al.,  
Expected performance of the DEPFET sensor with signal compression: A large format X-ray imager with mega-frame readout capability for the European XFEL,  
NIMA, Vol. 624, Issue 2, 11 December 2010, pp. 509–519.
- Thil, Ch., Baron, A.Q.R., Fajardo, P., Fischer, P., Graafsma, H. and Ruffer R.,  
Pixel readout ASIC for an APD based 2D X-ray hybrid pixel detector with sub-nanosecond resolution,  
NIMA, Vol. 628, Issue 1, 1 February 2011, pp. 461–464.
- Schulz, V., Weissler, B., Gebhard, P., Fischer, P., Ritzert, M., Mlotok, V. et al.,  
SiPM based preclinical PET/MR insert for a human 3T MR: first imaging experiments,  
Nuclear Science Symposium and Medical Imaging Conference (NSS/MIC), 2011, pp. 4467–4469.

#### Chair of Computer Architecture

- Fröning, H., Montaner, H., Silla, F. and Duato, J.,  
On Memory Relaxations for Extreme Manycore System Scalability  
2nd Workshop on New Directions in Computer Architecture (NDCA-2),  
held in conjunction with the 38th International Symposium on Computer Architecture (ISCA-38),  
San Jose, California, June 5, 2011.
- Leber, C., Geib, B. and Litz, H.,  
High Frequency Trading Acceleration using FPGAs  
21st International Conference on Field Programmable Logic and Applications (FPL 2011),  
Chania, Greece, Sept 5–7, 2011.
- Lemke, F., Kapferer, S., Giese, A., Fröning, H. and Brüning, U.,  
A HT3 Platform for Rapid Prototyping and High Performance Reconfigurable Computing,  
Second International Workshop on HyperTransport Research and Applications,  
Mannheim, Germany, Feb 9, 2011.
- Litz, H., Leber, C. and Geib, B.,  
DSL Programmable Engine for High Frequency Trading Acceleration  
4th Workshop on High Performance Computational Finance at SC11 (WHPCF 2011), co-located with SC11,  
Seattle, USA, Nov 13, 2011.

- Mohr, B., Zimmermann, N., Wang, Y., Thiel, B. T., Negra, R., Heinen, S.;  
Lemke, F., Schenk, S., Leys, R. and Brüning, U.,  
Implementation of an RF-DAC based Multistandard Transmitter System,  
CDNLIVE! 2011, Academic Track,  
Munich, Germany, May 3–5, 2011.
- Montaner, H., Silla, F., Fröning, H. and Duato, J.,  
A New Degree of Freedom for Memory Allocation in Clusters  
Cluster Computing: Special Issue (HPDC 2010), Springer, accepted for publication in 2011.
- Montaner, H., Silla, F., Fröning, H. and Duato, J.,  
MEMSCALE: a Scalable Environment for Databases,  
13th IEEE International Conference on High Performance Computing and Communications (HPCC-2011),  
Banff, Canada, Sept 2–4, 2011.
- Montaner, H., Silla, F., Fröning, H. and Duato, J.,  
Unleash your Memory-Constrained Applications: a 32-node Non-coherent Distributed-memory Prototype  
Cluster,  
13th IEEE International Conference on High Performance Computing and Communications (HPCC-2011),  
Banff, Canada, Sept 2–4, 2011.
- Wohlfeld, D., Lemke, F., Fröning, H., Schenk, S. and Brüning, U.,  
High Density Active Optical Cable: from a Concept to a Prototype,  
SPIE Photonics West, Optoelectronic Interconnects and Component Integration XI,  
San Francisco, California, January 22–27, 2011.

#### Chair of Computer Science V

- Beier, F., Diederich, S., Schmieder, K. and Männer, R.,  
NeuroSim - The Prototype of a Neurosurgical Training Simulator, Studies in health technology and informatics,  
Vol. 163, pp. 51–56, 2011.
- Bruni, G., Bruschi, M., D'Antone, I., Dopke, J., Falchieri, D., Flick, T., Gabrielli, A., Grosse-Knetter, J., Joseph, J.,  
Krieger, N., Kugel, A., Morettini, P., Polini, A., Rizzi, M., Schroer, N. C., Travaglini, R., Zannoli, S. and Zoccoli, A.,  
ATLAS IBL: integration of new HW/SW readout features for the additional layer of Pixel Detector,  
Journal of Instrumentation, Vol 6., Nr. 1, 2011.



- Kugel, A.,  
Linux on reconfigurable platforms, The 1st Embed With Linux (EWiLi) mini-Workshop, 2011.
- Kugel, A., Dopke, J., Falchieri, D., Flick, T., Gabrielli, A., Grosse-Knetter, J., Heim, T., Joseph, J., Krieger, N., Morettini, P., Neumann, M., Polini, A. and Schroer, N.,  
The IBL BOC Demonstrator, 2011 IEEE Nuclear Science Symposium Conference Record (NSS/MIC), 2011.
- Marcus, G.,  
Acceleration of Astrophysical Simulations with Special Hardware,  
Dissertation, University of Heidelberg, 2011.
- Marcus, G., Gao, W., Kugel, A. and Männer, R.,  
The MPRACE framework: An open source stack for communication with custom FPGA-based accelerators, Programmable Logic (SPL), 2011 VII Southern Conference on, pp.155–160, 2011.
- Spurzem, R., Berczik, P., Hamada, T., Nitadori, K., Marcus, G., Kugel, A., Männer, R., Berentzen, I., Fiestas, J., Klessen, R. and Banerjee, R.,  
Astrophysical Particle Simulations with Large Custom GPU Clusters on Three Continents, Proceedings of the ISC2011, 2011.

#### Chair of Computer Vision, Graphics and Pattern Recognition

- Andres, B., Kappes, J. H., Beier, T., Köthe, U. and Hamprecht, F.,  
Probabilistic Image Segmentation with Closedness Constraints, Proceedings of 2011 IEEE International Conference on Computer Vision (ICCV), 2011.
- Breitenreicher, D., Lellmann J. and Schnörr, C.,  
Sparse Template-Based Variational Image Segmentation, Advances in Adaptive Data Analysis, Vol. 3, pp. 149–166, 2011.
- Breitenreicher, D. and Schnörr, C.,  
Model-Based Multiple Rigid Object Detection and Registration in Unstructured Range Data, Int. J. Comp. Vision, Vol. 92, pp. 32–52, 2011.
- Kappes, J. H., Speth, M., Andres, B., Reinelt, G. and Schnörr, C.,  
Globally Optimal Image Partitioning by Multicuts, EMMCVPR, Springer, 2011.

- Lellmann, J., Lenzen, F. and Schnörr, C.,  
Optimality Bounds for a Variational Relaxation of the Image Partitioning Problem, Energy Min. Meth. Comp. Vis. Patt. Recogn., Springer, 2011.
- Lellmann, J., Lenzen, F. and Schnörr, C.,  
Optimality Bounds for a Variational Relaxation of the Image Partitioning Problem, Technical report, Dec 2011.
- Lellmann, J. and Schnörr, C.,  
Continuous Multiclass Labeling Approaches and Algorithms, CoRR, abs/1102.5448, 2011.
- Lellmann J. and Schnörr, C.,  
Continuous Multiclass Labeling Approaches and Algorithms, SIAM J. Imaging Sciences, Vol. 4, Nr. 4, pp. 1049–1096, 2011.
- Lellmann J. and Schnörr, C.,  
Regularizers for Vector-Valued Data and Labeling Problems in Image Processing, Control Systems and Computers, Vol. 2, pp. 43–54, 2011.
- Nicola, A., Petra, S., Popa, C. and Schnörr, C.,  
A general extending and constraining procedure for linear iterative methods, Int. J. Comp. Math., Note: In press, 2011.
- Rathke, F., Schmidt, S. and Schnörr, C.,  
Order Preserving and Shape Prior Constrained Intra-Retinal Layer Segmentation in Optical Coherence Tomography, MICCAI, Note: In press, Springer, 2011.
- Savchynskyy, B., Kappes, J. H., Schmidt, S. and Schnörr, C.,  
A Study of Nesterov's Scheme for Lagrangian Decomposition and MAP Labeling, IEEE International Conference on Computer Vision and Pattern Recognition (CVPR), 2011.
- Schmidt, S., Savchynskyy, B., Kappes, J. H. and Schnörr, C.,  
Evaluation of a First-Order Primal-Dual Algorithm for MRF Energy Minimization, EMMCVPR, Vol. 6819 of LNCS, pp. 89–103, Springer, 2011.



#### Chair of Optoelectronics

- Auer, M. and Brenner, K.-H.,  
Enhancement of Photodetector Responsivity in Standard SOI CMOS Processes by introducing Resonant Grating Structures, JEOS:RP 6, 110145, 2011.
- Brenner, K.-H.,  
Aspekte der Lichtausbreitung zwischen verkippten Ebenen, DGaO-Proceedings (Online-Zeitschrift der Deutschen Gesellschaft für angewandte Optik e. V.), ISSN: 1614-8436-urn:nbn:de:0287-2011-B009-2, 112. Jahrestagung, Ilmenau, June 14–18, 2011.
- INVITED: Brenner, K.-H.,  
Parallel non-mechanical image scanning with micro lenses and binary phase gratings!, 10th Euro-American Workshop on Information Optics (WIO 2011), Benicassim/Spain, June 20-24, 2011.
- Brenner, K.-H. and Buschlinger, R.,  
Parallel image scanning with binary phase gratings, Journal of European Optical Society: Rapid Publications 6, 11024 (JEOS:RP), ISSN 1990-2573, 2011.
- Merchán, F. and Brenner, K.-H.,  
A concept for the assembly and alignment of arrayed microelectronic and micro-optical systems for Optical Multi-Gigabit Communication, Optoelectronic Interconnects and Component Integration XI Conference OE112, Jan 22.–27. 2011, San Francisco, California, USA, 2011, submitted.
- Merchán, F. and Brenner, K.-H.,  
Monolithisches Fertigungskonzept für die kostengünstige Herstellung optischer Mikrosysteme, (Online-Zeitschrift der Deutschen Gesellschaft für angewandte Optik e. V.), ISSN: 1614-8436-urn:nbn:de:0287-2011-B004-0, 112. Jahrestagung, Ilmenau, June 14–18, 2011.
- Slogsnat, E. and Brenner, K.-H.,  
Design des Beleuchtungspfad für ein miniaturisiertes paralleles Fluoreszenz-Mikroskop, (Online-Zeitschrift der Deutschen Gesellschaft für angewandte Optik e. V.), ISSN: 1614-8436-urn:nbn:de:0287-2011-P00x-x, 112. Jahrestagung, Ilmenau, 2011, June 14–18, 2011.

- Stenau, T., Liu, X. and Brenner, K.-H.,  
Analyse eines neuen Systemkonzepts zur parallel scannenden Mikroskopie, (Online-Zeitschrift der Deutschen Gesellschaft für angewandte Optik e. V.), ISSN: 1614-8436-urn:nbn:de:0287-2011-P005-9, 112. Jahrestagung, Ilmenau, June 14–18, 2011.

#### Juniorprofessorship/Chair of Computer Engineering

- Montaner, H., Silla, F., Fröning, H. and Duato, J.,  
MEMSCALE: In-Cluster-Memory Databases, 20th ACM Conference on Information and Knowledge Management (CIKM2011), demo session, Glasgow, UK, Oct 24–28, 2011.
- Fröning, H., Giese, A., Montaner, H., Silla, F. and Duato, J.,  
Highly Scalable Barriers for Future High-Performance Computing Clusters, 18th annual IEEE International Conference on High Performance Computing (HiPC 2011), Bangalore, India, Dec 18–21, 2011.
- Fröning, H.,  
Network Interfaces, David Padua (Ed.): Encyclopedia of Parallel Computing, Springer, New York, ISBN 978-0-387-09765-7, to appear, 2011.



## PATENTS

Title	Date of Submission	Chair
DE 10 2011 111 432.0: Ortsempfindlicher Detektor zur Detektion von Photonen- oder Teilchenverteilungen	Aug 25, 2011	Circuit Design

## COLLOQUIA AND CONFERENCES

Title	Place	Date	Chair
Symposium on Variational Image Analysis	Heidelberg	July 4, 2011 July 6, 2011	Computer Vision, Graphics and Pattern Recognition
Third Symposium of the HyperTransport™ Center of Excellence and the Second International Workshop on HyperTransport Research and Applications	Mannheim	Feb 8–9, 2011	Computer Architecture
8th International Workshop on DEPFET Detectors and Applications	Bad Dürkheim	Sept 20–22, 2011	Circuit Design
Annual Colloquium on Probabilistic Graphical Models (RTG)	Heidelberg	Nov 23–25, 2011	Computer Vision, Graphics and Pattern Recognition

